

**Metal oxide catalysts for the low temperature selective oxidation of
propane to iso-propanol**

Thesis submitted in accordance with the requirements of the University of
Cardiff for the degree of Doctor of Philosophy by
Thomas Edward Davies

October 2006

UMI Number: U584969

All rights reserved

INFORMATION TO ALL USERS

The quality of this reproduction is dependent upon the quality of the copy submitted.

In the unlikely event that the author did not send a complete manuscript and there are missing pages, these will be noted. Also, if material had to be removed, a note will indicate the deletion.



UMI U584969

Published by ProQuest LLC 2013. Copyright in the Dissertation held by the Author.
Microform Edition © ProQuest LLC.

All rights reserved. This work is protected against
unauthorized copying under Title 17, United States Code.



ProQuest LLC
789 East Eisenhower Parkway
P.O. Box 1346
Ann Arbor, MI 48106-1346

Summary

A range of $\text{Ga}_2\text{O}_3/\text{MoO}_3$ and Co_3O_4 catalysts have been prepared and tested for the oxidative dehydrogenation of propane to propene. The $\text{Ga}_2\text{O}_3/\text{MoO}_3$ physical mixture demonstrated appreciable activity for propane conversion, with selectivity to propene comparable to existing known catalysts. The major products were propene and carbon dioxide with trace amounts of acrolein in some cases. The bulk Co_3O_4 catalyst was active for the conversion of propane at temperatures as low as ambient. The conversion at such low temperatures was very low but the selectivity to propene was near 100%. At temperatures lower than 100°C the catalyst showed rapid deactivation but at temperatures nearing 140°C the catalyst was capable of steady state conversion. Further study led to the creation of a high surface area nano-crystalline Co_3O_4 catalyst that was more active and selective than the original Co_3O_4 sample. The catalyst activity was probed by varying the reaction conditions and it was demonstrated that the selectivity and activity could be improved by varying the flow rate, feed composition and catalyst preparation method. Further studies looked into combining the low temperature Co_3O_4 catalyst with an acid hydration catalyst for the one step selective oxidation of propane to iso-propanol. The nano-crystalline sample was tested alongside various heteropolyacids and supported phosphoric acid catalyst. Co-feeding water had a negative effect on the activity of the nano-crystalline Co_3O_4 catalyst but trace amounts of iso-propanol were found in the reaction product indicating that the process investigated was possible.

Abstract

The oxidative dehydrogenation of propane to propene has been studied over a series of $\text{Ga}_2\text{O}_3/\text{MoO}_3$ and Co_3O_4 catalysts in an attempt to find a suitable catalyst that can be used in conjunction with an acid hydration catalyst for the direct one-step catalytic selective oxidation of propane to iso-propanol. The catalysts were created as a result of using a design approach recognising that the suitable catalyst should be able to activate the alkane and facilitate the desorption of the alkene without over oxidation to CO_x at temperatures low enough to allow the subsequent conversion of the product propene to iso-propanol. It has been demonstrated that the $\text{Ga}_2\text{O}_3/\text{MoO}_3$ catalyst synergistically combined the alkane activation properties of Ga_2O_3 with the selective oxidation function of MoO_3 producing appreciable propene yields in the temperature range 300-500°C. Studies have probed the influence of varying the Ga/Mo ratio. Catalysts with a 1/1 and 1/3 ratio showed similar catalytic activity, whilst reducing the ratio to 1/10 significantly reduced the propene yield. Comparison of the 1/1 $\text{Ga}_2\text{O}_3/\text{MoO}_3$ catalyst with a 6 wt% $\text{V}_2\text{O}_5/\text{TiO}_2$ catalyst, which is known to be active for selective propane oxidation, showed that the propene yields were greater for $\text{Ga}_2\text{O}_3/\text{MoO}_3$.

A series of bulk Co_3O_4 catalysts were prepared by various methods including precipitation from the nitrate and solid-state reaction. Propane conversion was observed at temperatures as low as 25°C, and this was a highly significant result as the low temperature activation of short chain alkanes is highly desirable. The catalyst prepared by solid-state reaction was more active than the catalyst prepared by precipitation. The selectivity to propene was near 100% at temperatures lower than 80°C but rapid deactivation of the catalyst occurred at these low temperatures. Steady-state activity was possible at 140°C but at the expense of propene selectivity which

was found to decrease with increasing reaction temperature. Comparison of propane conversion was made with a commercial sample of Co_3O_4 , and it was clear that the prepared catalysts were significantly more active. The commercial cobalt oxide catalyst was not active below 120°C .

The nano-crystalline Co_3O_4 catalyst was tested in conjunction with a number of different acid catalysts in an effort to probe the ability of a dual functioning catalyst for the direct one-step conversion of propane to iso-propanol. The best results were found over a phosphomolybdic- Co_3O_4 catalyst operating in the $100\text{-}140^\circ\text{C}$ temperature range. The co-feeding of water had a negative effect on the Co_3O_4 activity resulting in a lower than average propane conversion. However iso-propanol was present in trace amounts in the product distribution indicating that the process was feasible. At this stage, no attempt has been made to optimise the reaction conditions to increase iso-propanol yield.

All catalysts tested have been characterised by a range of techniques including BET, powder XRD, TPR/TPO, SEM and Raman spectroscopy the results of which are presented and discussed along with the catalytic data.

Abstract (Microfiche)

The oxidative dehydrogenation of propane to propene has been studied over a series of $\text{Ga}_2\text{O}_3/\text{MoO}_3$ and Co_3O_4 catalysts in an attempt to find a suitable catalyst that can be used in conjunction with an acid hydration catalyst for the direct one-step catalytic selective oxidation of propene to iso-propanol. Both the $\text{Ga}_2\text{O}_3/\text{MoO}_3$ and Co_3O_4 catalyst were active and selective for the reaction. The $\text{Ga}_2\text{O}_3/\text{MoO}_3$ was prepared by physically mixing the component oxides and was found to be active and selective for the reaction in the temperature range 300-500°C. A series of Co_3O_4 catalysts were prepared by both precipitation and solid-state reaction with the latter preparation method resulting in a nano-crystalline sample that was highly active and selective. The nano-crystalline Co_3O_4 was active at temperatures as low as ambient with a selectivity to propene near 100%. Combination of the catalyst with a phosphomolybdic acid catalyst resulted in a dual functioning catalyst capable of converting propane to iso-propanol in trace quantities. The catalysts developed were characterised using a wide range of techniques.

Acknowledgments

First and foremost I would like to thank my supervisor Dr Stuart Taylor for his constant support and guidance over the last three years. Thanks also to Jon, Phil, Dan, Ben and Tomas for taking the time to show me how to work those infernal machines. Everyone in lab. 1.88 and 1.44 Javier, Nick, Jenny, Chris, Graham, Sarah, Darragh, Nian Xue, Hong Mei, Leng Leng and of course Marco for taking the time to show me how to fix those infernal machines. Thanks to the techs. Dave, Rob, Gaz, Alun and Ricky for having the solutions to all my problems. Many thanks to those friends outside of university; Rhys, James, Owen, Pete, Jo, Ed, Shem, Will and Alun, for tolerating my awkward behaviour and being a constant source of entertainment. Special thanks goes to my family, especially mum, Laura, Nan and Gramps.

Abbreviations/Nomenclature

GHSV = Gas Hourly Space Velocity

BET = Brunauer Emmet Teller (Surface area analysis)

HC = Hydrocarbon

ODH = Oxidative Dehydrogenation

SEM = Scanning Electron Microscopy

TCD = Thermal Conductivity Detector

FID = Flame Ionisation Detector

TPO = Temperature Programmed Oxidation

TPR = Temperature Programmed Reduction

XRD = X-Ray Diffraction

GC = Gas Chromatograph

i.d. = Internal Diameter

Iso-propanol = Propan-2-ol

Acrolein = Propenal

Propylene = Propene

Table of Contents

Chapter 1: Introduction	1
1.1 Catalysts and catalysis	1
1.2 Basic principles of catalysis	2
1.3 Heterogeneous catalysis	5
1.4 The petrochemical industry and the production of propene	6
1.4.1 Steam Cracking	7
1.4.2 Catalytic cracking	8
1.4.3 Alkane dehydrogenation	9
1.4.4 Alkane oxidative Dehydrogenation	11
1.5 Aims of project	14
1.6 Literature review	16
1.6.1 Vanadium oxide based catalysts	16
1.6.2 Molybdenum oxide based catalysts	21
1.6.3 Gallium oxide based catalysts	24
1.6.4 Cobalt oxide based catalysts	27
1.5 Iso-propanol production	29
1.6 References	32
Chapter 2: Experimental	39
2.1 Catalyst preparation	39
2.1.1 Ga ₂ O ₃ /MoO ₃ mixed oxide catalyst	39
2.1.2 Precipitated GaOOH precursor	39

2.1.3 Precipitated Co_3O_4 catalyst	40
2.1.4 Nanocrystalline Co_3O_4	40
2.1.5 Higher Co_3O_4	41
2.1.6 Silica supported H_3PO_4	41
2.1.7 Acid hydration catalysts	42
2.1.8 Dehydrogenation/Hydration catalyst	42
2.2 Reactor design	42
2.2.1 Oxidative dehydrogenation reactor	42
2.2.2 Low temperature oxidative dehydrogenation reactor	43
2.2.3 $\text{Ga}_2\text{O}_3/\text{MoO}_3$ reaction conditions	43
2.2.4 Small bed Co_3O_4 reaction conditions	44
2.2.5 Ambient temperature reaction conditions	45
2.2.6 Propane/propene hydration reaction conditions	45
2.2.7 Reduction of Co_3O_4	47
2.2.8 Sample delivery	47
2.2.9 Valve sequence and temperature programme	49
2.2.9.1 Data handling	49
2.3 Characterisation	51
2.3.1 Powder X-ray diffraction (XRD)	52
2.3.2 Raman spectroscopy	55
2.3.3 Thermogravimetric analysis (TGA)	56
2.3.4 Brunauer Emmet Teller surface area determination (BET)	57
2.3.5 Temperature programmed reduction/oxidation (TPR/TPO)	58
2.3.6 Scanning electron microscope (SEM)	58
2.4 References	60

Chapter 3: The oxidative dehydrogenation of propane using gallium-molybdenum oxide based catalysts	61
3.1 Introduction	61
3.2 Characterisation	62
3.2.1 BET surface areas	62
3.2.2 Powder X-ray diffraction	63
3.2.3 Raman spectroscopy	68
3.2.4 Temperature programmed reduction	70
3.2.5 Scanning electron microscopy	72
3.3 Results	74
3.3.1 Propane oxidative dehydrogenation over 1:1 Ga ₂ O ₃ /MoO ₃	76
3.3.2 Propane oxidative dehydrogenation over individual components : effect of heat treatment	79
3.3.3 Propane oxidative dehydrogenation over modified Ga ₂ O ₃ /MoO ₃	82
3.3.4 Propane oxidative dehydrogenation over Ga ₂ O ₃ /MoO ₃ : Layered bed	84
3.4 Discussion	87
3.5 Conclusions	91
3.6 References	92
Chapter 4: Cobalt oxide catalyst for the low temperature oxidative dehydrogenation of propane	93
4.1 Introduction	93
4.2 Characterisation	94
4.2.1 BET surface areas	94

4.2.2 X-ray diffraction (XRD)	95
4.2.3 Temperature programmed reduction	97
4.3 Results	101
4.3.1 Initial experiments	101
4.3.2 Variation in O ₂ concentration	106
4.3.3 Variation in calcinations conditions	109
4.3.4 Variation in flow rate	112
4.3.5 Steady state activity	114
4.3.6 Improved conversion with lower space velocities	118
4.3.7 Comparison with commercial sample	119
4.3.8 <i>in situ</i> reduction	121
4.4 Discussion	124
4.5 Conclusions	127
4.6 References	128
Chapter 5: Nanocrystalline cobalt oxide catalysts for selective propane oxidation under ambient conditions	130
5.1 Introduction	130
5.2 Characterisation	132
5.2.1 BET Surface areas	132
5.2.2 X-ray diffraction	133
5.2.3 Temperature programmed reduction	136
5.2.4 Scanning electron microscopy	140

5.3 Results	142
5.3.1 Variation in preparation method	142
5.3.2 Cobalt oxide nanoparticles	147
5.2.3 Steady state measurements	150
5.2.4 Effect of water on Co_3O_4 nanoparticles	152
5.2.5 Conversion of propene to iso-propanol over acid catalysts	155
5.2.6 Direct conversion of propane to iso-propanol over bi-functional Catalyst	159
5.4 Discussion	163
5.4.1 Propane oxidative dehydrogenation over bulk Co_3O_4 catalyst	163
5.4.2 Direct oxidation of propane to iso-propanol	168
5.5 Conclusions	170
5.6 References	171
Chapter 6: Conclusions and future work	173
6.1 $\text{Ga}_2\text{O}_3/\text{MoO}_3$ catalyst	173
6.2 Co_3O_4 catalyst	174
6.3 References	178
Chapter 7: Appendix	

Chapter 1

Chapter 1

Introduction

1. Introduction to catalysis

1.1 Catalysts and catalysis

A catalyst may be defined simply as a substance, which increases the rate at which a chemical reaction approaches equilibrium, without itself undergoing a chemical change or being consumed in the process. A more precise definition states that ‘a catalyst is a substance which increases the rate of attainment of equilibrium of a reacting system without causing any great alteration in the free energy changes involved’ ^[1]. Berzelius first used the word ‘catalysis’ in 1836 to describe a series of observations and discoveries made by others; Thenard (1813) discovered that metals could decompose ammonia and Dobereiner (1825) found that manganese oxide affected the rate of decomposition of potassium chlorate. Berzelius suggested that the surface of some solids possessed a ‘catalytic force’ ^[2].

Catalysts fall into two main classes: *homogeneous* and *heterogeneous*. A catalyst is described as ‘homogeneous’ when the reaction takes place in any one phase and ‘heterogeneous’ when the reaction occurs at an interface. Examples of the two systems are given in table 1.1. Homogeneous catalysts usually operate in the liquid-liquid phase and involve soluble metal complexes in solution. The selectivity is typically high with moderate activity and the reaction temperatures are usually low (<250°C). Limitations to homogeneous methods include product separation and catalyst recycling which can be problematic and expensive.

In heterogeneous catalysis the reactants are typically gaseous or liquid and pass over a solid catalyst. Catalytic activity is usually high but selectivity to the desired products can be quite low, the reaction temperatures are relatively high (250-600°C). Recycling of the catalyst is quite simple and product separation can be easier but the high temperatures of reaction make the process energy intensive and environmentally unsound.

Table 1.1 Examples of *homogeneous* and *heterogeneous* catalysts

Catalytic system	Phase	Example
Homogeneous	Liquid + Liquid	Acid/base catalysed hydrolysis of esters
	Gas + Gas	Oxidation of sulphur dioxide catalysed by nitric oxide $\text{SO}_2 \xrightarrow{\text{NO}} \text{SO}_3$
Heterogeneous	Liquid + Gas	Phosphoric acid catalysed polymerisation of olefins $\text{C}_2\text{H}_4 \xrightarrow{\text{H}_3\text{PO}_4} \text{-}(\text{-CH}_2\text{CH}_2\text{-})_n\text{-}$
	Solid + Liquid	Gold catalysed hydrogen peroxide decomposition $\text{H}_2\text{O}_2 \xrightarrow{\text{Au}} \text{H}_2\text{O} + 1/2\text{O}_2$
	Solid + Gas	Iron catalysed production of ammonia (Haber process) $\text{N}_2 + 3\text{H}_2 \xrightarrow{\text{Fe}} 2\text{NH}_3$

1.2 Basic principles of catalysis

A catalyst works by providing another route for the reaction i.e. providing an alternative reaction mechanism with a lower energy of activation (figure 1.1).

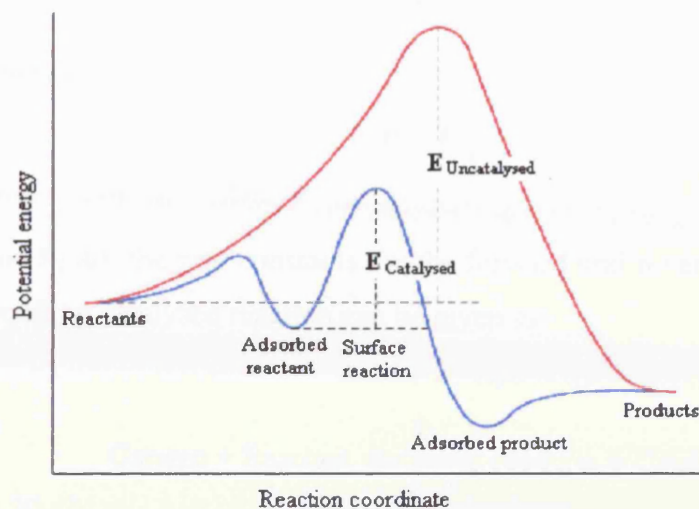


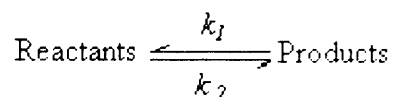
Figure 1.1 Potential energy profile of an exothermic reaction: red line, uncatalysed; blue line, catalysed

A catalyst can only alter the rate at which the reaction attains equilibrium; it cannot alter the position of equilibrium in a reversible reaction. This can be easily shown. The Gibbs free energy ΔG° is a state function, and for any reaction there can be only one value for the standard Gibbs free energy change ΔG° . Since:

$$-\Delta G^\circ = RT \ln K$$

where K is the equilibrium constant, there can be only one value for K .

Given that the equilibrium attained in a catalysed reaction must be the same as the corresponding uncatalysed reaction it follows that the catalyst must equally affect the rate of both the forward and reverse reactions. The equilibrium constant K of the uncatalysed reaction:

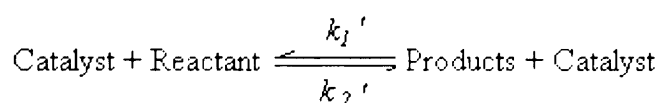


can be defined as:

$$K = k_1/k_2$$

Where k_1 and k_2 are the rate constants for the forward and reverse reaction respectively.

The corresponding catalysed reaction can be given as:



and

$$K = k_1'/k_2'$$

Given

$$-\Delta G^{\circ}_T = RT \ln(k_1/k_2)$$

and

$$-\Delta G^{\circ}_{T'} = RT \ln(k_1'/k_2')$$

By definition

$$-\Delta G^{\circ}_T = -\Delta G^{\circ}_{T'}$$

where $-\Delta G^{\circ}_T$ is the standard free energy change at T° Kelvin, and so

$$(k_1/k_2) = (k_1'/k_2')$$

It is therefore apparent that a catalyst can only accelerate the rate of a chemical reaction that is already thermodynamically feasible i.e. a reaction that involves a decrease in free energy [3].

1.3 Heterogeneous catalysis

Many industrial processes are now carried out by heterogeneous catalysts, some of the most important being the Haber process for the production of ammonia, the Bosch process for hydrogen, the contact process for sulphuric acid, the refining of petroleum and the synthesis of vinyl chloride, aldehydes, butadiene, styrene, phenol, alcohols and many other important organic compounds. One of the earliest observations of such catalysis was Paul Sabatier's observation that nickel hydrogenated ethene giving ethane (1900) ^[4]. Many more industrial applications followed. A number of materials are used for heterogeneous catalysis and they can be divided into two distinct groups: (i) metals and (ii) non-metals. Table 1.2 highlights some of the more important reactions with examples of catalysts used. The metallic and supported metallic catalysts are some of the most important catalysts and are used in dehydrogenation, hydrogenation, hydrogenolysis and in some cases oxidation. Metal oxides and sulphides such as NiO, Cr₂O₃ and WS₂ are proven catalysts for oxidation, reduction, cyclisation and desulphurisation reactions. Ceramic metal oxides such as MgO, Al₂O₃ and SiO₂ are often used as supports for metals because of their high stability and inactivity, and are also used in dehydration and isomerisation reactions. Zeolites are important catalysts for the catalytic cracking of petroleum fractions to C₂-C₁₄ hydrocarbons. Zeolites, H₃PO₄ and H₂SO₄ are examples of acid catalysts and as well as catalytic cracking reactions are also useful for polymerisation, isomerisation and alkylation reactions ^[3].

Table 1.2 Typical catalysed reaction

Reaction	Catalyst	Type of reaction
$\text{CH}_3\text{CH}=\text{CH}_2 \rightarrow \text{CH}_3(\text{CH}_2)_3\text{CH}=\text{CH}_2$	$\text{NiO}/\text{SiO}_2/\text{Al}_2\text{O}_3$	Polymerisation
Petroleum fractions \rightarrow C ₄ -C ₁₂ hydrocarbons	$\text{Al}_2\text{O}_3/\text{SiO}_2$	Hydrocarbon cracking
But-1-ene \rightarrow Buta-1,3-diene	$\text{MoO}_3/\text{V}_2\text{O}_5$	Oxidation
Ethylene \rightarrow $\text{H}_2\text{C}(\text{O})\text{CH}_2$	Ag	
$\text{CO} + \text{H}_2 \rightarrow$ alcohols, aldehydes, acids, hydrocarbons	Fe, Co, Ni	Synthesis
Olefines \rightarrow Paraffins	Pd, Pt, Ni, Rh, Os,	Reduction
Acetylenes \rightarrow Olefines	Ni, Rh, Pd, Pt	
But-1-ene \rightarrow cis/trans but-2-ene	Ni, Pd, Pt, Ru, Rh	Isomerisation
$\text{CO} + 3\text{H}_2 \rightarrow \text{CH}_4 + \text{H}_2\text{O}$	Ni	Shift reactions
$\text{CO} + \text{H}_2\text{O} \rightarrow \text{CO}_2 + \text{H}_2$	$\text{Fe}_3\text{O}_4/\text{Cr}_2\text{O}_3$	

1.4 The petrochemical industry and the production of propene

Many materials and chemical intermediates are derived from propene, some of the most important materials include: propene oxide, acrylonitrile, cumene, polypropene, oxoalcohols and iso-propanol. In turn, each of these chemicals is an important precursor in the manufacture of consumer products. Propene oxide is a precursor to polyurethane resins and propene glycols, which are used in flame-retardants and synthetic lubricants. Acrylonitrile is converted to acrylic fibres and coatings. Dimerization of acrylonitrile affords adiponitrile, which is used in the synthesis of nylon. Cumene is used to make epoxy resins and polycarbonate and is also a constituent of vinyl floor tiles, carpets, foam

insulation and other rubber floor/wall coverings. Polypropene is an important thermoplastic polymer with countless applications in areas such as food packaging, textiles, plastic parts and containers to name but a few. High-grade polypropene is used in various fabrication processes such as injection moulding, thermoforming, blow moulding and laminating. Iso-propanol is typically used as a solvent and disinfecting agent as well as being an additive in fuels. Oxo-alcohols are used in coatings and plasticers ^[5].

Propene is produced primarily as a by-product of petroleum refining and of ethene production by the steam cracking of hydrocarbons. For example it is estimated that 66% of the total amount of propene produced in 2003 was obtained as co-product in ethene manufacture by steam cracking processes. Fluid catalytic cracking (FCC) units supply around 32% with propane dehydrogenation and metathesis estimated to account for only 2% of the market ^[6]. The current demand for propene is primarily driven by the high growth rate of propylene for the plastics industry and it is estimated that future demand will increase by 5% annually. With the demand for olefins ever increasing the principle methods of steam cracking and FCC may not have the capacity to meet future needs. Indeed, with an increasing demand for all alkenes the operating conditions in many steam and catalytic cracking processes are being optimised for ethene production at the expense of propene yield ^[7].

1.4.1 Steam Cracking

Although a number of modern processes use catalysts, steam or naphtha cracking is an example of one that does not. The process works by naphtha being vaporised with super heated steam and cracked to smaller molecules via free radical mechanisms in the absence of a catalyst. Oil or gas fired burners are used to heat the reactor tubes to 750-900°C with

temperatures up to 1100°C (high severity cracking). Light olefins are formed in the gaseous state before the reaction mixture is cooled and quenched. The effluent is then passed through a series of heat exchangers before primary fractionation and compression. The gasoline and fuel oil streams are separated into liquids and gas fractions with the products at this stage being uncrude fuel oil, aromatic gasoline, toluene, benzene and xylene. The final stage is product recovery where the products are separated by distillation, refrigeration and extraction. C₃ compounds are removed in a depropanizer stage with consequent splitting of the alkane and alkene^[7, 8].

The steam cracking of ethane is similar to naphtha cracking and gives rise to propene as a by-product. Cracking is a massively energy intensive process and is estimated to be the single most energy intensive process in the chemical industry, it is estimated that the pyrolysis stage of the steam cracker consumes 65% of the total process energy alone^[7].

1.4.2 Catalytic cracking

Since its early beginnings research into catalytic chemistry has been stimulated by the needs of industry. The use of catalysts has led to better reaction control and product selectivity as well as improved process efficiency and economics. Indeed, a number of existing processes may well become obsolete as the development of catalytic processes increases. The first major catalytic cracking processes were introduced in 1940's America and originally used clay catalysts operating at 500°C. Since then development has seen the introduction of newer processes such as modern fluidised-bed catalytic cracking (FCC) and hydrocracking.

Fluid Catalytic Cracking (FCC) is an acid cracking process that uses acidic ZSM catalysts and heavy feedstocks. By using a zeolite catalyst the process is less energy

intensive than steam cracking and typically operates in the 450-600°C temperature range. Efficient heat transfer is managed by good contact between the catalyst and reactant along with the moving/riser reactor technology. The low temperatures mean that excess heat can be recycled and used as a source of process energy. The use of a catalyst also means that the reaction is more selective towards the desired product.

The hydrocracking process is less efficient and more expensive than the FCC process and operates at about 450°C and 150-200 atm hydrogen. The catalyst used is usually a zeolite-supported palladium^[7-9].

1.4.3 Alkane dehydrogenation

The direct catalytic dehydrogenation of alkanes provides a selective way of alkene production from abundant alkane feedstocks and was first commercialised in the 1930's. Areas such as the Middle East where alkane feedstocks are in good supply have been paying a lot of attention to propane dehydrogenation for propene production^[7, 10]. Alkene production via catalytic dehydrogenation takes up only a small portion of total alkene production but offer more selective routes to the desired product. Current industrial processes in or near operation include:

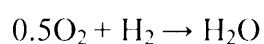
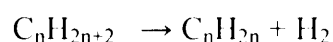
- (i) The Catofin or Houdry process licensed and developed by Sud-Chemie and Lummus is a cyclical process using an adiabatic fixed bed reactor comprising alkali promoted $\text{CrO}_x/\text{Al}_2\text{O}_3$. The operating temperature is around 590-650°C and converts alkanes to alkenes with 85% selectivity^[10-11].

- (ii) The STAR process (Steam Active Reforming), under licence from Philips uses a cyclical dehydrogenation and oxydehydrogenation process with a Pt/Sn on $ZnAl_2O_4/CaAl_2O_4$. The STAR reactor uses a combination of dehydrogenation and oxydehydrogenation processes giving selectivity to alkenes of around 90%^[10-11].
- (iii) The UOP Oleflex process for C_3 and C_4 production uses an alkali promoted Pt/Sn/ Al_2O_3 catalyst and achieves a selectivity to alkenes of around 91%^[11].
- (iv) FBD (Fluidised Bed Dehydrogenation) operates under licence from Snamprogetti/Yarsintiz and uses an alkaline promoted CrO_x/Al_2O_3 catalyst for the production of alkenes. Process gives selectivity to propene of around 90%^[11].

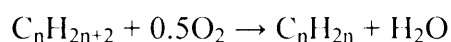
Due to the relative stability of ethane and hence the vigorous reaction conditions required for dehydrogenation, there is as yet, no commercial ethane dehydrogenation process. Indeed one of the main problems with catalytic dehydrogenation processes is that the conversion and selectivity are restricted thermodynamically and high temperatures are necessary to supply energy to the strongly endothermic main reaction. In turn, the high temperatures can lead to a number of unwanted side reactions resulting in irreversible catalyst deactivation. Even when there isn't complete deactivation it is still necessary to regenerate the catalyst, sometimes after only minutes online. The high temperatures also make the process energy and capital intensive^[6].

1.4.4 Alkane oxidative dehydrogenation

The oxidative dehydrogenation of alkanes provides an alternative route for the production of alkenes, which overcomes the thermodynamic restrictions, allows operation under relatively mild conditions and avoids the necessity of continuous catalytic regeneration. Dioxygen can facilitate the conversion of molecular hydrogen into water and thus shift the equilibrium towards the formation of dehydrogenated products. Oxygen acts as a hydrogen acceptor which gives rise to an exothermic reaction and overcomes the thermodynamic limitations of a reversible endothermic reaction.



Overall:



The oxidant also prevents coking by burning off any carbonaceous deposits that can decrease catalyst lifetime. However, there are a number of drawbacks. Controlling selectivity can be difficult due to the possibility of a large number of oxygenated products such as aldehydes and acids (figure 1.2).

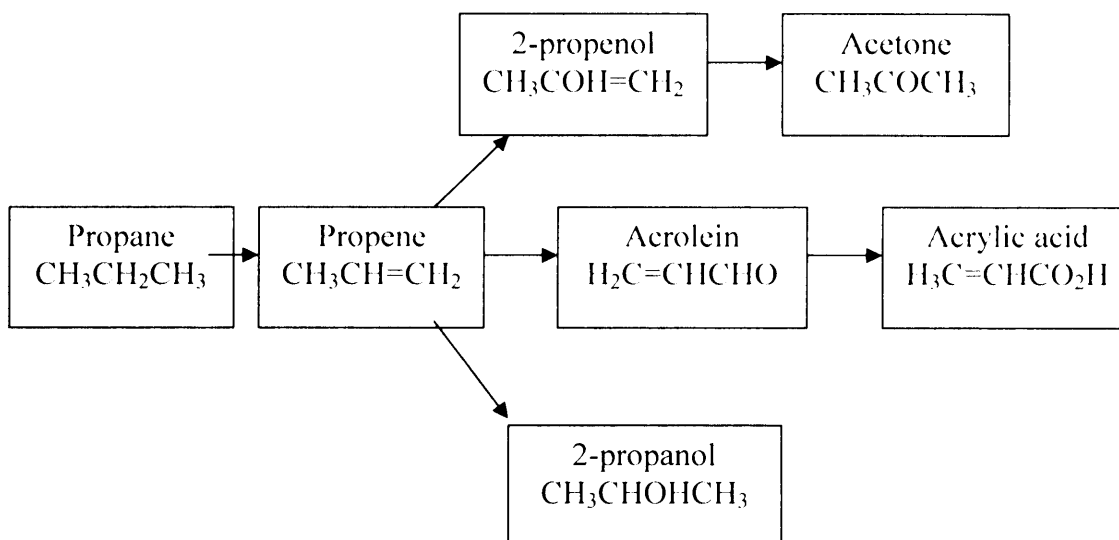


Figure 1.2 Oxygenated products of propene ^[12]

The other major problem is controlling the consecutive oxidation to carbon oxides; figure 1.3 shows the reaction network for the oxidative dehydrogenation of propane. Propene is formed from the oxidative dehydrogenation of propane (k_1), and CO_x is formed as a result of the direct combustion of propane (k_2) or the subsequent total oxidation of propene (k_3). For a selective reaction the k_2/k_1 ratio is usually low (~ 0.1), but with increasing conversion there is usually a decrease in alkene yield corresponding to an increased k_3/k_1 ratio ($\sim 10-50$). The large k_3/k_1 ratio occurs as a result of the weaker allylic C-H bond in propene and the fact that alkenes are more strongly bound to oxide surfaces. The strongly bound alkene is susceptible to further oxidation ^[13].

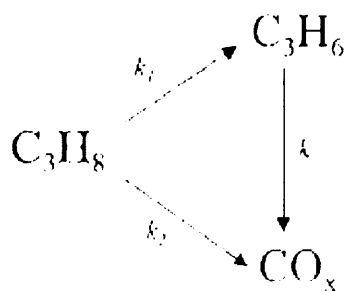


Figure 1.3 Reaction network in the ODH of propane

Other difficulties include the flammability of the reaction mixture and controlling the heat produced, due to the exothermic reaction the process can be auto-thermal, but this can also lead to a runaway reaction. It is therefore necessary to operate within the flammability limits and to carefully control the feed mixture. With oxygen in excess there is an increased conversion, but also the increased likelihood of total combustion resulting in poor selectivity to the desired product.

There is a general agreement that propane oxidative dehydrogenation involves redox cycles whereby the organic molecule is oxidised by lattice oxygen resulting in a reduced centre which is then reoxidised by O_2 ^[14-16], i.e the Mars-van Krevelen mechanism. When in equilibrium with the gas phase the surface is populated by short lived oxygen species capable of removing the methylene C-H in the propane molecule. A second hydrogen abstraction then takes place before desorption of the propene molecule and subsequent reoxidation of the reduced site (figure 1.4).

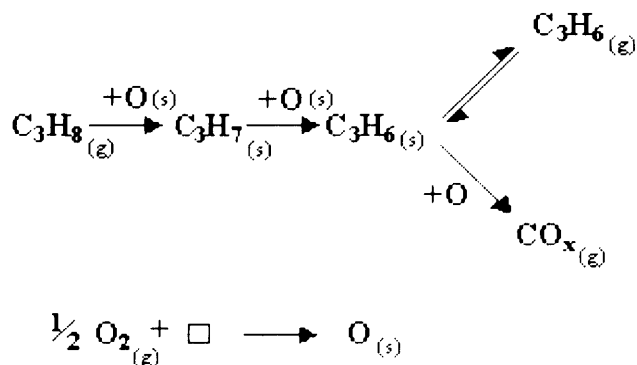


Figure 1.4 Proposed reaction mechanism for the ODH of propane (\square denoted surface vacancy)^[14]

Propane oxidative dehydrogenation remains a viable route for the production of propene but as yet no catalyst has been developed which meet the requirements of industrial processes. Also the problem of propene stability towards consecutive unselective oxidative attack makes finding a suitable catalyst for the oxidative dehydrogenation of propane a difficult task.

1.5 Aims of project

The overall aim of this project is to find a catalyst capable of the direct conversion of propane to iso-propanol, which historically has not been extensively studied. A vast portion of the research will focus on the initial propane oxidative dehydrogenation step in an effort to find a catalyst capable of activating propane at temperatures low enough to allow the subsequent hydration step to take place. One of the main problems will be the incompatibility of the reaction conditions for the two different processes. To date the best catalysts found for the ODH of propane usually operate in the 400-600°C temperature range at atmospheric pressure. Even the most active catalysts can only operate at

temperatures not less than 350°C and this is usually at the expense of propane conversion and propene yield. Such reaction conditions are too severe for the hydration of propene: a process that is thermodynamically limited by the reverse reaction at high temperatures. Current propene hydration processes operate in the 100-300°C temperature range and at pressures typically between 25-250 atms.

Based on this, two possible approaches are possible. One is to develop a range of multi-component catalysts that possess both oxidative dehydrogenation and acid catalytic properties combined synergistically. Simplistically, it can be imagined that synergistic combinations may exist in which one component is principally responsible for propane activation and the other for oxygen insertion. As an example it has been shown previously that Ga₂O₃/MoO₃ is a selective catalyst for methane oxidation to methanol ^[17]. Even if the reaction proposed for this investigation is very different, such materials represent an excellent starting point, since they contain redox elements (Ga,Mo). The acid function could then be introduced by direct impregnation of the ODH catalyst e.g. by the addition of a strong acid such as phosphoric acid.

A second possible approach would be to keep the oxidative dehydrogenation and hydration catalyst separate but in contact i.e. by layering the catalyst beds or creating a mechanical mixture. Such an approach would prevent modification of the individual functions by addition of one catalyst to the other e.g. impregnation of the ODH catalyst with a strong acid such as phosphoric acid may increase the acid character of the catalyst but at the expense of its selectivity to propene.

Either way, one of the most difficult problems will be finding an oxidative dehydrogenation catalyst capable of operating at such low temperatures. Although it is theoretically possible to convert propane to propene with 100% selectivity at ambient temperature using an oxidative dehydrogenation process, this has not yet been realised.

Conversion is limited at such low temperatures, so in order to achieve appreciable yield the propene selectivity would have to be near 100%. Catalyst selectivity is of vital importance in the production of olefins and in the cases of large-scale applications it can often be more important than activity.

1.6 Literature review

1.6.1 Vanadium based catalysts

Vanadium oxide based catalysts are active and selective for a number of catalytic reactions including: the selective oxidation of short chain alkanes and alkenes such as oxylene, 1,3-butadiene and methane; the oxidation of methanol; the oxidation and ammoxidation of aromatic hydrocarbons; the decomposition of iso-propanol, as well as the selective catalytic reduction of NO_x ^[18-23]. Industrial processes currently in operation using vanadia based catalysts and short chain alkane feedstocks are n-butane to maleic anhydride on VPO and propane ammoxidation on $\text{VSbO}/\text{Al}_2\text{O}_3$. Vanadium catalysts for alkane oxidative dehydrogenation have also been the subject of much research and to date there has been a number of reviews detailing the current state of the art^[24-26]. Bulk V_2O_5 is a proven catalyst for alkane oxidation but not a good catalyst for propane oxidative dehydrogenation. Propane conversions of 22% at 540°C have been reported in the literature but the selectivity to propene was low at 18%^[26]. Other groups found similar results^[29]. However, the spreading of the oxide onto a suitable support leads to modification of the vanadia properties resulting in a highly active and selective catalyst.

Supported V_2O_5 catalysts are very active and selective catalysts for the ODH of propane to propene. Some of the earliest work was done on V-Mg-O catalyst with interesting results. Early work by Chaar *et al* on V impregnated MgO showed how it was capable of 10% propane conversion at 540°C with a propene selectivity of 65% [26]. Interestingly, the only products formed were propene, CO_x and ethane(ene) with no other oxygenates found in the feed. The absence of oxygenated products was attributed to the absence of V=O bonds in the orthovanadate ($Mg_3V_2O_8$) system which are believed to cause over-oxidation of the hydrocarbon. In a similar study Sew *et al* assigned the activity to the pyrovanadate phase (α - $Mg_2V_2O_7$) and stated that it was the orthovanadate phase that was responsible for the total oxidation [27]. Further work confirmed the pyrovanadate phase to be the most selective and reducible with the reactivity of each phase found to decrease in the order $Mg_2V_2O_7 > MgV_2O_6 > Mg_3V_2O_8$. Gao suggested that the phases work in a cooperative manner with the selectivity to propene over $Mg_3V_2O_8$ (orthovanadate) being promoted by the presence of the α - $Mg_2V_2O_7$ (pyrovanadate) phase or excess MgO in intimate contact [28-29]. Overall there is a general agreement that the reaction proceeds via abstraction of hydrogen from the alkane with the reduction of tetrahedrally co-ordinated V^{5+} species. The influence of the preparation methods of V-Mg-O catalysts on their catalytic properties has been studied and, again, an Mg enriched surface was found to be beneficial [30].

More recent studies have looked into altering the activity of the established V-Mg-O by modification of the active site or the addition of certain promoters. Solid state catalysts prepared by mechanical mixing of the two component oxides have been investigated but the results were poorer than those over the impregnated sample [31]. The significant increase in the selectivity over the impregnated sample has been related to the highly dispersed Mg in the meso-VMg. The addition of Mg to vanadia has been found to

increase the activity by the formation of VO_x tetrahedra with the activity of the catalyst being related to the presence of VO_x tetrahedra and the absence of exposed $\text{V}=\text{O}$ bonds from V_2O_5 crystallites ^[32-35]. Certain recent studies have focused on the preparation of magnesium vanadates with higher concentrations of these VO_x tetrahedra. The preparation method studied was found to inhibit the formation of the less selective double $\text{V}=\text{O}$ bonds resulting in a more active $\text{Mg}_3\text{V}_2\text{O}_7$ ^[36]. It appears that the strong interaction of the acidic and basic MgO is an important factor for the formation of active magnesium vanadates, the formation of isolated or clustered VO_x units is necessary to prevent over oxidation of the alkane: many groups support the theory that the high selectivity is as a result of the limited oxygen availability within these systems.

Supporting vanadia on other metal oxides also results in an active catalyst. VO_x supported on Al_2O_3 , SiO_2 and MgO has been the subject of a number of catalytic and structural studies. Silica supported catalyst have received a lot of attention over the last few years, primarily for the oxidation of ethane and butane ^[37-39]. The oxidative dehydrogenation of propane over SiO_2 supported vanadia has received less attention but certain studies have shown it to be an active catalyst for the production of propene. Parmaliana *et al* ^[40] found that V_2O_5 greatly enhanced the performance of pure SiO_2 for the production of propene. However, the temperature of the reaction was relatively high, typically operating in the 500-655°C temperature range. At lower temperatures of 450°C the conversion is relatively poor at 2.8% with selectivity to propene of 66%, although, with an alkane rich reaction feed the conversion was increased to 3.3% with a propene selectivity of 73%. The catalyst also showed traces of other oxygenates in the feed (ca.<5%). At higher temperatures (>500°C) the conversion is increased but at the expense of selectivity as methane, ethane and carbon oxides become the dominant products. Other groups found similar results with higher temperatures being necessary for appreciable

conversion of propane ^[41]. The best propene yields were achieved at 550°C but again, at these temperatures traces of ethane, ethene and methane were found. The higher reaction temperature required for the activation of propane on VSiO₂ catalysts is consistent with the evidence that the V species is highly dispersed over the acidic silica surface. Increasing the vanadia loading results in an increase in conversion due to the formation of polymeric vanadium species which, although more active, cause over oxidation of the alkane.

Silica supported VMgO catalysts are active and selective for the oxidative dehydrogenation of both propane and n-butane ^[42] but as with other silica supported catalysts tend to show low selectivity to oxygenates at higher reaction temperatures, in this case acrolein. Higher Mg/V ratios were required for better selectivity due to the loss of Mg within the system to the formation of Mg₂SiO₄. As with previous studies the presence of ortho-Mg₃V₂O₈ and pyro-Mg₂V₂O₇ are necessary to obtain the most selective catalyst.

In studies by Lemonidou *et al* V₂O₅ impregnated TiO₂ and Al₂O₃ were found to be more active and selective than V-Mg-O catalyst ^[43]. The activity was related to the reducibility and structure of the V species on the surface. Under the conditions tested the activity and selectivity was found to decrease in the order VAl₂O₃>VTiO₂>VZrO₂>VMgO. The VAl₂O₃ catalyst was 60% selective to propene at 8% conversion at 450°C, results comparable to those over Mg-vanadates. The addition of alkali metals (Li, Na and K) was found to increase the selectivity to around 80% but at the expense of decreased conversion. Recently V₂O₅/Al₂O₃/SiO₂ catalysts have been shown to activate propane in the 400-500°C temperature range ^[44]. Propane conversion over the catalysts were quite high at around 20% but the selectivity to propene was below average at <50%. The addition of Ni, Cr, Mo, and Nb to V-SiO₂ catalysts was found to increase the overall activity and selectivity ^[45]; at 500°C, and with conversions of 10%, a

selectivity to propene of around 40% was achieved. The selectivity to propene was found to decrease with the increasing electronegativity of the additive. The addition of an alkali potassium promoter increased the selectivity but decreased the activity. Interestingly the addition of K to VO_x/MgO resulted in a decrease of both activity and selectivity.

Alumina-supported basic vanadates containing ZnO are also active for propane conversion but the selectivity to propene is very low^[46]. As with previous work it was found that good interaction of the active phase with the support was necessary for increased propene selectivity. Interestingly the temperature of the reaction was relatively low at 350°C. This is some 50-100°C lower than many of the other V containing catalysts reported in the literature. The addition of Mg modifiers to $\text{V}_2\text{O}_5/\text{Al}_2\text{O}_3$ and $\text{V}_2\text{O}_5/\text{TiO}_2$ catalyst was investigated by Machli *et al.*^[47] Addition of Mg to $\text{V}_2\text{O}_5/\text{TiO}_2$ almost doubled the selectivity of the catalyst. The effect on $\text{V}_2\text{O}_5/\text{Al}_2\text{O}_3$ is less pronounced. This increased selectivity was related to the beneficial effect of Mg in the rate of primary formation of propene from propane. The specific surface activity of the catalyst was found to be related to the acidity; the higher the acidity the higher the activity.

Vanadium phosphates are well known to be active and selective in the oxidation of n-butane to maleic anhydride^[48] as well as the selective oxidation of ethane to ethane^[43]. The ability of VPO to catalyse the ODH of propane is generally quite poor. Vanadyl phosphates give predominately carbon oxides with very low concentrations of propene, ethane, acrylic acid and acrolein^[49-50]. The highest propene selectivity reported is 12.5% over $\alpha\text{-VOPO}_4$ although a selectivity of up to 75% has been reported when the reaction is carried out in the presence of ammonia^[51]. Higher propane selectivity has been obtained over vanadium aluminophosphates. VAPO catalysts containing small amounts of vanadia were very selective, and this selectivity was attributed to the increased concentration of VO_x tetrahedra on the surface^[52].

Vanadium oxide containing catalysts are active and selective materials for the oxidative dehydrogenation of propane, as well as ethane and butane. The spreading of the catalyst over various supports and carriers is found to greatly increase the activity of the V species. The activity and selectivity of the catalyst is found to be influenced by a number of factors including: the preparation method, presence of dopants, vanadia loading, the nature of the support and hence the nature of the surface V species. Acidic supports give a highly dispersed vanadia monolayer whereas basic supports tend to form stable mixed oxidic phases. Although vanadium containing catalysts show some of the highest conversion and propene selectivity the temperature of the reaction is typically in excess of 500°C.

1.6.2 Molybdenum based catalysts

Molybdenum oxide based catalysts are active for a number of reactions including the selective oxidation and ammoxidation of propene. Bismuth molybdates and vanadyl molybdates have proven to be active in the (amm)oxidation of propene to acrolein, acrylic acid and acrylonitrile^[53] but it is only recently that significant attention has been paid to molybdenum based catalysts for the oxidation and oxidative dehydrogenation of propane. Some of the earliest reported work was done in 1978 on cobalt molybdates that showed high selectivity to propene (77.9%) at temperatures in excess of 500°C but the reported propane conversion was very low at just 4.1%^[54]. It is only in the last 10 or so years that serious effort has been directed towards the study of various metal molybdates for the

ODH of propane and although promising results have been seen one of the major problems with molybdenum oxide based catalyst is the high temperature required for activation of the alkane. Indeed the majority of molybdenum catalysts studied are only active at temperatures greater than 450°C with few exceptions.

Yoon *et al* ^[55-56] studied propane oxidation over a series of metal molybdate catalysts and found that most of the catalysts predominately promoted the ODH of propane to propene. Each catalyst attained 80% selectivity but with varying activity. The most active catalysts were found to be those containing Mg, Ca, Ni, Al and Cr but selectivity at these conversions was relatively low. The most active and selective catalyst was $\text{Co}_{0.95}\text{MoO}_x$, which gave 60% selectivity at 20% conversion at 450°C, these results are comparable to those obtained over $\text{V}_2\text{O}_5/\text{MgO}$ catalysts ^[57]. Precipitated magnesium molybdates such as $\text{Mg}_{0.95}\text{MoO}_x$ are active at temperatures as low as 400°C but with low conversion. The authors report a maximum conversion of 22%, with a selectivity to propene of 61% ^[58]. Bulk and supported magnesium molybdates have also displayed promising results. Cadus and co-workers ^[59] reported an $\text{MgMoO}_4\text{-MoO}_3$ catalyst, which displayed high catalytic performance in the ODH of propane to propene. The maximum selectivity observed was 91% at 10% conversion at 550°C. The activity was attributed to a synergistic cooperation between the two phases in the $\text{MgMoO}_4\text{-MoO}_3$ mechanical mixture. Bulk MoO_3 shows little activity for propane oxidation but when used in conjunction with MgMoO_x there is an overall increase in the conversion and selectivity ^[58-59]. The activity was found to be strongly dependent on the acidity of the catalyst. Further studies indicated that excess MoO_3 in the MgMoO_x system plays an important part in the ODH reaction with surface MoO_x clusters contributing to the overall activity ^[60].

The selectivity to propene over certain MgO-MoO₃ systems is influenced by the presence of promoters. The addition of K and Sm to a MgO/ γ -Al₂O₃-supported molybdenum catalyst resulted in an increase in selectivity but a decrease in conversion^[61]. Addition of Cs, K and Li to a MoO_x/ZrO₂ catalyst resulted in a similar decrease in activity with subsequent increase in selectivity^[62]. The increased propene selectivity of ODH catalysts with alkaline addition is well known, with the effect being attributed to modification of the acid sites responsible for activity. Similar results were found over alkali modified VO_x/TiO₂ for the ODH of propane to propene^[63].

A number of studies have focused on supported molybdenum catalysts with a lot of attention paid to the effect of various supports on catalytic activity. Desikan and co-workers^[64] investigated propene oxidation over MoO₃ supported on SiO₂, Al₂O₃ and TiO₂. The oxidation products formed were found to be dependant upon the support used (acetone on MoO₃/TiO₂, acrolein on MoO₃/SiO₂ and acetaldehyde on MoO₃/Al₂O₃). The activity for propene oxidation increased in the order SiO₂< Al₂O₃<TiO₂ and was found to correlate with the interaction of MoO₃ with the support.

Other groups found similar results for the ODH of propane to propene^[65]. Propane conversion was tested over MoO₃ supported on Nb₂O₅, TiO₂, Al₂O₃, SiO₂, MgO and ZrO₂. Of these, the MoO₃/TiO₂ catalyst was the most selective at iso-conversion with a propene selectivity of 77% at 5% conversion. The rate of the reaction over the MoO₃/TiO₂ catalyst was increased by the addition of vanadia and niobia promoters which gave a catalyst with activity similar to that of NiMoO₃; one of the better catalysts reported for the reaction^[66]. An extensive study conducted by Grasselli *et al*^[67-69] showed how silica-supported Ni_{0.5}Co_{0.5}MoO₄ was capable of 67% selectivity to propene at 20% propane conversion. The maximum propene yield was found to be 16% at 34% conversion.

Molybdena-manganese catalysts have been shown to be highly effective for propane ODH, especially at low temperatures ^[70-71]. A Mo-Mn-O system prepared from dry impregnation of Mo on Mn₂O₃ was active at temperatures as low as 350°C. The propene yield was 1.5% with a selectivity to propene of 76%; the only other product was CO₂. This temperature was reported to be 100°C lower than other more commonly tested catalysts. It is interesting to note that Mn₂O₃ and CuMn₂O₄ are proven catalysts for combustion of CO and small chain olefins ^[72-73]. Mn₃O₄ has also been shown to activate propane and propene at temperatures as low as 100°C ^[74]. Combination of the highly active Mn₂O₃ with the relatively stable MoO₃ led to a selective catalyst that was active at a lower than average temperature.

1.6.3 Gallium based catalysts

Catalysts based on gallium oxide have been proven for a number of catalytic reactions. These include gallia exchanged or impregnated ZSM-5, gallium in mordenite or ferrierite, gallium with sulfated zirconia or sulfated ZSM-5, and combinations of gallium with zirconium on sulfated and unsulfated ZSM-5 which are all active for the reduction of NO_x by methane and hydrocarbons ^[75]. Recently Choudry *et al* showed that MCM-41 supported Ga₂O₃ was active for Friedel-Craft benzene benzylation and acylation of aromatic compounds ^[76].

One of its most important applications is in the Cyclar process where a Ga-ZSM-5 catalyst is used for the aromatization of propane and butane. Early work by Chen and Cattanch showed ZSM-5 was an effective catalyst for the conversion of alkanes to

aromatics ^[77-79]. Subsequent research and improvements led to the development of the Cyclar process ^[80] using gallium modified ZSM-5 ^[81-82]. The reaction is generally recognised to involve the synergistic interaction between the zeolite and the active gallium species. It is believed that the reaction follows a bi-functional process whereby the gallium catalyzes the dehydrogenation reaction and the zeolite acid sites facilitate the oligomerisation and cyclization of the propene ^[81].

Since its initial beginning continuing efforts have been made to improve the activity of the catalyst and also to probe the nature of the active sites. Buckles and Hutchings ^[83-84] tested the effect of co-feeding NO, O₂ and H₂ on the activity of Ga-ZSM-5 for the activation and conversion of propane and found that the addition of NO resulted in a decrease in overall conversion and methane yield, the propene yield however, remained constant. The addition of H₂ to the system was also found to decrease the activity and aromatic yield. Interesting results were found when the Ga₂O₃ was kept separate from the zeolite or was combined as a mechanical mixture. By having Ga₂O₃ separate from the ZSM-5 a propane conversion of around 34% was achieved with a selectivity to propene of 9%. Again the temperature of the reaction was high at 550-600°C. Pre-treatment of the catalyst with H₂ resulted in a decrease in both conversion and selectivity for catalysts with higher concentrations of Ga₂O₃. Combination of the Ga₂O₃ and ZSM-5 in a physical mixture gave promising results for the conversion of propane to propene. Increasing the concentration of Ga₂O₃ within the mixture resulted in an increase in propane conversion and propene selectivity. Methane, ethane and aromatic selectivity decreased. The addition of H₂ to the reaction mixture increased the activity of the physically mixed catalyst relative to having N₂ in the feed. A 100% Ga₂O₃ catalyst at 600°C with H₂ in the feed achieved 21.8% conversion with a propene selectivity of 71.9%. With N₂ in the reaction mixture the conversion decreases to 8.8% with a selectivity to propene of 74%. The

authors attribute the higher activity of the physical mixture to contact synergy within the Ga₂O₃/ZSM-5 system. They suggest that the propane molecule is activated at the interface between the Ga₂O₃ and the zeolite. In related studies on the conversion of methane to methanol, deuterium exchange experiments showed how at 500°C the rate of CH₄/D₂ exchange was greatest over Ga₂O₃ (4.71×10^{19} molecules s⁻¹) [85-86]. This would support the theory that the key role of Ga₂O₃ in these catalysts is to aid C-H bond activation via heterolytic cleavage caused by bond polarisation induced by the Ga₂O₃.

Gallium oxide based catalysts have also been considered for the conversion of propane to propene via alkane dehydrogenation, typically in the presence of CO₂ [87-88]. Work by Michorczyk *et al* showed how both propane conversion and propene selectivity could be increased by the use of CO₂ as a mild oxidant. The temperature of the reaction was very high in comparison to those typical for oxidative dehydrogenation using O₂ but the results are quite interesting. At 600°C the propane conversion and propene selectivity over bulk Ga₂O₃ was 33 and 93% respectively [87]. The use of CO₂ in this process allows the reaction to be run at relatively low temperatures with a high selectivity to C₃H₆. Yue *et al* studied the same reaction and found that due to its stability, the promotional effect of CO₂ was only evident above 550°C [89]. However, at 500°C the selectivity to propene over β-Ga₂O₃ was >95% with a propane conversion of 25%, this is better than the chromium oxide catalyst typically used in this reaction.

Gallium promoted zeolites have also been tested for the oxidative dehydrogenation of propane. The rate of propane conversion over a faujasite catalyst was found to significantly increase with the addition of a few gallium ions, lowering the temperature of activity compared to the bare zeolite [90-91]. Very few studies have focused purely on bulk Ga₂O₃ for the ODH of propane with the majority focused in mixed metal oxides incorporated with gallium. Pérez Pujol *et al* found interesting results in studying V-Ga-O

catalysts ^[92]. The catalysts tested were active at very low temperatures, showing 5% conversion at 350°C. The main reaction products were propene CO and CO₂ with no partial oxidation products. Although the pure Ga₂O₃ show some activity, it was not as active as the vanadia-impregnated sample, the activity of which increased with increasing vanadia loading. The selectivity to propene was in range of 60-80% and increased with decreasing O₂ feed concentration. The V-Ga-O catalyst showed the highest activity at the lowest temperature out of all of the catalyst with the best reported results of 3.3% propane conversion at 300°C, with a selectivity to propene of 70%. The performance of the catalyst is comparable to that of the best V-Mg-O catalyst.

1.6.4 Cobalt oxide based catalysts

Cobalt oxides have a wide range of industrial applications and are used in rechargeable batteries, CO sensors and magnetic materials ^[93-96]. Cobalt oxide catalysts are of great interest due to their high activity in hydrocarbon oxidation ^[97-98] and CO oxidation ^[99-102]. There has been little research into bulk or supported cobalt oxide catalysts for the oxidative dehydrogenation of propane. The few catalysts that have been studied usually contain cobalt as a promoter within an established catalytic system. CoMoO₃ catalysts are particularly good at converting propane and outperform other metal molybdates ^[103-104] with addition of Co to bulk MoO₃ found to increase both activity and selectivity ^[105] and its addition to V-Mg-O systems has been found to increase propane conversion ^[106]. Cobalt impregnated MCM-41 catalysts are also active and selective in the ODH of

propene but with a lower than average conversion and selectivity ^[107]. One of the most interesting aspects of Co_3O_4 is its activity at low temperatures. In the oxidation of CO , Co_3O_4 is found to be active at temperatures as low as -63°C ^[108]. Cunningham *et al* found a light-off temperature of -54°C ^[109]. Such high activity at low temperatures has been linked to the interaction of Co_3O_4 with oxygen in the gas phase. Studies have shown Co_3O_4 to have the highest rate of oxygen exchange with the gas phase, giving rise to high concentrations of chemisorbed and physisorbed electrophilic (O_2^- , O^- and O_2^{2-}) and nucleophilic (O^{2-}) oxygen species on the surface ^[7,18]. Haber and Turek proposed that propene was activated on the surface by electrophilic oxygen species giving rise to surface oxygenates which break down to CO_2 and H_2O (figure 1.5)

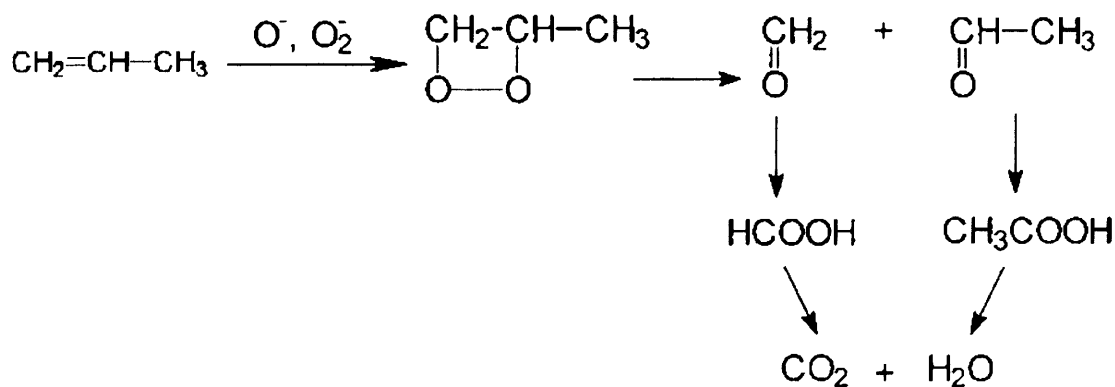


Figure 1.5. Proposed mechanism for propene oxidation on the surface of Co_3O_4 ^[110]

There is no evidence in the literature of cobalt oxide being capable of propane conversion to propene at these low temperatures. However work by Finocchio *et al* attempted to determine the reaction mechanism for propane activation by FTIR. It was found that

Co_3O_4 was more active than other oxides tested, giving rise to substantial conversion of propane at ca. 250°C [111] although the primary product was CO_2 . Its activity in the total oxidation of propene was similar to that of propane. The FTIR studies by this group go some way to suggesting a simple mechanism. It states: "On Co_3O_4 we found that propene is oxidised at the allylic position giving rise to acrylate species already at room temperature". Also: "Propane is also activated at very low temperatures, at C (1) and at C (2). Activation at C (2) gives rise to acetates" [111]. Although they present these results no mention is made of low temperature reaction studies on Co_3O_4 that give rise to propene in the gas phase, they merely state the presence of such species on the surface. Nevertheless, if bulk Co_3O_4 is capable of activating propane at such low temperature it may be a good catalyst for the oxidative dehydrogenation of propane providing the reaction conditions are carefully controlled. As mentioned previously Co_3O_4 is an excellent catalyst for the total combustion of organic molecules but as long as desorption of the propene molecule occurs before total oxidation Co_3O_4 could be a good catalyst for the low temperature ODH of propane.

1.5 Isopropanol production

Iso-propanol is classed by the US Environmental Protection Agency and the Organisation for Economic Cooperation and Development as a high production volume chemical, with a production at least 1 million tonnes per annum worldwide. Chemical grade iso-propanol is used as an intermediate for the manufacturing of acetone, ethers, alkylchlorides and amines. Industrial uses are numerous, for example iso-propanol is used in the manufacture of pharmaceuticals, paints, semiconductors, rubber, and has many

applications in industries such as electroplating and printing. Iso-propanol is currently produced by industrial hydration processes using concentrated sulphuric acid, supported phosphoric acid catalysts or acidic cation exchange resins. In the conventional process, used since 1930, aqueous sulphuric acid is used as the catalyst. Alkyl sulphates are formed initially and then hydrolysed by the addition of water to form the alcohol product. The use of such strong acid catalysts can be problematic however, causing corrosion to reactors and pollution ^[8,112]. It is also necessary to re-concentrate the used acid. Figure 1.6 shows a simplified version of the homogeneous reaction mechanism. The addition of water to the alkene obeys Markovnikov's rule resulting in the secondary alcohol iso-propanol. Oligomerisation of the alkene as well as dehydration and dehydrogenation of the alcohol can give rise to various by-products such as ketones, aldehydes and alkene oligomers

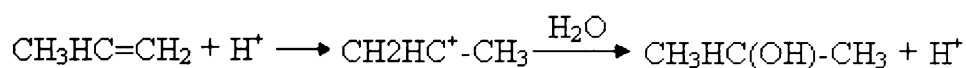


Figure 1.6 Homogeneous acid catalysed hydration of propene

There are also a number of heterogeneous processes in operation using solid acid catalysts. In the ICI process $\text{WO}_3/\text{SiO}_2 + \text{ZnO}$ is used as catalyst at 270°C and 250 atm. and in the Huls process a $\text{H}_3\text{PO}_4/\text{SiO}_2$ catalyst is used at 190°C and 25-45 atm., in the latter process a selectivity of 95% is achieved at ca. 6% conversion^[112]. Again it is often necessary to re-concentrate the acid catalyst, which can be unstable and degrade over time. Figure 1.7 shows a proposed mechanism for the heterogeneous conversion of propene to isopropanol.

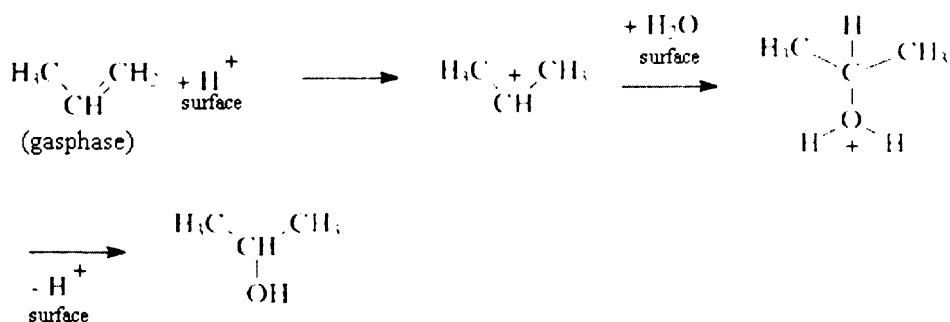


Figure 1.7 Proposed mechanism for heterogeneous propene hydration over acid catalyst ^[113]

Because of the inherent problems of existing processes there has been a continuing effort to find more suitable catalysts. One of the most recent developments has been in Japan with the introduction of a large scale commercial process using aqueous solutions of heteropolyacids. In the Tukuyama process alkene conversions of 60-70% are achieved with a alcohol selectivity of 99%. The temperature of the reaction is quite high at around 240-280°C ^[114].

To date there has been little or no research into a process for the direct conversion of propane to iso-propanol and given the large worldwide resources of propane such a process has many advantages. Two possible routes have been proposed in the literature which include a method whereby the two reactions works in series: the propene is first formed via dehydrogenation before being passed to a second reactor where hydration to iso-propanol takes place ^[115]. The second method promotes the use of enzyme mimicking catalysts such as metaloporphyrins and phthalocyanin complexes, the results are promising but far from commercialisation.^[116] Heterogeneous processes using bi-functional catalysts have received no attention of late but it is envisaged that such a catalyst could be fine-tuned to give the desired results.

1.7 References

- [1] S.J. Thomson and G. Webb, *Heterogeneous Catalysis*. University Chemical text 1968
- [2] G.C Bond, *Heterogeneous Catalysis*. 2nd edition. Oxford university press 1987
- [3] G.C Bond, *Principles of Catalysis*. Monographs for teachers. The Royal Institute of Chemistry. 1963
- [4] C.G. Silcocks, *Physical Chemistry*, Second Edition. Macdonald and Evans LTD. 1972
- [5] *Propene chronic toxicity summary*. (www.oehha.ca.gov.) Cas. Reg.115-07-1
- [6] *Basic Principles of Applied Catalysis*. M. Baerns(Ed.), Springer-Verlag Berlin Heidelberg New York 2004
- [7] T. Ren, M. Patel and K. Blok, *Energy* 31 (2006) 425-451
- [8] *An Introduction to Industrial Chemistry*. A. Heaton (Ed.). Blackie Academic and Professional. Third edition. 1996
- [9] *Catalyst Handbook*. M.V. Twigg (Ed.). Manson Publishing Ltd. Second Edition 1996
- [10] M. M Bhasin, J. H. McCain, B. V. Vora, T. Imai, P. R. Pujadó, *Appl. Catal. A. Gen.*, 221 (2001) 397–419.
- [11] S. Airaksinen, *Industrial Chemistry Publication series*. (<http://lib.tkk.fi/Diss>) 2005
- [12] M. Bowker, *The Basis and Applications of Heterogeneous Catalysis*. Oxford University Press. 1998.
- [13] D. Creaser and B. Andersson, *Appl. Catal. A. Gen.*, 141 (1996) 131
- [14] J. N. Michaels, D. L. Stern and R K. Grasselli, *Catal. Lett.*, 1996, 42: 139
- [15] D. Patel, P.J. Andersen and H.H. Kung, *J. Catal.*, 125 (1990) 132.

- [16] P. Mars and D.W van Krevelen, *Chem. Eng. Sci.*, 3 (1954) 41
- [17] C.A. Cooper, C.R Hammond, G.J Hutchings, S.H. Taylor, D.J. Willock and K. Tabata, *Cat. Today* 71 (2001) 3-10
- [18] G.C. Bond, K. Bruckman, *Faraday Disc. Chem. Soc.*, 72 (1981) 235
- [19] G.C. Bond and S.F. Tahir, *Appl. Catal. A. Gen.* 71 (1991) 1
- [20] P. J. Pomonis and J. C. Vickerman, *Faraday Disc. Chem. Soc.*, 72 (1981) 247
- [21] M.S. Wainwright and N.F Foser, *Catal. Rev. Sci. Eng.*, 19 (1979) 211
- [22] D.B Dadyburjor, S.S. Jewur and E. Ruckenstein, *Catal. Rev. Sci. Eng.*, 19 (1979) 293
- [23] E.A Mamedov and V. Cortes Corberan, *Appl. Catal. A. Gen.*, 127 (1995) 1-40
- [24] T. Blasco and J.M. Lopez Nieto, *Appl. Catal. A. Gen.*, 157 (1997) 117-142
- [25] H.H. Kung and M.C. Kung, *Appl. Catal. A. Gen.*, 157 (1997) 105-116
- [26] M. A. Chaar, D. Patel, H.H. Kung, *J. Catal.*, 109 (1988) 463-467
- [27] D. Siew Hew Sam, V. Soenen and J.C Volta, *J. Catal.*, 123 (1990) 417-435
- [28] P.M. Michalakos, M. C. Kung, I. Jahan and H.H. Kung, *J. Catal.*, 140 (1993) 226-242
- [29] X. Gao, P. Ruiz, Q. Xin, X. Guo and B. Delmon, *J. Catal.*, 148 (1994) 56-67
- [30] A. Corma, J.M. Lopez Nieto and N. Paredes, *J. Catal.*, 144 (1993) 425-438
- [31] Z. Chau and E. Ruckenstein, *Catal. Lett.*, 94 (204) Nos. 3-4
- [32] M. A. Chaar, D. Patel, H.H. Kung and M.C. Kung., *J. Catal.*, 105 (1987) 483
- [33] O. S. Owen, M.C Kung and H.H. Kung, *Catal. Lett.*, 12 (1992) 45
- [34] A. Corma, J.M. López Nieto, N. Paredes and M. Pérez, *Appl. Catal.* 97 (1993) 159
- [35] D. Patel, P.J. Andersen and H.H.Kung, *J. Catal.* 125 (1990) 132
- [36] L. Balderas-Tapia, I. Hernández-Pérez, P. Schacht, I.R. Córdova, G.G. Aguilar-

- Ríos, *Catal. Today*, 107-108 (2005) 371-376
- [37] S.T.Oyama, *J. Catal.*, 128 (210) 1991
- [38] L.Owens and H.H.Kung, *J. Catal.*, 144 (1993) 202
- [39] J.Le Bars, J.C. Vedrine, A. Auroux, S. Trautmann and M. Baerns, *Appl. Catal. A. Gen.*, 88 (1992) 179
- [40] A. Parmaliana, V. Sokolovskii, D. Miceli and N. Giordano, *Appl. Catal. A. Gen.*, 135 (1996) L1
- [41] J. Santamaría-González, J. Luque-Zambrana, J. Mérida-Robles, P. Maireles-Torres, E. Rodríguez-Castellón and A. Jiménez-López, *Catal. Lett.*, 68 (2000) 67-73
- [42] B. Solsona, A. Dejoz, M.I. Vázquez, F. Márquez and J.M. López Nieto, *Appl. Catal. A. Gen.*, 208 (2001) 99-110
- [43] A.A. Lemonidou, L. Nalbandian and I.A. Vasalos, *Catal. Today*, 61 (2000) 333-341
- [44] R. Monaci, E. Rombia, V. Solinas, A. Sorrentino, E. Santacesaria, G. Colon, *Appl. Catal. A. Gen.*, 214 (2001) 203-212
- [45] A. Klisin'ska, K. Samson, I. Gressel, B. Grzybowska, *Appl. Catal. A. Gen.*, 309 (2006) 10-15
- [46] Arthur R.J.M. Mattos, Rosane Aguiar da Silva San Gil, Maria Luiza M. Rocco, Jean-Guillaume Eon, *J. Mol. Catal. A. Chem.*, 178 (2002) 229-237
- [47] M. Machli, E. Heracleous, A. A. Lemonidou, *Appl. Catal. A. Gen.*, 236 (2002) 23-24
- [48] G. Centi, F. Triferó, J. R. Ebner and V.M Franchetti, *Chem. Rev.*, 88 (1988) 55
- [49] P.M. Michalakos, M.c. Kung, I. Jahan and H.H. Kung, *J. Catal.*, 140 (1993) 226

- [50] G. Centi and F. Triferó, *Catal. Today*, 3 (1988) 151
- [51] G. Centi, T. Tosarelli and F. Triferó, *J. Catal.*, 142 (1993) 70
- [52] P. Concepción, J.M. Lopez Nieto and J. Perez Pariente, *Catal. Lett.*, 19 (1993) 333
- [53] S. Williams, M. Puri, A.J. Jacobson, C.A. Mims, *Catal. Today*, 37 (1997) 43-49
- [54] H.F. Hardman, U.S patent 4131631 19781226 (1978)
- [55] Y.-S. Yoon, N. Fujikawa, W. Ueda, Y. Moro-oka, K-W. Lee, *Catal. Today*, 24 (1995) 327-333
- [56] Y.-S. Yoon, N. Fujikawa, W. Ueda, Y. Moro-oka, *Chem. Lett.*, (9) (1994) 1635-6
- [57] M. A. Char, D. Patel, H.H. Kung, *J. Catal.*, 109 (1988) 463-467
- [58] Y. -S. Yoon, W. Ueda and Y. Moro-oka, *Catal. Lett.*, 35 (1995) 57-64
- [59] L.E. Cadus, M.F Gomez and M.C Abello, *Catal. Lett.*, 43 (1997) 229-223
- [60] K.H. Lee, Y.-S. Yoon, W. Ueda and Y. Moro-oka, *Catal. Today*, 44 (1998) 199-203
- [61] M.C. Abello, M.F. Gomez and L.E. Cadus, *Catal. Lett.*, 53 (1998) 185-192
- [62] K. Chen, S. Xie, A. T. Bell and E. Iglesia, *J. Catal.*, 195 244-252 (2000)
- [63] A.A. Lemonidou, L. Nalbandian, I.A Vasalos, *Catal. Today*, 61 (2000) 333-341
- [64] A.N. Desikan, W. Zhang and S.T. Oyama, *J. Catal.*, 157 (1995) 740-748
- [65] F.C. Meunier, A. Yasmeen and J.R.H Ross, *Catal. Today*, 37 (1997) 33-42
- [66] C. Mazzocchia, C. Aboumrad, C. Daigne, E. Tempesti, J.M. Herrmann and G. Thomas, *Catal. Lett.*, 10 (1991) 181.
- [67] J.N. Michaels, D.L. Stern and R.K. Grasselli, *Catal. Lett.*, 42 (1996) 135 and 139
- [68] D.L. Stern, J.N. Michaels, L. DeCaul and R.K. Grasselli, *Appl. Catal. A. Gen.*,

153 (1997) 21

- [69] D.L. Stern and R.K. Grasselli, *Stud. Surf. Sci. Catal.*, 110 (1997) 357.
- [70] L. E. Cadus and O. Ferretti, *Catal. Lett.*, 69 (2000) 199-202
- [71] L. E. Cadus and O. Ferretti, *Appl. Catal. A. Gen.*, 233 (2002) 239-253
- [72] P.-O. Larsson and A. Andersson, *Appl. Catal. B. Env.*, 24, Iss. 3-4, (2000) 175-192
- [73] G. Busca, M. Baldi, V.S. Escribano, J.M.G Amores and F. Milella, *Appl. Catal. B. Env.*, 17 (1998) L175-L182
- [74] G. Busca, E. Finocchio, V. Lorenzelli, G. Ramis and M. Baldi, *Catal. Today*, 49 (1999) 453-465
- [75] J.N. Armor, *Catal. Today*, 31 (1996) 191-198
- [76] V. Choudhary, S.K. Jana and B.P. Kiran, *J. Catal.*, 192 (2000) 257
- [77] N.Y. Chen, *Australian Patent* 465697 (1973)
- [78] J. Cattanach, *Australian Patent* 484975 (1974)
- [79] J. Cattanach, *Australian Patent* 484974 (1974)
- [80] T.K. McNiff, *U.S. Patent* 462403 (1987)
- [81] D. Sedden, *Catal. Today* 6 (1990) 351
- [82] M. Guisnet, N.S. Gnep and F. Alerio, *Appl. Catal.*, 89 (1992) 1
- [83] G.J. Buckles and G.J Hutchings, *J. Catal.*, 151 (1995) 33-43
- [84] G.J. Buckles and G.J Hutchings, *Catal. Today.*, 31 (1996) 233-246
- [85] J. S. J. Hargreaves, G. J. Hutchings, R. W. Joyner, S. H. Taylor, *Appl. Catal. A. Gen.*, 227(1-2), (2002) 191-200.
- [86] S.H. Taylor, *Ph.D. Thesis, University of Liverpool*, 1994.
- [87] P. Michorczyk and J. Ogonowski, *Appl. Catal. A. Gen.*, 251 (2003) 425-433
- [88] B. Xu, B. Zheng, W. Hua, Y. Yue and Z. Gao, *J. Catal.*, 239 (2006) 470-477

- [89] B. Zheng, W. Hua, Y. Yue and Z. Gao, *J. Catal.*, 232 (2005) 143-151
- [90] B. Sulikowski, Z. Olejniczak and V. Cortes Corberan, *J. Phys. Chem.*, 100 (1996) 10323-10330
- [91] B. Sulikowski, V. Cortes Corberan, R.X. Valenzuela, M. Derewinski, Z. Olejniczak and J. Krysiak, *Catal. Today*, 32 (1996) 193-204
- [92] V. Cortes Corberan, R.X. Valenzuela, Z. Olejniczak, B. Sulikowski, A. Perez Pujol, A. Fuerte and E. Wloch, *Catal. Today*, 78 (2003) 247-256
- [93] E. Antolini and E. Zhecheva, *Mater. Lett.*, 35 (1998) 380
- [94] S.-D. Choi, B.-K. Min, *Sens. Actuators, B.*, 77 (2001) 330
- [95] H. Yamaura, K. Moriya, N. Miura and N. Yamazoe, *J. Electrochem. Soc.*, 144 (1997) 158
- [96] S.A Makhlof, *J. Magn. Mater.*, 246 (2002) 184
- [97] E. Garbowski, M. Guenin, M.C. Marion and M. Primet, *Appl. Catal.*, 64 (1990) 209
- [98] G. Busca, M. Daturi, E. Finocchio, V. Lorrenzelli, G. Ramis and R.J. Willey, *Catal. Today*, 33 (1997) 239-249
- [99] J. Jansson, A.E.C Palmqvist, E. Fridell, M. Skoglundh, L. Osterlund, P. Thormählen and V. Langer, *J. Catal.*, 211 (2002) 387-397
- [100] Y.-F. Yu Yao, *J. Catal.*, 33 (1974) 108
- [101] K. Omata, T. Takada, S. Kasahara and M. Yamada, *Appl. Catal. A. Gen.*, 146 (1996) 255-267
- [102] J. Jansson, *J. Catal.*, 194 (1) (2000) 55-60
- [103] Y.-S. Yoon, N. Fujikawa, W. Ueda, Y. Moro-oka, K.-W. Lee, *Catal. Today*, 24 (1995) 327-333
- [104] Y.-S. Yoon, N. Fujikawa, W. Ueda, Y. Moro-oka, *Chem. Lett.*, (9)(1994) 1635-6

- [105] L. A. Palacio, A. Echavarría, L. Sierra and E. A. Lombardo, *Catal. Today*, 107-108, (2005) 338-345
- [106] W. Oganowski, J. Hanuza, H. Drulis, W. Mišta and L. Macalik, *Appl. Catal. A. Gen.*, 136 (1996) 143-159
- [107] B. Jibril and S. Ahmed, *Cat. Comm. In press. Available 2006*
- [108] P. Thormählen, M. Skoglundh E. Fridell and B. Andersson, *J. Catal.*, 188 (1999) 300
- [109] D.A.H. Cunningham, T. Kobayashi, N. Kamijo and M. Haruta. *Catal. Lett.*, 25 (1994) 257
- [110] J. Haber and W. Turek., *J. Catal.*, 190 (2000) 320-326
- [111] E. Finocchio, R.J Willey, G. Busca and V. Lorenzelli, *J. Chem. Soc.*, 93 (1997) (1), 175-180
- [112] M.M. Bhasin, J.H. McCain, B.V. Vora, T. Imai and P.R. Pujadó, *Appl. Catal. A. Gen.*, 221 (2001) 397
- [113] N. Essayem, Y. B. Taârit, E. Zausa and A.V. Ivonov, *Appl. Catal. A. Gen.*, 256 (2003) 225-242
- [114] Y. Izumi, *Catal. Today*, 33 (1997) 371-409
- [115] US Patent, 5 198580
- [116] R. Raja, C. R. Jacob, P. Ratnasamy, *Catal. Today*, 49 (1999) 171-175

Chapter 2

Chapter 2

Experimental

2.1 Catalyst Preparation

2.1.1 Ga₂O₃/MoO₃ mixed oxide catalyst

The mixed oxide catalyst Ga₂O₃/MoO₃ was prepared by physical mixing. The catalyst was prepared by grinding the two components, Ga₂O₃ (Aldrich 99.9%) and MoO₃ (Aldrich 99.9%), in a pestle and mortar in a 1:1 molar ratio. The catalyst was ground for a minimum of 10 minutes to ensure good mixing. The mixed oxide was calcined at 650°C for 3 hours in static air. The sample was allowed to cool to below 100°C before being removed from the tube furnace and ground in the pestle and mortar for a further 10 minutes. A second uncalcined sample was also prepared. For certain experiments the molar ratios were varied as well as the calcination time and temperature. All samples were pelleted between 250-600µm. The sample was compressed in a 12mm die at a pressure of 10,000 Kg and then broken down through a sieve with grinding to give pellets between 250-600µm.

2.1.2 Precipitated GaOOH precursor

Gallium hydrate was prepared by precipitation from the nitrate (Aldrich 99.9%) with aqueous ammonia solution. Gallium nitrate (2.6g) was dissolved in distilled water (50ml) and the solution stirred for 30 minutes. Aqueous ammonia (50%) was then added until pH 9.0 was attained. The resulting white precipitate was stirred for a further 30 min. before being filtered and dried for 16h at 40°C.

2.1.3 Precipitated Co₃O₄ catalyst

Co₃O₄ was prepared by precipitation of the oxide from the nitrate. Typically, 40g of cobalt nitrate (Co(NO₃)₂ · 6H₂O; Aldrich 99.9+%) was added to distilled H₂O (800ml) with vigorous stirring. The solution was heated to 80°C before the dropwise addition of 35% (aq) NH₄(OH). The ammonia was added at a rate of approximately 2ml min⁻¹ until pH 8.5. Beyond this the rate of addition was halved until pH 9.0 was attained. The purple precipitate was aged between 0-5 h at 80°C with continuous stirring, before being filtered and washed with hot distilled water (1000ml).

The precursor was dried in an oven at 120°C for 16 hours before being calcined in static air. The calcination temperatures were 250°C, 400°C and 550°C. Each precursor was calcined for a period of 2h.

For comparison, a commercial Co₃O₄ sample (Avacado 99.9%) was obtained and used as received from the suppliers.

2.1.4 Nano-crystalline Co₃O₄

Nano-crystalline Co₃O₄ was prepared by solid-state reaction according to methods described elsewhere^[1]. The starting materials used were Co(NO₃)₂ · 6H₂O (Aldrich) and NH₄HCO₃ (Aldrich). 5g of the starting materials were mixed in a pestle and mortar with Co(NO₃)₂ · 6H₂O: to NH₄HCO₃ molar ratio of 2:5. The starting materials were ground for 0.5h before being thoroughly washed with distilled water and filtered by suction. The reaction proceeded according to the equation:



The reaction was very fast with the reaction mixture turning a deep purple. The smell of ammonia gas was also noticeable. The catalyst precursor was then dried for 16h at 100°C before calcination at 300°C for 2h in static air. Samples were also calcined at 200°C, 400°C and 600°C to investigate the effect of calcination temperature on surface area and activity.

2.1.5 Higher cobalt oxide

The higher cobalt oxide system was prepared using the precipitation-oxidation process described elsewhere ^[2]. A cobalt nitrate solution (0.4M) was added to a mixture of aqueous solutions of NaOH (4 M) and NaOCl (1 M). NaOH was used as a precipitating agent to instead of NH₄OH in order to avoid the formation of water-soluble Co(II) ammonia complexes. Precipitation was carried out using NaOH at 70°C with constant stirring. The solution was maintained at pH-9.0. The resulting black precipitate was aged for 1h before being filtered and washed with plenty of hot distilled water to remove Cl⁻ and NO³⁻. The precursor was then dried at 90°C for 6h.

2.1.6 Silica supported H₃PO₄

The silica supported phosphorous catalysts were prepared by insipient wetness impregnation. An appropriate amount (70wt%) of phosphoric acid (Aldrich 99.9%) was dissolved in distilled water before addition to the fumed silica (Aldrich 99.8%). The resultant slurry was stirred thoroughly before being allowed to dry in an oven at 110°C for 16 h.

2.1.7 Acid hydration catalysts

The bulk acid catalysts were used as supplied from Aldrich. They included tungstophosphoric acid (HPW) (Aldrich 99.995+%), phosphomolybdic acid (Aldrich 99.99+%), tungstosililic acid (Aldrich 99.9+%) and zeolite ZSM-5 (Zeolyst).

2.1.8 Dehydrogenation/hydration catalyst

Catalysts were prepared by direct mechanical mixing of nano-crystalline Co_3O_4 and phosphomolybdic acid in a 1:1 ratio by mass, or by direct impregnation of the cobalt oxide catalyst with an aqueous solution containing (70wt%) phosphoric acid.

2.2 Reactor Design

2.2.1 Oxidative Dehydrogenation Reactor

The reactor consisted of an 8 ml i.d quartz tubular reactor running at atmospheric pressure. Studies were performed using propane (BOC 99.99%) with oxygen (BOC 99.5%) as the oxidant and helium (BOC 99.5%) as balance. The flow rates were controlled by MKS digital flow meters. Calibration data for the MFC's can be found in the appendices. The catalyst was secured in the quartz tube between silica wool plugs. The catalysts bed was heated with a Carbolite furnace with the catalyst sitting in the hottest part of the catalyst hot zone. The temperature of the reaction was monitored using a thermocouple placed directly above the catalyst bed, in contact with the silica wool. Flow rates for all experiments were between 20-40 ml min^{-1} except where contact times were varied.

For hydration experiments water was introduced to the system using a 150cc stainless steel sample cylinder. The temperature of the water was controlled with heating tape attached by a Eurotherm temperature controller. The temperature was monitored with a thermocouple inside the sample cylinder (figure 2.1).

Online analysis was conducted using a Varian 3800 GC with Haysep Q and Molsieve 13X columns in a series/bypass configuration. Reaction products were detected using a thermal conductivity detector (TCD) and flame ionisation detector (FID).

2.2.2 Low Temperature Oxidative Dehydrogenation Reactor

The low temperature oxidative dehydration reactor (figure 2.2) consisted of a stainless steel reactor tube submersed in a temperature controlled water bath. The temperature of the catalyst bed was monitored with a thermocouple placed directly above the catalyst bed. The rest of the system was as described previously.

2.2.3 Ga₂O₃/MoO₃ reaction conditions

0.25g of catalyst was used, in each case the flow rate was 40 ml min⁻¹ (He/O₂/C₃H₈ = 85/5/10%). For certain experiments the bed composition was varied. Two tests were done using a Ga₂O₃/SiC/MoO₃ layered bed where the pure metal oxides were separated by a silicon carbide layer (0.1g). Experiments were done with Ga₂O₃ in both the upper and lower portion of the bed (figure 2.3). For comparison, the metal oxides were also tested on their own, the bed volume being maintained using inert silicon carbide. The data for silicon carbide blank reaction can be found in the appendices.

The effect of layering the catalysts in contact with no silicon carbide was also investigated; again experiments were done with Ga₂O₃ in both the upper and lower portion of the bed.

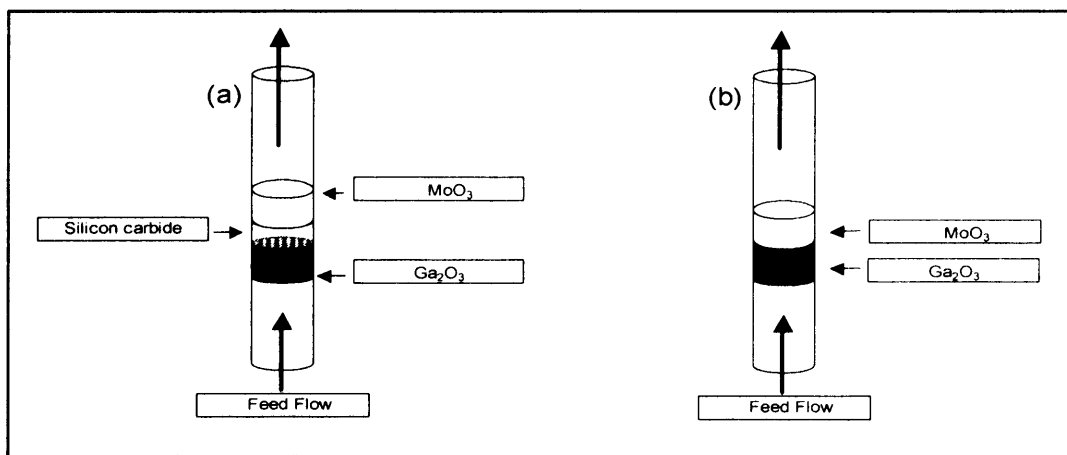


Figure 2.3 (a) Dual bed with silicon carbide separating layer (b) Dual bed with metal oxides in contact

2.2.4 Small bed Co_3O_4 reaction conditions

0.25g of catalyst was used, in each case the total flow rate was 20 ml min^{-1} (He/O_2 / $\text{C}_3\text{H}_8 = 80/19/1\%$) $\text{GHSV}=4800 \text{ h}^{-1}$. The temperature of the reaction was between 25-140°C. Contact times were changed by varying the flow rates of the gases, and in certain tests the O_2 concentrations were also varied. Steady state measurements were conducted at temperatures between 25-140°C with a constant flow rate. The catalyst was activated in the reactor prior to the reaction at 400°C for 2hrs in a $20 \text{ ml}/\text{min}^{-1}$ 10% O_2/He flow. Figure 2.1 shows the reactor arrangement.

2.2.5 Ambient temperature reaction conditions

Ambient temperature reactions were conducted in the water bath reactor (figure 2.2) using between 5-10g of catalyst. The catalyst was pelleted to uniform particle size (250-600 μm .). In each case the total flow rate was 20 ml min⁻¹ (He/O₂/C₃H₈ = 80/19/1%) GHSV=4800 h⁻¹. The temperature of the reaction was varied between 25-60°C.

2.2.6 Propene/propane hydration reaction conditions

0.25g of the phosphomolybdic-Co₃O₄ catalyst was used in each case. The reaction was performed at 70-150°C. The total flow rate was 40 ml min⁻¹ (He/O₂/Hydrocarbon = 80/19/1%). The concentration of water in the feed was varied between 2-35KPa. The catalyst was heated up to 70°C in a He/O₂ mix. Once the temperature had been allowed to stabilise propane and H₂O were introduced to the system. The sample cylinder was heated in 10°C steps and allowed to stabilise at each temperature for approx. 15-20

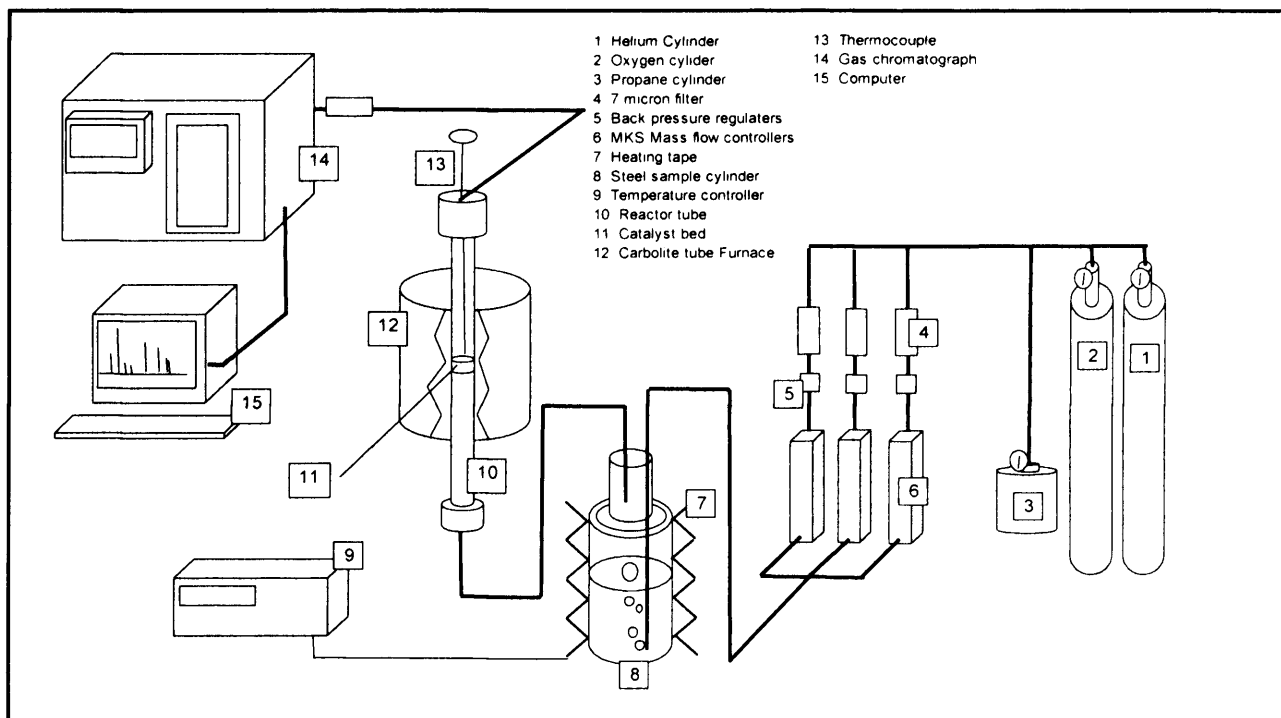


Figure 2.1 Oxidative dehydrogenation reactor and hydration reactor

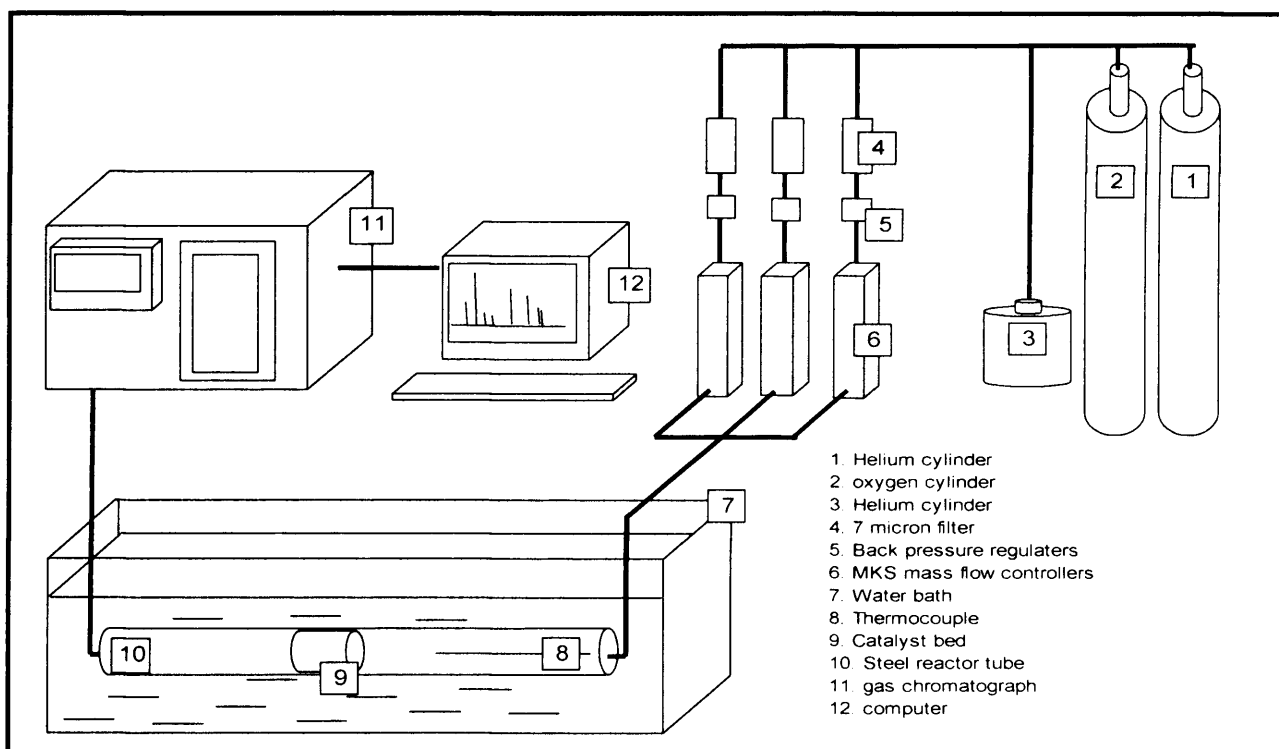


Figure 2.2 Low Temperature oxidative dehydrogenation reactor

minutes before sample injection. Three injections were done at each temperature and the average taken. CO₂, propene and iso-propanol were the primary products present with trace amounts of other oxygenates formed at higher temperatures.

2.2.7. Reduction of Co₃O₄

After activation (400°C, 2h, 10% O₂/He) the catalyst was reduced in a 10%H₂/He flow, 20 ml min⁻¹ at 80, 150 and 200°C for 2h.

2.2.8. Sample delivery

The sample delivery program was built in conjunction with the GC oven temperature program to get good separation of the reactants and products along with acceptable retention times. Samples were injected into the GC using a six-port valve (V1) heated to 200°C. Separation of the reactants and products was done on two columns fitted in series (figure 2.4) with the Molsieve in the second position.

The Molsieve could be bypassed at the second valve (V2) (figure 2.5). The Molsieve 13X was used to separate the N₂, O₂ and CO. The Haysep Q separated the hydrocarbons and CO₂. The bypass configuration meant that the CO₂ could be separated efficiently. CO₂ irreversibly adsorbs on the Molsieve and can deactivate the column.

2.2.9. Valve sequences and temperature programming

Valve 1 (V1) controls the flow through the HAYSEP Q column and valve 2 (V2) controls the flow through the MOLSIEVE column. The sequence of the valves can be programmed to perform different operations. The sequence of the valves can be seen in the following diagrams.

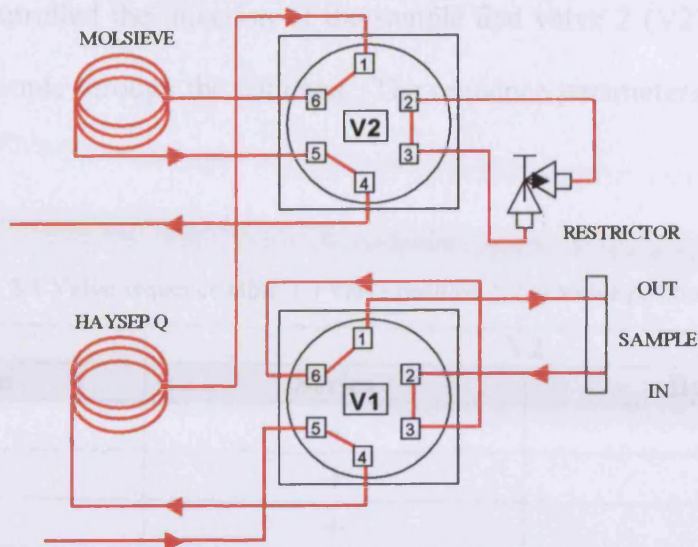


Figure 2.4 Valve position 1. Columns in series configuration.

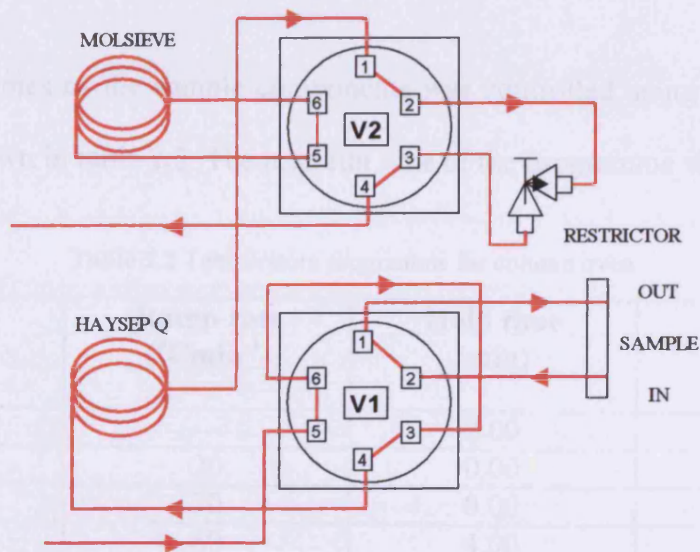


Figure 2.5 Valve position 2. Columns in bypass configuration.

2.2.9. Valve Sequence and temperature programme

Valve 1 (V1) controlled the injection of the sample and valve 2 (V2) controlled the passage of the sample through the columns. The sequence parameters can be seen in table 2.1.

Table 2.1 Valve sequence table. (-) Valve position 1. (+) Valve position 2

V1	V2	
	Series	Bypass
Injection		
Initial	-	-
0.01	+	-
0.8	+	+
2.20	+	-
3.50	+	+

The retention times of the sample components was controlled using the temperature programme shown in table 2.2. The total run time of the programme was 10 minutes.

Table 2.2 Temperature programme for column oven

Temperature (°C)	Ramp rate (°Cmin ⁻¹)	Hold time (min)	Total time (min)
100	---	2.00	2.0
140	20	0.00	4.0
180	30	0.00	5.3
220	60	4.00	10.00

2.2.9.1 Data handling

The GC was calibrated for analysis by injecting known amounts of reactants and products. The peak areas corresponded to a specific concentration determined by multiplying the raw counts by the response factor (RF). The response factor (RF) is the taken from the gradient of the calibration chart (see appendix).

Hydrocarbon conversions were calculated using the following method:

$$((\text{HC}_{\text{in}} - \text{HC}_{\text{out}}) / \text{HC}_{\text{in}}) \times 100\%$$

The HC_{in} value was obtained by taking the average initial counts at the beginning of a run prior to light-off. By subtracting the average concentrations of the HC over the temperature range studied the percentage conversion is calculated.

The selectivity to products was determined as follows:

$$(\text{Amount of product } X / \text{Total amount of products including } X) \times 100$$

The proportion of products determined percentage selectivity after correcting for the carbon number of the product. Carbon balances were in the range of 95-105%.

Each data point at a given temperature is the average of three injections. To determine the accuracy of the conversion measured the standard deviation of three runs for each catalyst was calculated, resulting in an average error of $\pm 4\%$. In the case where the conversion is below 1% the catalysts were repeatedly tested to ensure that the trends seen were real and reproducible. Rapid deactivation of certain catalysts meant that the timing of the injection was crucial for reproducible results and repeated calibration of both the GC and flow rates was necessary to ensure accuracy.

2.3. Characterisation

2.3.1 Powder X-ray Diffraction (XRD)

X-ray diffraction (XRD) is one of the oldest and most frequently used techniques for catalyst characterisation and it was the discovery of X-rays in 1895 that enabled scientists to probe crystalline structures at the atomic level. X-rays are electromagnetic radiation that occurs in the spectrum in the region between ultraviolet and gamma rays. They have wavelengths in the region of 10^{-10} m (1 Å), which is about the same size of an atom and the diffraction technique depends upon the constructive interference of radiation that is scattered by the larger parts of the sample. As a consequence, XRD techniques require long-range order. X-ray diffraction has two main uses: the fingerprint characterisation of crystalline materials, and the determination of their structure. Each crystalline solid has its unique characteristic X-ray powder pattern, which may be used as a "fingerprint" for its identification. Once the material has been identified, X-ray crystallography may be used to determine its structure, i.e. how the atoms pack together in the crystalline state and what the interatomic distance and angle are etc. X-rays scattered by atoms in an ordered lattice interfere constructively and destructively in directions given by Bragg's law^[3].

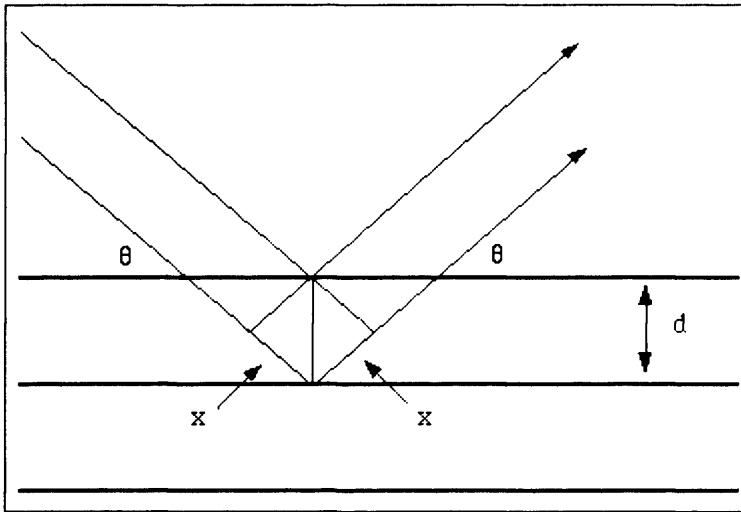


Figure 2.6 Reflection of x-rays from two planes of atoms in a solid

The path difference between two waves:

$$2x = 2d\sin(\theta)$$

For constructive interference between these waves, the path difference must be an integral number of wavelengths:

$$n\lambda = 2x$$

This leads to the Bragg equation:

$$n\lambda = 2d\sin(\theta)$$

Where

n is an integer ($n=1,2,3\dots$) called the order of the reflection

λ is the wavelength of the X-rays

d is the distance between two lattice planes

θ is the angle of incidence

For a powdered sample the XRD pattern is usually measured with a stationary X-ray source (in this case Cu K α) and a movable detector that scans the intensity of the diffracted radiation as a function of the angle 2θ . In the case of powdered samples a diffraction pattern is formed because, by chance, a small proportion of the particles will be orientated such that a certain crystal plane is at the right angle θ with the incident beam for constructive interference. Diffraction patterns are mainly used to identify the crystallographic phases present in the catalyst. However, the applicability of the technique is limited to compounds with particle sizes greater than 4nm, since extensive line broadening occurs for smaller particles, and clear diffraction peaks are only observed when the sample possesses sufficient long-range order.

Analysis was performed on an Enraf Nonius FRS90 Bragg Brentano geometry with CuK α radiation and a Ge(111) single crystal monochromator. Detection of the X-rays was done using a curved position sensitive scintillater X-ray operated at 1.2KW (40mA and 30kV). Each sample was run for ½ hour and the diffractogram compared to known patterns on the JCPDS database. Crystallite size calculations were determined using the Scherrer equation. Peak broadening was referenced to crystalline silicon standard (see appendix).

$$\text{Crystallite size} = (K \times \lambda) / (FW \times \cos)$$

Where:

K= The Scherrer constant

λ = Wavelength of X-ray

FW = Full peak width at half maximum

2.3.2 Raman Spectroscopy

Irradiating a molecule with an incident beam of radiation gives rise to scattering, absorption or transmission. Such conditions give rise to Rayleigh scattering where the

scattered energy consists almost entirely of radiation of the incident frequency. In Raman spectroscopy the incident beam of radiation ($h\nu$) interacts with the molecule and the scattered beams consist of energies above and below that of the incident beam of radiation. The gain or loss of energy from the beam corresponds to the energy differences in the vibrational and rotational energy levels of the molecule. The quantum theory behind the Raman effect is as follows. Radiation of frequency ν is treated as a stream of photons of energy $h\nu$. The photons can undergo inelastic or elastic collisions with the irradiated molecule. In the case of Rayleigh scattering the collision is elastic and there is no energy change. With an inelastic collision however the molecule can gain or lose energy ΔE . If the molecule gains energy there is a loss of energy from the photon as in $h\nu - \Delta E$ and if the molecule loses energy there is a gain of energy in the photon as in $h\nu + \Delta E$. These two forms are referred to as Stokes and anti-Stokes radiation respectively. This can be seen schematically in figure 2.7 where $\nu=0$ and $\nu=1$ are the ground state and first energy level of the molecule^[4].

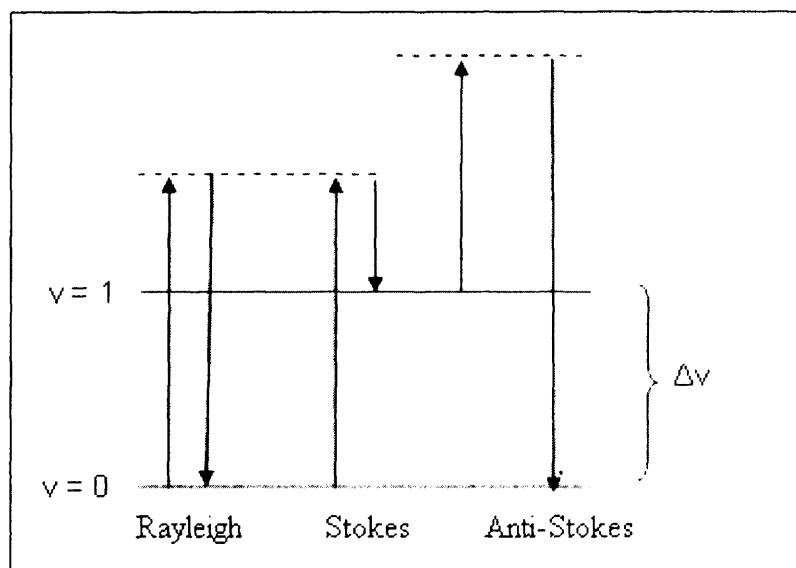


Figure 2.7 Energy changes in Raman and Rayleigh scattering

In situ raman analysis was conducted using a linkam TSIS00 in situ cell attached to a Renishaw system 1000 dispersive laser Raman microscope. The argon ion laser

(514.5 nm) was focused with a BH2-UMA microscope fitted with an optical CCD camera. Spectra was collected in the 200-1200 cm^{-1} range with 10s exposures and 20 accumulations using 100% laser power. The gas mixture, $\text{C}_3\text{H}_8/\text{O}_2/\text{N}_2 = 1.5/17.5/79\%$ (BOC 99.5%), was passed over the catalyst at 40 ml/min. The temperature was raised from 40 to 140°C in 25°C increments at a rate of 10°Cmin⁻¹.

2.3.3 Thermogravimetric analysis (TGA)

Thermogravimetric analysis measures the weight loss of material as a function of temperature. Weight loss is given as percentage of the total sample weight and can be used to identify species lost during the course of the temperature ramp. Analysis was conducted using a Perkin Elmer TGA 7 with approximately 10 mg of catalyst in an N₂ atmosphere. The temperature of the analysis was in the range of 40-700°C with a ramp rate of 20°C min⁻¹.

2.3.4 Brunauer Emmet Teller surface area determination

It was Brunauer Emmet and Teller who developed the BET equation for the determination of the surface area of a solid [5]. The method is based on the non-specific physisorption of a gas (N₂ or Ar) onto the surface of a solid close to the condensation temperature of the adsorbing gas. The results of the BET process are characterised by an isotherm, which displays the equilibrium amount of gas adsorbed on a surface at a given temperature as a function of pressure. There are a number of isotherms ranging from type I to type V (Figure 2.8). Langmuir developed one of the most widely used theoretical descriptions of adsorption but it is the type II isotherm that forms the basis for the BET

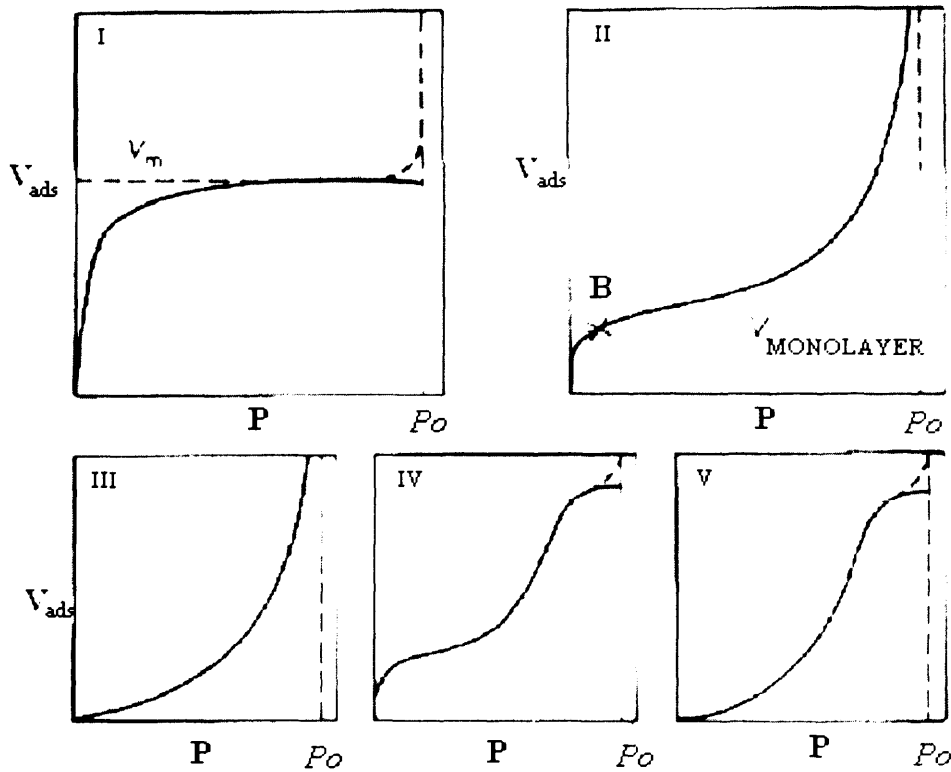


Figure 2.8 The 5 types of adsorption isotherm

analysis. The type II isotherm displays how, at low pressures, there is a build up of monolayer on the surface and, as the pressure increases; there is accelerated multilayer growth. As with other isotherms the type II isotherm exhibits hysteresis (hysteresis refers to the way the shape of the isotherms differ depending upon whether the isotherm is formed by the progressive addition or removal of a gas from the system). Monolayer coverage occurs at the point circled in the diagram although this value is approximate.

The BET equation is actually an extension of the Langmuir equation to accommodate multilayer adsorption (the Langmuir isotherm ignores multilayer coverage to focus on monolayers).

$$\frac{P}{V(P_0 - P)} = \frac{1}{V_m C} + \frac{(C - 1)P}{C V_m P_0}$$

Where:

V is the volume of gas adsorbed.

P_0 is the saturation pressure

V_m is the volume of gas adsorbed at (STP) per unit mass of adsorbent, when the surface is covered by a unimolecular layer of adsorbate

The assumption is made that the first layer is adsorbed with a heat of adsorption H_1 , while the second and subsequent layers that form on the surface are all characterised by the heats of adsorption equal to the latent heat of evaporation H_L . And, it is by considering the dynamic equilibrium between each layer and the gas phase that the BET isotherm is obtained. The constant C is given by:

$$C = \exp(H_1 - H_L) / RT$$

A plot of $p/V(p_0 - p)$ vs. p/p_0 yields V_m , the monolayer uptake. Because this value has to be expressed as an area an assumption is made about the packing of the adsorbed molecules on the surface and the area occupied by each; a nitrogen molecule occupies 16 \AA^2 and a krypton atom is assumed to be 19.5 \AA^2

BET analyses were performed on a Micromeritics Gemini 2360 surface analyser. All samples were degassed for 2 hours at 120°C . For the surface area experiment there is a $\pm 10\%$ error in the recorded values due limitations in the technique and the varying amounts of catalyst tested in each case.

2.3.5 Temperature programmed reduction/oxidation (TPR/TPO)

Temperature programmed reduction (TPR) is a technique for the determination of the reducibility of a material as a function of temperature. Temperature programmed oxidation (TPO) can be thought of as the reverse process and determines how readily oxidised the material is at a specific temperature. Powdered samples are placed in the elbow of the quartz analyser tube and fitted into the furnace. In the case of TPR, diluted H₂ is passed over the sample and a stable baseline reading established at a low enough temperature that no reduction of the sample is occurring. The temperature is then changed and at the critical temperature the H₂ reacts with the sample to form H₂O. The H₂O is removed from the stream using a liquid N₂/IPA cold trap. Because of the reaction, the amount of H₂ in the sample decreases and the proportion between the carrier and reactant shifts towards the carrier as does the mixtures thermal conductivity. A thermal conductivity detector (TCD) is used to measure the signal.

Analysis was performed using a Micromeritics Autochem 2910. Approximately 0.05-0.1g of powdered sample was secured in the elbow of the quartz U-tube using quartz wool plugs. The gas mixtures used were a 10% H₂/Ar and a 10% O₂/Ar mixture. The flow rate was set to 50 ml min⁻¹. The temperature scan was between 40 - 700°C with a 10°C min⁻¹. For certain experiments the ramp was 20°C min⁻¹.

2.3.6 Scanning electron microscope (SEM)

Scanning electron microscopy uses a beam of high energy electrons to examine the topology, morphology and composition of a sample. The electron beam is generated from a field emission gun (FEG) which comprises a very fine single crystal of tungsten. A series of fine apertures and lenses focus the beam to a fine point and

direct it onto the sample producing secondary electrons, which are detected and accumulated into the final image.

Analysis was performed using an A-SEM LEO S360 SEM. Ground catalyst was mounted on 12.5mm stubs and coated with a thin layer of gold. The gold coating provides an electrical contact over the whole specimen during analysis.

2.4 References

- [1] H. Yang, Y. Hu, X. Zhang and G. Qui, *Mats. Lett.*, 58 (2004) 387-389
- [2] St. G. Christoskova, M. Stoyanova, M. Georgieva and D. Mehandjiev, *Mat. Chem. and Phys.*, 60 (1999) 36-43
- [3] W. Clegg. *Crystal structure determination*. Oxford Chemistry Primer (2001)
- [4] N. B. Colthup and L. H. Daly. *Introduction to infra-red and Raman spectroscopy* Academic Press inc. (1964)
- [5] S. Brunauer, P.H Emmet and E. Teller. Adsorption of Gases in Multimolecular Layers, *J. Am. Chem. Soc.*, 60 (1938) 309-319

Chapter 3

Chapter 3

The oxidative dehydrogenation of propane using gallium-molybdenum oxide based catalysts

3.1 Introduction

Given the increasing industrial demand for propene, for the production of acrolein, acrylic acid, acrylonitrile and iso-propanol, it has been desirable to develop catalysts capable of producing propene by dehydrogenation of the more abundant alkane. Studies have probed the oxidative dehydrogenation (ODH) of alkanes as a potential route for alkene production. Unlike non-oxidative dehydrogenation, oxidative propene dehydrogenation is exothermic and avoids the thermodynamic constraints that limit propene yield from non-oxidative dehydrogenation. However, the introduction of an oxidant may also lead to lower than maximum predicted propene yields as deep oxidation to carbon oxides are more thermodynamically favoured.

In previous studies catalysts based on a mixture of Ga_2O_3 and MoO_3 have been developed for the partial oxidation of methane^[1]. The $\text{Ga}_2\text{O}_3/\text{MoO}_3$ catalyst showed an increased yield of partial oxidation products by combining the alkane activation properties of Ga_2O_3 and the partial oxidation behaviour of MoO_3 in a synergistic manner. It is apparent that similar catalytic properties are also required for the partial oxidation of propane to propene Ga_2O_3 itself is known to be highly effective for the activation of methane. In earlier studies investigating CH_4/D_2 exchange it has been shown that the rate of reaction for Ga_2O_3 was at least two orders of magnitude greater than any other metal oxide^[2-3]. Molybdenum too is known to be highly selective and active in many reactions and supported molybdenum oxides have been studied extensively in the ODH of propane^[4]. It is against this background that the current

study has been undertaken to probe the efficacy of Ga₂O₃/ MoO₃ catalysts for the ODH of propane to propene. For propane ODH the most active and selective catalysts are based on vanadium and molybdenum based oxides. A series of variously loaded V₂O₅/TiO₂ were also prepared as a comparison.

3.2 Characterization

3.2.1 BET Surface Areas

Table 3.1 BET surface areas of prepared catalysts (maximum error \pm 10%)

Catalyst	BET surface area/m ² g ⁻¹
1:1 Ga ₂ O ₃ /MoO ₃ calcined	13
1:1 Ga ₂ O ₃ /MoO ₃ uncalcined	13
Ga ₂ O ₃	25
MoO ₃	2
1:3 Ga ₂ O ₃ /MoO ₃ uncalcined	9
1:10 Ga ₂ O ₃ /MoO ₃ uncalcined	6
TiO ₂	50
3 wt% V ₂ O ₅ /TiO ₂	50
6 wt% V ₂ O ₅ /TiO ₂	47
10 wt% V ₂ O ₅ /TiO ₂	46

Catalyst surface areas determined by the BET method are summarized in table 3.1. The MoO₃ surface area was low whilst Ga₂O₃ was considerably greater at 25m²g⁻¹. The surface areas for the calcined and uncalcined Ga₂O₃/MoO₃ catalysts were 13m²g⁻¹, the expected value for a 1:1 physical mixture. It was also apparent that the surface area was not decreased by calcination. Varying the ratio of the components resulted in a decreased surface area due to the higher MoO₃ content: the surface area decreased from 13m²g⁻¹ to 9 and 6m²g⁻¹ for the 1:3 and the 1:10 Ga₂O₃/MoO₃ catalysts respectively. Addition of 3wt% V₂O₅ to the TiO₂ support had no measurable effect

on the surface area. It is only near the calculated point of monolayer formation (6wt%) that there is a noticeable effect, with the surface area decreasing with increased V_2O_5 content. This is due to the formation of V_2O_5 crystallites over the surface of the support.

3.2.2 Powder X-ray Diffraction

The powder X-ray diffraction patterns for Ga_2O_3 , MoO_3 and the 1:1 Ga_2O_3/MoO_3 catalysts are shown below. The powder pattern for uncalcined Ga_2O_3 (figure 3.1) showed that diffraction peaks were broad and relatively low in intensity demonstrating that the structure was relatively disordered. Ga_2O_3 has five polymorphs: α -, β -, γ -, δ - and ϵ - Ga_2O_3 . The Ga_2O_3 from Aldrich contains predominately β - Ga_2O_3 with about 5% α - Ga_2O_3 and hydroxy gallium oxide ^[5]. The peaks at 33.0° , 36.7° , 50.3° and 55.7° are the (104), (110), (024) and (116) diffractions of α - Ga_2O_3 . Also traces of γ - Ga_2O_3 are present although it is difficult to assign exact peaks.

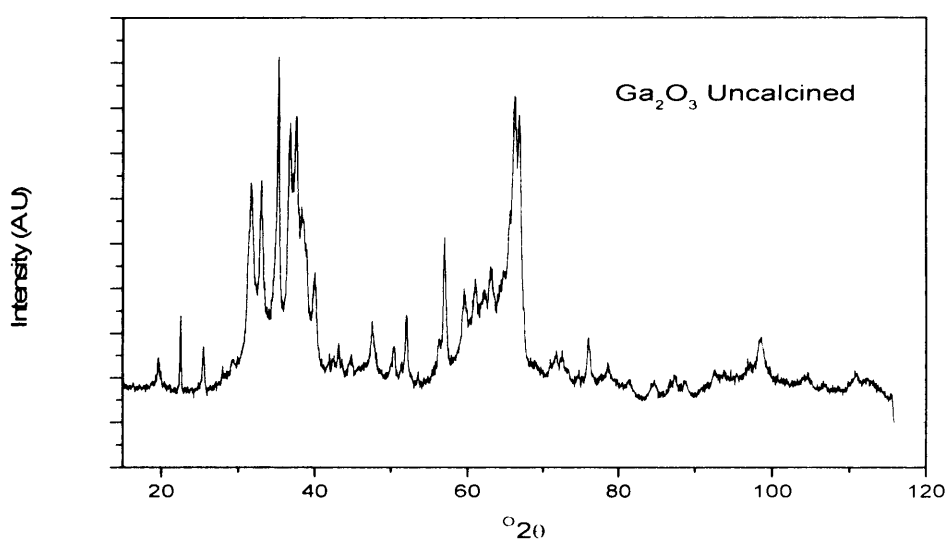


Figure 3.1 XRD pattern of uncalcined Ga_2O_3

Calcination of Ga_2O_3 at 650°C (figure 3.2) leads to the formation of the thermodynamically more stable $\beta\text{-Ga}_2\text{O}_3$ with the loss of the hydroxy gallium oxide. The peaks corresponding to the diffractions of 110 and 100 planes of $\text{GaO}(\text{OH})$ are missing from the calcined catalyst. TGA analysis of the hydroxide by C. Otero Arean *et al* showed that it lost water over the temperature range 390-650 K ($117\text{-}377^\circ\text{C}$)^[6], evidence that the hydroxyl gallium oxide decomposes during calcination.

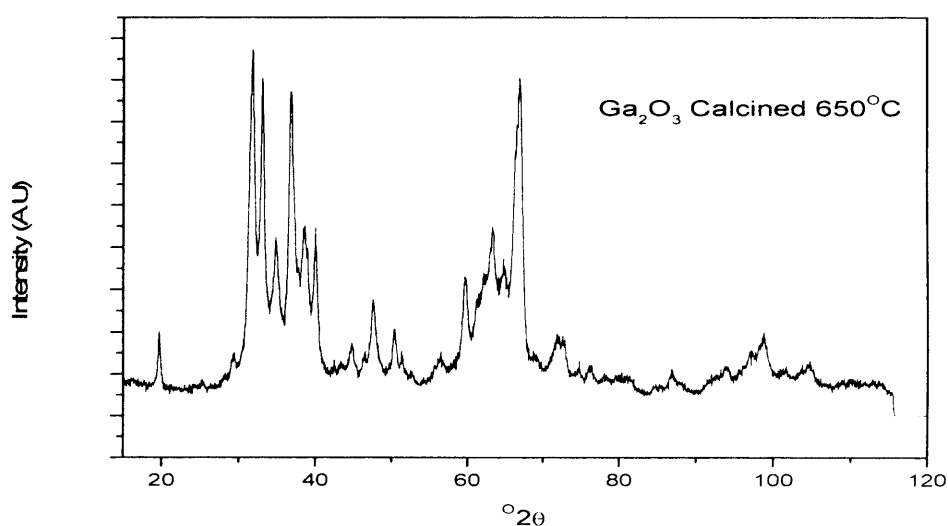
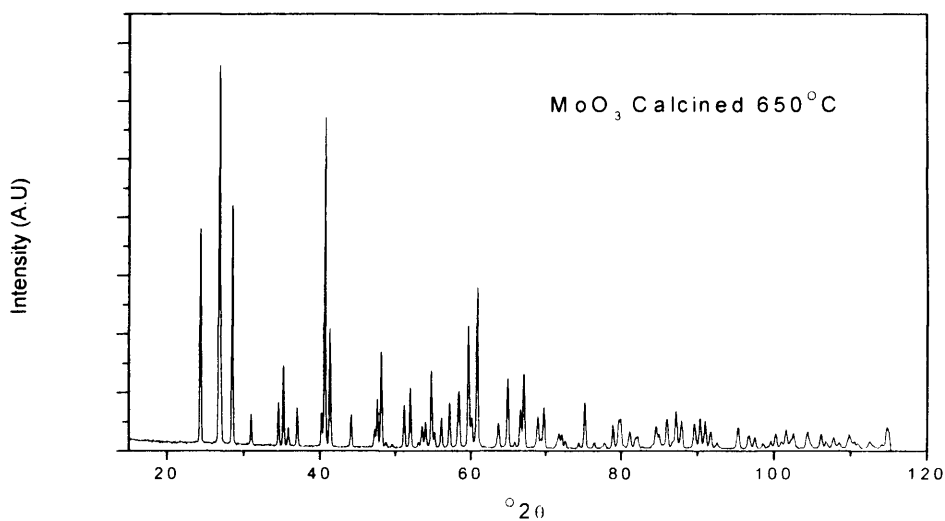
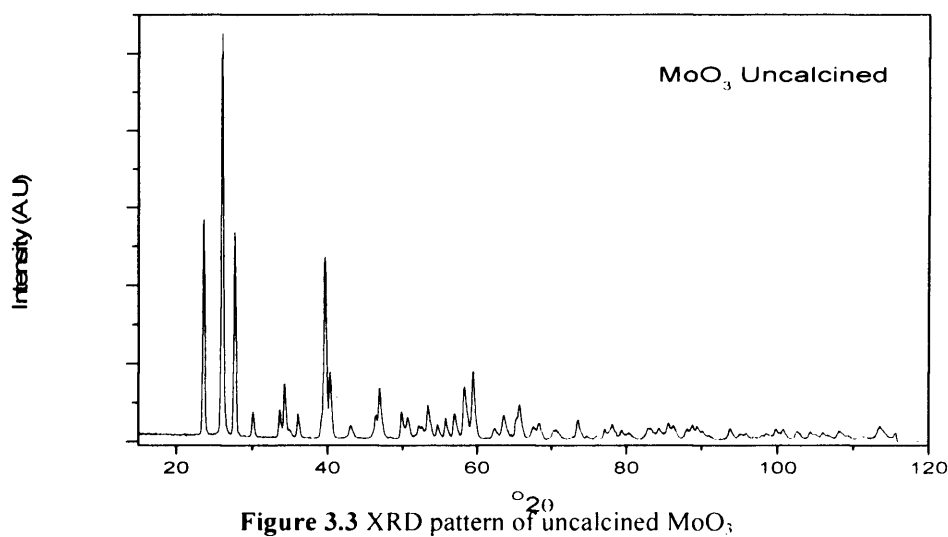


Figure. 3.2 XRD pattern of Ga_2O_3 calcined 650°C

On the other hand diffraction data from MoO_3 (figure 3.3) showed that the phase was highly crystalline. Calcination of MoO_3 at 650°C led to an increase in peak intensity due to crystal growth (figure 3.4).



The 1:1 Ga₂O₃/MoO₃ catalysts showed largely diffraction peaks from MoO₃ (figure 3.5). Careful inspection of the diffraction data revealed that diffraction from Ga₂O₃ was observed, but due to the low intensity of the peaks they were barely discernable. This is not surprising considering the differences of diffraction intensity between the diffraction patterns from MoO₃ and Ga₂O₃.

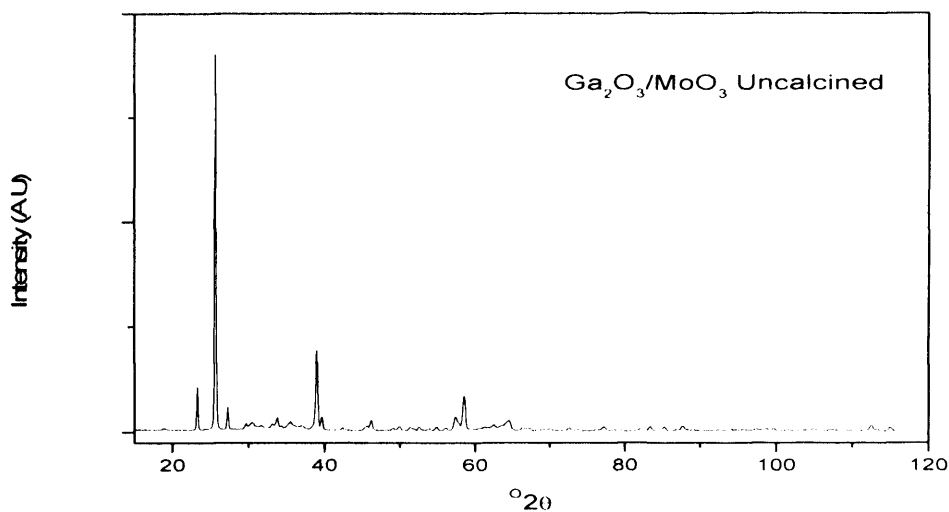


Figure 3.5 XRD pattern of uncalcined $\text{Ga}_2\text{O}_3/\text{MoO}_3$ mechanical mixture

Calcination of 1:1 $\text{Ga}_2\text{O}_3/\text{MoO}_3$ at 650°C had little effect upon its structure, no new mixed phases were produced, neither was there any recordable distortion of the MoO_3 unit cell. Furthermore, after use in the reaction there were no significant changes to the powder XRD patterns (not shown). The change in intensity of the MoO_3 diffraction peaks post calcination is also observable in the 1/1 $\text{Ga}_2\text{O}_3/\text{MoO}_3$. An additional diffraction peak at ca. 22° was observed in the uncalcined 1/1 $\text{Ga}_2\text{O}_3/\text{MoO}_3$ catalyst. The peak was attributed to the presence of $\text{GaO}(\text{OH})$ and it is interesting that this catalyst alone also demonstrated low selectivity to acrolein at high temperatures.

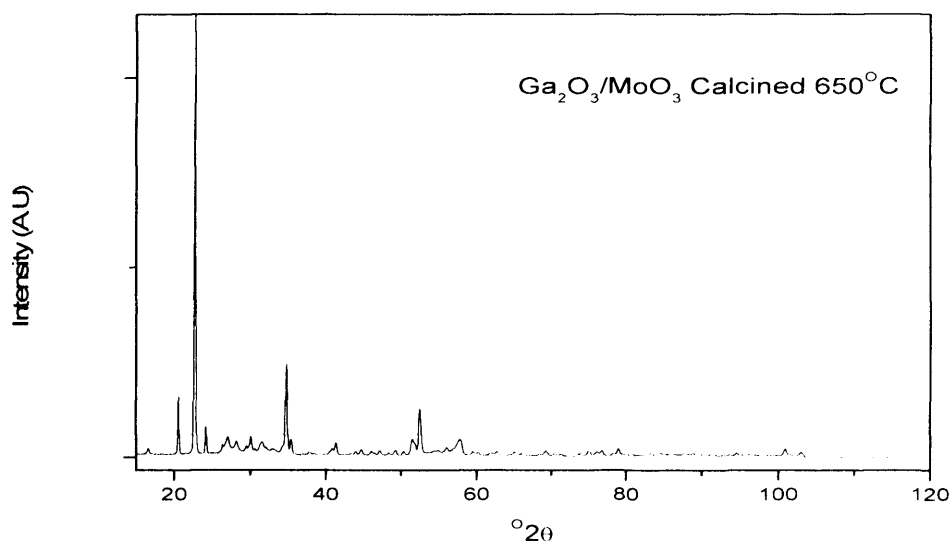


Figure 3.6 XRD pattern of $\text{Ga}_2\text{O}_3/\text{MoO}_3$ mechanical mixture calcined 650°C

The presence of GaOOH can be seen in figure 3.7 with diffraction peaks at $2\theta=22.5^\circ$ and 25.5° corresponding to the (110) and (120) planes respectively. $\gamma\text{-Ga}_2\text{O}_3$ was also present as indicated by peaks at $2\theta=36.2^\circ$, 64.2° and 76.0° . The main phase present was $\beta\text{-Ga}_2\text{O}_3$.

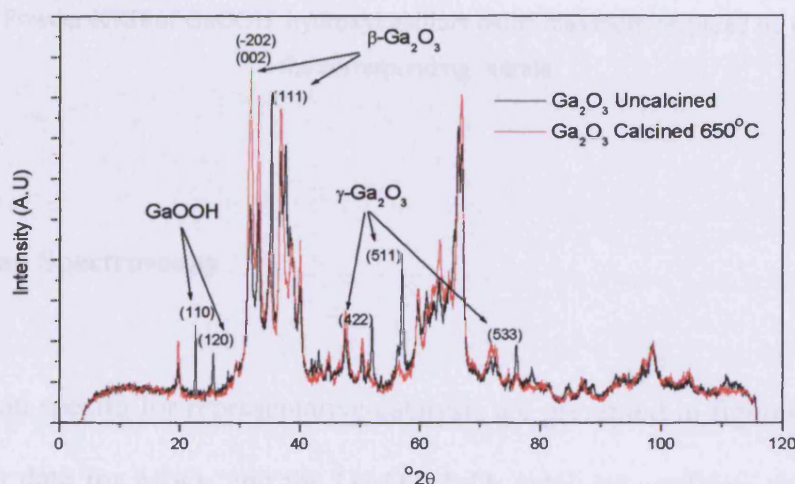


Figure 3.7 Overlaid X-ray diffraction patterns for gallium oxide before and after calcinations. Ga_2O_3 calcined (red). Ga_2O_3 uncalcined (black)

The studies indicate that the $\text{Ga}_2\text{O}_3/\text{MoO}_3$ catalysts comprised a mixture of Ga_2O_3 and MoO_3 and there was no evidence for the formation of any new mixed phases. The noticeable differences between the calcined and uncalcined catalyst were the increased crystal growth in a specific plane direction in MoO_3 along with the formation of the more stable $\beta\text{-Ga}_2\text{O}_3$ polymorph and the loss of $\text{GaO}(\text{OH})$. The diffraction pattern for a pure $\text{GaO}(\text{OH})$ sample can be seen in figure 3.8.

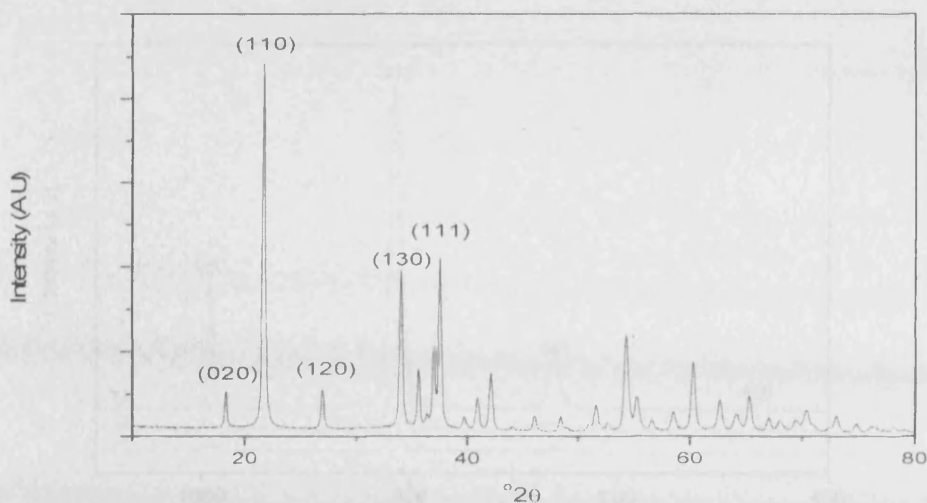


Figure 3.8 Powder XRD of GaOOH hydroxyl gallium oxide diasopore prepared by precipitation of the corresponding nitrate

3.2.3 Raman Spectroscopy

The Raman spectra for representative catalysts are presented in figures 3.9 and 3.10. The Raman data for MoO₃ and the Ga₂O₃/MoO₃ catalysts confirms the conclusions obtained from the powder X-ray diffraction data. The Raman spectrum for MoO₃ was the same as both of the Ga₂O₃/MoO₃ catalysts, reiterating the conclusion that MoO₃ is not significantly altered on production of the two component catalysts. The characterization studies indicate that the Ga₂O₃/MoO₃ catalysts were comprised from a mixture of Ga₂O₃ and MoO₃ and there was no evidence for the formation of any new mixed phases.

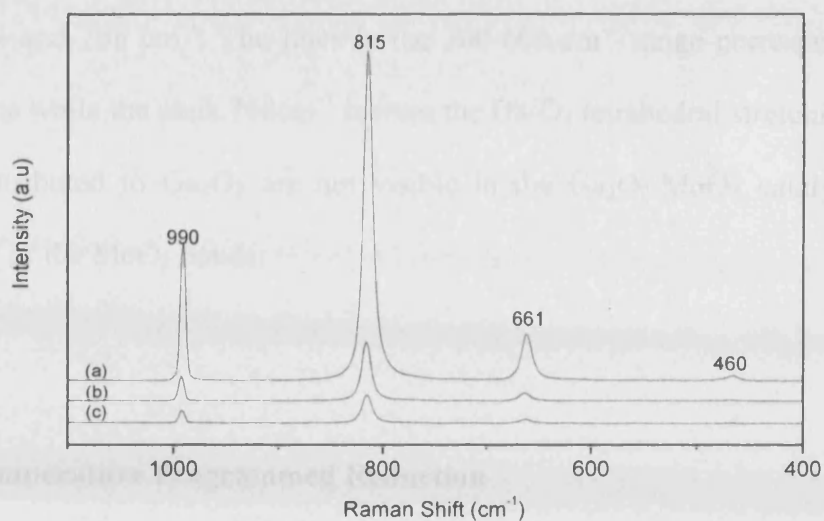


Figure 3.9 Comparison of micro laser Raman spectra for MoO_3 and $\text{Ga}_2\text{O}_3/\text{MoO}_3$ catalysts. (a) MoO_3 (b) $\text{Ga}_2\text{O}_3/\text{MoO}_3$ calcined (c) $\text{Ga}_2\text{O}_3/\text{MoO}_3$ uncalcined

It was also apparent that calcined and uncalcined catalysts were not significantly different. Weak Raman bands corresponding to the stable $\beta\text{-Ga}_2\text{O}_3$ are visible in the uncalcined gallia and become more prominent upon calcinations (Figure 3.10). The raman spectra of the calcined sample show lines at 201, 229, 319, 348, 418, 476,

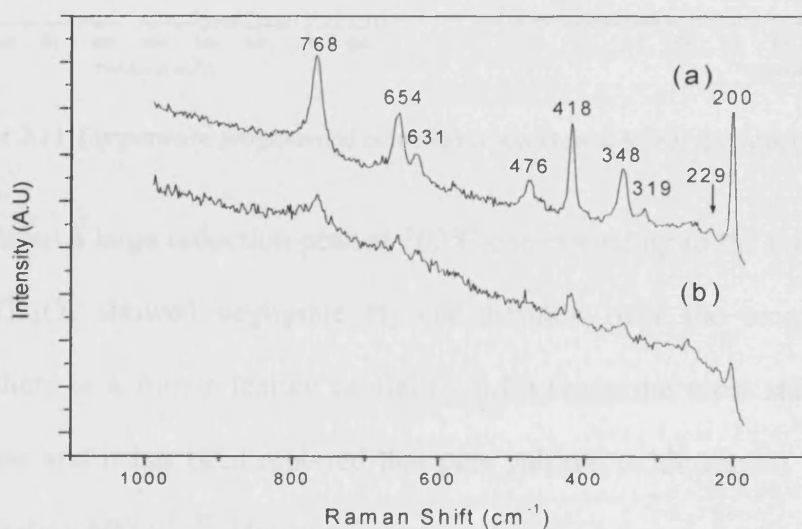


Figure 3.10 Micro Laser Raman Spectra for Ga_2O_3 showing the formation of the stable $\beta\text{-Ga}_2\text{O}_3$ polymorph: (a) Ga_2O_3 calcined 650°C ; (b) Ga_2O_3 Uncalcined

631, 654 and 768 cm^{-1} . The lines in the 300-600 cm^{-1} range correspond to bending vibrations while the peak 768 cm^{-1} is from the Ga-O₄ tetrahedral stretching mode. The bands attributed to Ga₂O₃ are not visible in the Ga₂O₃/MoO₃ catalyst due to the intensity of the MoO₃ bands.

3.2.4 Temperature Programmed Reduction

The temperature-programmed reduction of the component oxides is shown in figure 3.11

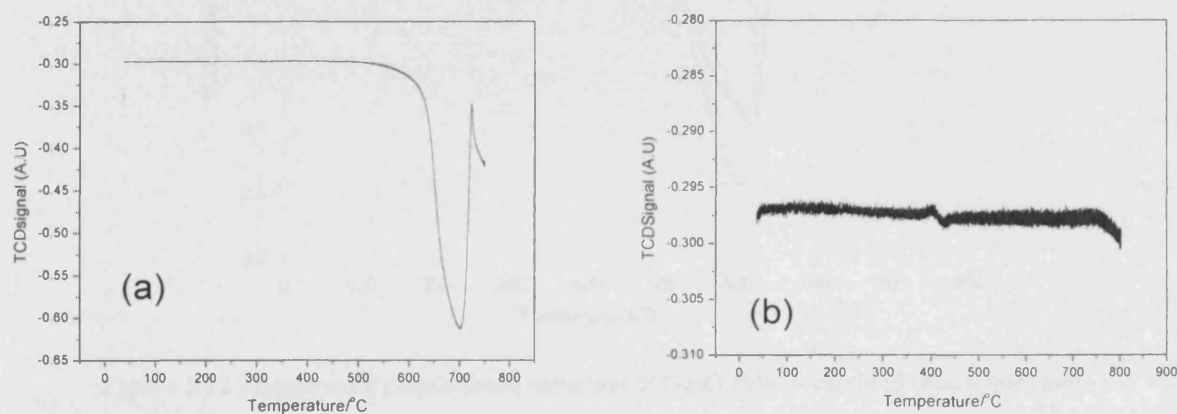


Figure 3.11 Temperature programmed reduction of Ga₂O₃ and MoO₃: (a) MoO₃; (b) Ga₂O₃

MoO₃ shows a large reduction peak at 702°C corresponding to the total reduction of MoO₃. Ga₂O₃ showed negligible H₂ consumption over the temperature range although there is a minor feature at 400°C. β -Ga₂O₃ is the most stable crystalline modification and it has been reported that pure gallium oxide cannot be reduced by hydrogen below 600°C^[7-8]. However, some studies have found small reducible peaks in the 250°C region indicating that small parts of the gallium oxide can be reduced. XPS analysis has confirmed the presence of a Ga₂⁺O species in a reduced sample^[9].

The temperature programmed reduction of the calcined and uncalcined mixtures of Ga₂O₃/MoO₃ catalysts can be seen in figure 3.12. Both mixtures show the presence of a minor reduction peak centred at ca.400°C. A second much larger peak is visible at ca. 610°C, which can be attributed to the MoO₃ component of the catalyst. It is interesting to note that reduction of MoO₃ occurs approximately 100°C lower when in combination with Ga₂O₃. Exact values for the reduction peaks can be found in table 3.2.

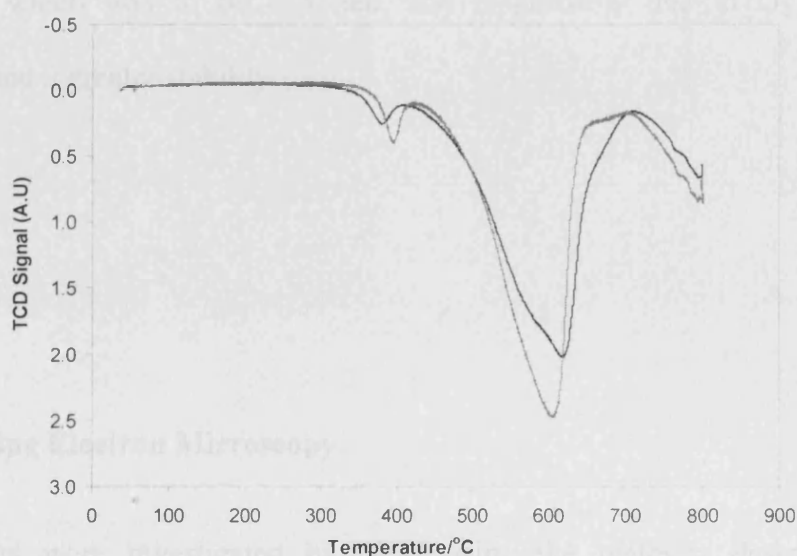


Figure 3.12 Temperature programmed reduction of Ga₂O₃/MoO₃ calcined (black line) and Ga₂O₃/MoO₃ uncalcined (redline)

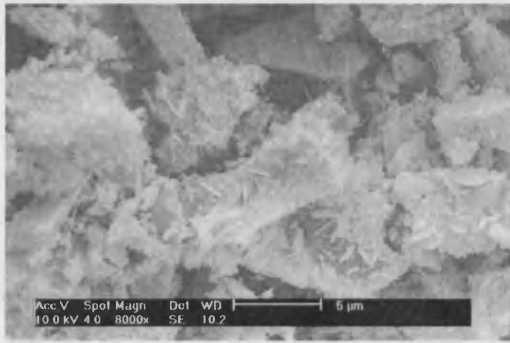
Table 3.2 Temperature of reduction peaks

Catalyst	Reduction Peak (°C)
Ga ₂ O ₃	400 (v. small)
MoO ₃	702
Ga ₂ O ₃ /MoO ₃ Uncalcined	394, 605
Ga ₂ O ₃ /MoO ₃ Calcined	400, 582 (shoulder), 703

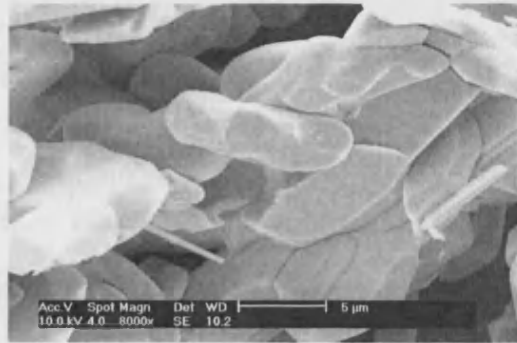
The shift to lower temperatures in the combined Ga₂O₃/MoO₃ catalyst could be due to interaction between the two component oxides. It is certainly the case that the combination of Ga₂O₃ and MoO₃ results in an increase in reducibility and an increased H₂ consumption. The appearance of the reduction peak at ca. 400°C is very interesting; this appeared as only a very minor peak in the single Ga₂O₃ catalyst and is tentatively attributed to the reduction of small parts of Ga₂O₃ to a Ga₂⁺O species. The calcined Ga₂O₃/MoO₃ catalyst showed a lower H₂ consumption relative to the uncalcined, which was to be expected, and is probably due to O₂ loss during calcination and a greater stability.

3.2.5 Scanning Electron Microscopy.

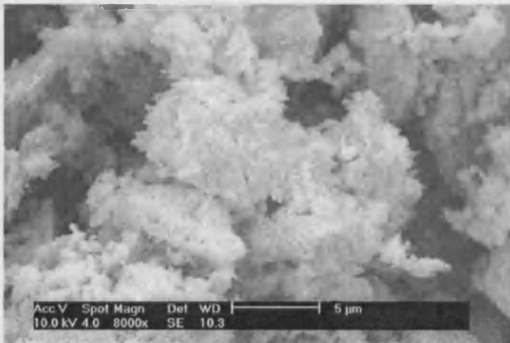
The catalysts were investigated by SEM using the methods described in the experimental section 2.3.6. The results can be seen in figure 3.13. Calcination time does not affect particle size or surface area to any noticeable extent. The Ga₂O₃ has an irregular particle size with a jagged edge structure. The MoO₃ has a platelet-like morphology with well-defined particles. Combination of the two components with additional grinding leads to an intimate mixture with the Ga₂O₃ particles covering the MoO₃ particles. The regular shaped particles of MoO₃ can just be seen underneath the layer of Ga₂O₃ in image (c) and can be seen more clearly in image (d). There is no difference in particle size or morphology for the calcined and uncalcined catalysts.



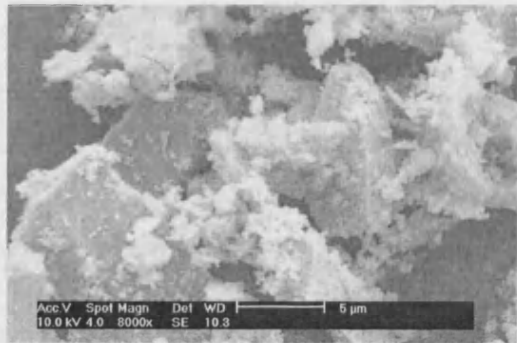
(a) Pure Ga₂O₃ (Aldrich)



(b) Pure MoO₃



(c) 1:1 Ga₂O₃/MoO₃ Uncanceled



(d) 1:1 Ga₂O₃/MoO₃ Calcined

Figure 3.13 SEM images of Ga₂O₃ and MoO₃ catalysts at 8000X magnification

3.3 Results

3.3.1 Propane oxidative dehydrogenation over 1:1 Ga₂O₃/MoO₃

Propane conversion over the 1:1 Ga₂O₃/MoO₃ catalysts and comparison with individual Ga₂O₃ and MoO₃ are shown in figure 3.14. The data were obtained at steady state conversion and there was no measurable deactivation for any of the catalysts. The reaction data in the work were reproducible with a precision of less than 5%.

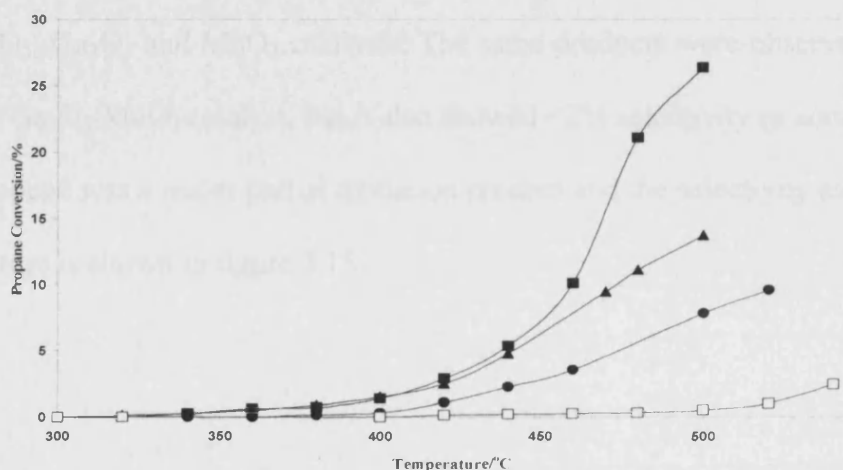


Figure 3.14 Propane conversion over the Ga₂O₃/MoO₃ catalysts and comparison with Ga₂O₃ and MoO₃ (C₃H₈/O₂/He=2/1/8.5, GHSV=9600 h⁻¹). ▲ Ga₂O₃/MoO₃ calcined; ■ Ga₂O₃/MoO₃ uncalcined; ● Ga₂O₃; □ MoO₃.

The Ga₂O₃ catalyst showed initial propane conversion at 375°C increasing to ca. 8% at 500°C. On the contrary the rate of propane oxidation over MoO₃ was considerably lower. Initial activity was detected at 425°C and only increased to ca. 3% at 500°C. Both of the 1:1 Ga₂O₃/MoO₃ catalysts showed considerably higher rates of propane oxidation. The light-off temperatures for the calcined and uncalcined catalysts were

325°C and 340°C respectively; approximately 50°C lower than the individual Ga₂O₃ catalyst. This trend continued over the entire temperature range with a maximum conversion of 26% for the uncalcined catalyst at 500°C. The profile of propane conversion with temperature was broadly similar for the calcined and uncalcined catalyst below 425°C. Above this temperature propane conversion over the uncalcined catalyst was greater than the calcined material. The calcined 1:1 Ga₂O₃/MoO₃ catalyst achieved a maximum conversion of 13% at 500°C as compared to 26% for the uncalcined catalyst. No appreciable activity was observed below 550°C in an empty quartz reactor (see appendix).

Propene, CO₂ and CO were the only reaction products over the calcined 1:1 Ga₂O₃/MoO₃, Ga₂O₃ and MoO₃ catalysts. The same products were observed with the uncalcined Ga₂O₃/MoO₃ catalyst, but it also showed <2% selectivity to acrolein above 440°C. Propene was a major partial oxidation product and the selectivity as a function of temperature is shown in figure 3.15.

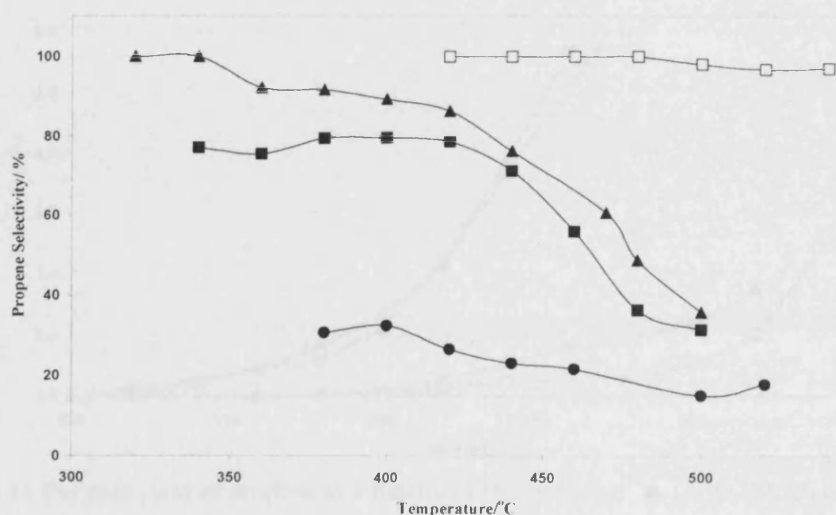


Figure 3.15 Selectivity to propene as a function of temperature ($C_3H_8/O_2/He=2/1/8.5$, GHSV=9600 h⁻¹):

▲ Ga₂O₃/MoO₃ calcined; ■ Ga₂O₃/MoO₃ uncalcined; ● Ga₂O₃; □ MoO₃.

Propene selectivity was lowest for the Ga_2O_3 catalyst; gradually decreasing from ca. 35 % at 375°C to ca. 20% at 520°C. MoO_3 was most selective for the partial oxidation of propane to propene. Selectivities in excess of 95% were observed even at 540°C, but it must be noted that these high selectivities were obtained at low propane conversion. The propene selectivity over the calcined and uncalcined 1:1 $\text{Ga}_2\text{O}_3/\text{MoO}_3$ catalysts demonstrated the same trends with temperature. The calcined catalyst showed initially 100 % selectivity to propene, this decreased gradually to 61 % at 470°C. The propene selectivity was lower over the uncalcined catalyst across the entire temperature range, but still remained greater than the Ga_2O_3 catalyst.

The per pass yields of propene for the 1:1 $\text{Ga}_2\text{O}_3/\text{MoO}_3$, Ga_2O_3 and MoO_3 catalysts are shown in figure 3.16 The MoO_3 catalyst gave the lowest propene yields. The propene yields over Ga_2O_3 were higher than MoO_3 and this was due to the higher propane conversion. It must also be noted that considerably higher temperatures were

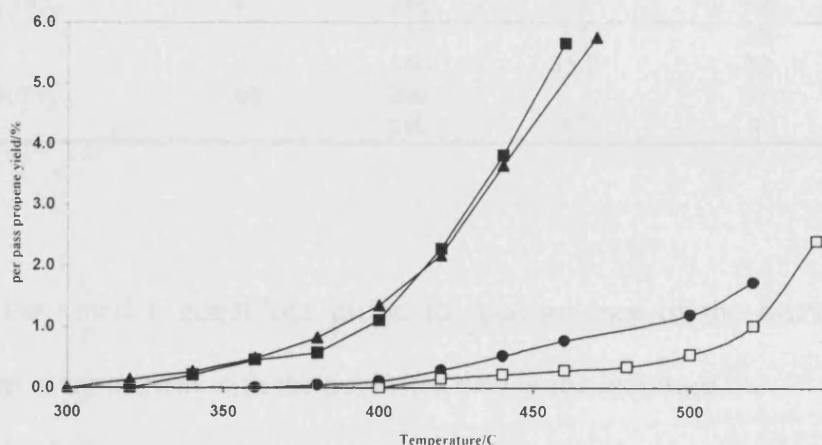


Figure 3.16 Per pass yield of propene as a function of temperature: ▲ $\text{Ga}_2\text{O}_3/\text{MoO}_3$ calcined; ■

$\text{Ga}_2\text{O}_3/\text{MoO}_3$ uncalcined; ● Ga_2O_3 ; □ MoO_3 .

required with the MoO₃ catalyst. The propene yields over both 1:1 Ga₂O₃/MoO₃ catalysts were markedly similar. Both exhibited a 5.7 % per pass yield at 470 °C for the calcined catalyst and, at 460 °C for the uncalcined catalyst.

For comparison with the catalytic data in this study a series of V₂O₅/TiO₂ catalysts were also prepared and tested. Vanadium and molybdenum based catalyst are one of the most widely studied for this reaction and are generally accepted to be the most efficient. The best performance of the V₂O₅/TiO₂ catalysts was shown with a 6wt% V₂O₅ loading. A comparison of propane partial oxidation, at approximately constant conversion, ca. 10% where possible, is presented in table 3.3.

Table 3.3 Comparison of catalyst performance for propane oxidative dehydrogenation. (C₃H₈/O₂/He=2/1/8.5, GHSV=9600 h⁻¹)^[6]

Catalyst	BET surface area/m ² g ⁻¹	Temp. /°C	Propane conversion/%	Propene selectivity/%	Per pass propene yield/%
Ga ₂ O ₃ /MoO ₃ calcined	13	470	9.9	62	5.7
Ga ₂ O ₃ /MoO ₃ uncalcined	13	460	10.1	56	5.7
Ga ₂ O ₃	25	520	9.6	18	1.7
MoO ₃	1.5	540	2.5	97	2.4
3 wt% V ₂ O ₅ /TiO ₂	50	260	0.9	50	0.5
		300	3.6	32	2.0
		325	10.1	19	1.9
6 wt% V ₂ O ₅ /TiO ₂	47	240	0.8	69	0.5
		315	7.5	28	2.0
		340	11.0	22	2.5
10 wt% V ₂ O ₅ /TiO ₂	46	240	1.2	65	0.7
		290	8.7	3	0.2

Although the reaction conditions differ, the performance of the 6wt% V₂O₅/TiO₂ catalyst was in agreement with the published data in the literature ^[7].

The V₂O₅/TiO₂ catalysts were active at lower temperatures than the 1:1 Ga₂O₃/MoO₃ catalysts, and such a decrease in temperature could be expected to produce higher propene selectivity by reducing over oxidation. However, this was not the case and the propene yield from the 6wt% V₂O₅/TiO₂ catalyst was lower than that

for the 1:1 Ga₂O₃/MoO₃ catalysts. Despite the higher temperatures the propene selectivities and yields for the 1:1 Ga₂O₃/MoO₃ catalysts were superior.

Studies have been performed replacing either the Ga₂O₃ or MoO₃ components of the 1:1 Ga₂O₃/MoO₃ catalysts with silicon carbide (SiC). The aim of these studies was to probe the effect of dilution for the two component catalysts. Representative data for comparison are presented in table 3.4. The replacement of the Ga₂O₃ component with SiC suppressed the propane conversion relative to MoO₃ alone. The propane conversion was also significantly lower than with the 1:1 Ga₂O₃/MoO₃ catalysts. The selectivity to propene was also very similar to MoO₃. Replacement of MoO₃ with SiC showed that propane conversion was increased when compared to Ga₂O₃ alone, interestingly the propene selectivity was also affected with a 15% increase at 450°C. The results from studies using SiC to dilute Ga₂O₃ and MoO₃ showed that dilution of the Ga₂O₃ may be beneficial in the performance of the Ga₂O₃/MoO₃ catalysts but is probably not solely responsible. Dilution with silicon carbide may help to control over oxidation by allowing heat removal from the bed. It is often the case that dilution of oxidation catalysts has a positive effect on product selectivity. Dilution of MoO₃ had a negative effect.

Table 3.4 Comparison of catalyst performance and the effect of dilution with SiC.

Catalyst	Temp. /°C	Propane conversion/%	Propene selectivity/%
MoO ₃ /SiC	560	0.3	100
	580	1.0	95
MoO ₃	520	1.0	97
Ga ₂ O ₃ /SiC	400	0.5	30
	420	1.4	32
Ga ₂ O ₃	420	1.1	28
Ga ₂ O ₃ /MoO ₃ calcined	380	0.9	92
Ga ₂ O ₃ /MoO ₃ uncalcined	380	0.7	80

These data clearly demonstrate that the 1:1 Ga₂O₃/MoO₃ catalysts showed promising activity for propane oxidative dehydrogenation. Furthermore, at this stage no attempt has been made to maximise the performance of the Ga₂O₃/MoO₃ catalysts and it is envisaged that further improvements in catalyst performance are possible.

3.3.2 Propane oxidative dehydrogenation over individual components: Effect of heat treatment.

The Ga₂O₃ and MoO₃ catalysts were tested for propane ODH before and after calcination (650°C, 3h.). The results for propane conversion are presented in figure 3.17. Calcination of the pure MoO₃ catalyst led to a decrease in overall activity with the calcined MoO₃ showing no activity within the experimental temperature range. Conversely calcination of Ga₂O₃ led to an increase in activity and selectivity. The catalyst showed initial conversion at 350°C with a maximum conversion of 12.6% at 500°C as compared to the uncalcined Ga₂O₃, which showed initial conversion at 380°C with a maximum conversion of 7.9% at 500°C. The propane conversion over the calcined Ga₂O₃ was similar to that of the calcined 1:1 Ga₂O₃/MoO₃ catalyst. This was not the case for propene selectivity however.

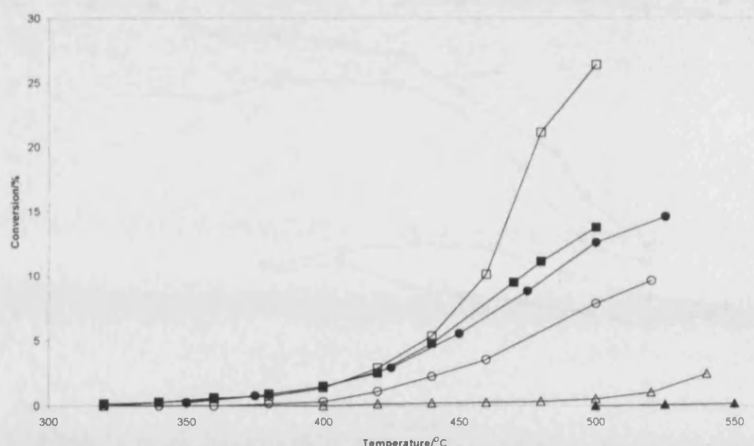


Figure 3.17 Propane conversion over component oxides Ga₂O₃ and MoO₃; Effect of heat treatment: ○ Ga₂O₃ Uncalcined; ● Ga₂O₃ Calcined; □ Ga₂O₃/MoO₃ Uncalcined; ■ Ga₂O₃ / MoO₃ Calcined; △ MoO₃ Uncalcined; ▲ MoO₃ Calcined.

The selectivity to propene is shown in figure 3.18. Calcination of Ga₂O₃ leads to an increase in selectivity from 20% to 37% at 450°C, decreasing to 20% at higher temperatures. Although the Ga₂O₃ catalyst showed similar activity to the 1:1 Ga₂O₃/MoO₃ this was not the case for the selectivity, which achieved no greater than 40% across the entire temperature range tested. It can be seen that calcination of the mixed 1:1 Ga₂O₃/MoO₃ actually leads to a decrease in activity but an increase in selectivity. This differs from the behavior displayed by the individual components (calcination of Ga₂O₃ increases both conversion and selectivity). It appears that the catalytic ability of the individual components is modified upon combination with one another. It may be the case that a superior catalyst could be made by combination of calcined Ga₂O₃ with uncalcined MoO₃.

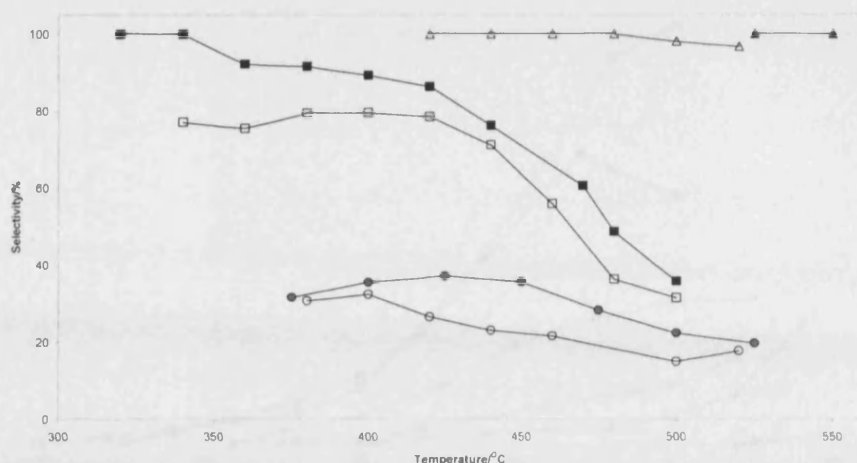


Figure 3.18 Selectivity to propene over component oxides: Effect of thermal heat treatment (450°C, 6h); ○ Ga₂O₃ Uncalcined; ● Ga₂O₃ Calcined; □ Ga₂O₃/MoO₃ Uncalcined; ■ Ga₂O₃ / MoO₃ Calcined; Δ MoO₃ Uncalcined; ▲ MoO₃ Calcined.

Table 3.5 shows the propane conversion and selectivity to propene for the catalysts at 400°C and 500°C. At 400°C both the calcined and uncalcined 1:1 Ga₂O₃/MoO₃ show the highest conversion and propene selectivity compared to the individual components. With the exception of the uncalcined MoO₃ catalyst the same was seen at the higher temperature of 500°C.

Table 3.5 Conversion and selectivity data at 400°C and 500°C for calcined and uncalcined catalyst.

Catalyst	Temperature of reaction (400°C)		Temperature of Reaction (500°C)	
	Conversion (%)	Selectivity (%)	Conversion (%)	Selectivity (%)
Ga ₂ O ₃	0.3	32	7.9	15
Ga ₂ O ₃ Calcined	1.5	36	12.6	22
MoO ₃	0.0	0	0.5	98
MoO ₃ Calcined	0.0	0	0.0	0
Ga ₂ O ₃ /MoO ₃ Calcined	1.5	89	13.7	36
Ga ₂ O ₃ /MoO ₃ Uncalcined	1.4	80	26.4	31

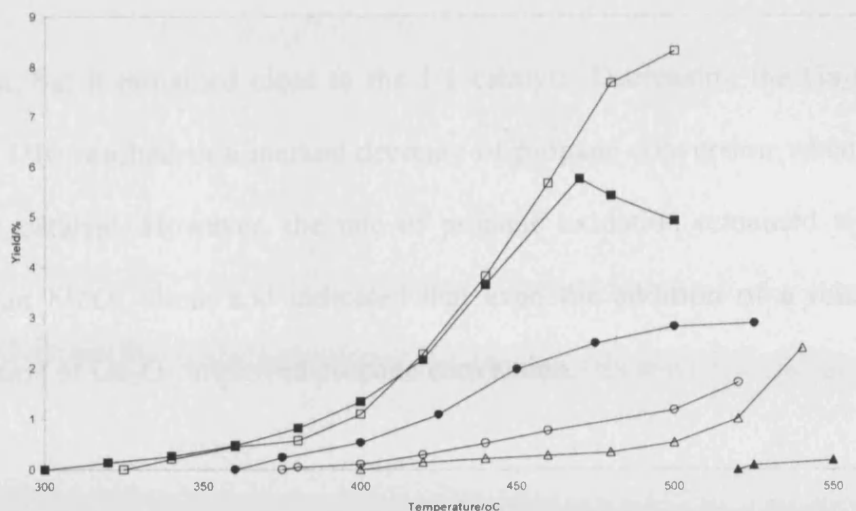


Figure 3.19 Propene yield over component oxides: Effect of thermal heat treatment (450°C, 6hrs); ○ Ga₂O₃ Uncalcined; ● Ga₂O₃ Calcined; □ Ga₂O₃/MoO₃ Uncalcined; ■ Ga₂O₃/MoO₃ Calcined; △ MoO₃ Uncalcined; ▲ MoO₃ Calcined.

Propene yields are shown in figure 3.19. The highest yields were obtained over the 1:1 mixed Ga₂O₃/MoO₃ catalysts. The uncalcined Ga₂O₃/MoO₃ catalyst showed the highest propene yield of 8.5% but at a low propene selectivity of just 31%. The propene yield over the calcined Ga₂O₃/MoO₃ catalyst was similar to the uncalcined below 450°C but decreased to 5% at 500°C. Calcination of Ga₂O₃ resulted in an increased propene yield and this is as a result of the increased conversion and selectivity. The overall yield was twice that of the uncalcined Ga₂O₃ rising from 1% at 425°C to 2.7% at 500°C. Calcination of MoO₃ resulted in a total loss of activity below 525°C and consequently a low propene yield.

3.3.3 Propane ODH over modified Ga₂O₃/MoO₃ (varying ratio)

The influence of changing the Ga₂O₃ to MoO₃ ratio has been investigated and the effect on propane conversion is shown in figure 3.20. The catalyst with Ga/Mo=1/1 was most active showing the greatest propane conversion across the temperature range. Decreasing the ratio to 1/3 resulted in a marginal decrease of propane

conversion, but it remained close to the 1/1 catalyst. Decreasing the Ga₂O₃ content further to 1/10 resulted in a marked decrease of propane conversion when compared to the 1/1 catalyst. However, the rate of propane oxidation remained significantly greater than MoO₃ alone and indicated that even the addition of a relatively low concentration of Ga₂O₃ improved propane conversion.

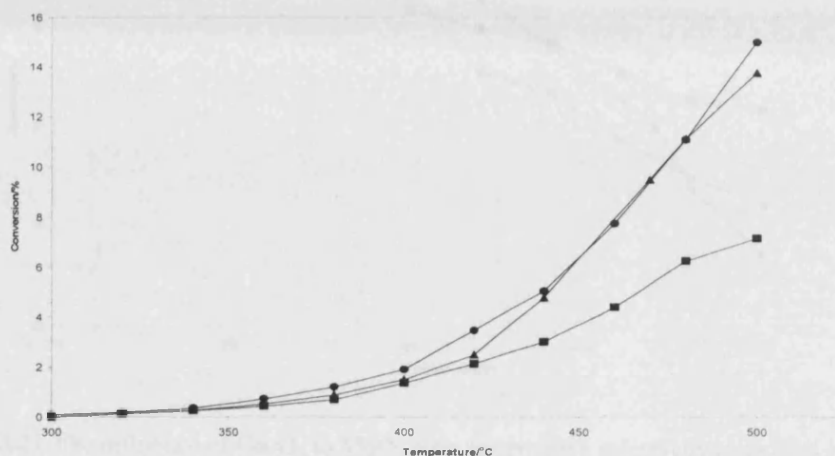


Figure 3.20 The influence of Ga₂O₃ to MoO₃ ratio for propane conversion over dual component Ga₂O₃/MoO₃ catalysts: ▲ 1/1 Ga₂O₃/MoO₃ calcined; ● 1/3 Ga₂O₃/MoO₃ calcined; ■ 1/10 Ga₂O₃/MoO₃ calcined.

The selectivity to propene for the Ga₂O₃/MoO₃ catalysts with varying Ga/Mo ratios is presented in figure 3.21. The propene selectivity for Ga₂O₃ /MoO₃ catalysts with ratios 1/1 and 1/3 were broadly similar with selectivities decreasing from ca. 90% at 360°C to less than 50% at 460°C. Decreasing the Ga/Mo ratio to 1/10 resulted in an increased selectivity to propene. This was evident across the whole temperature range, although it must be noted that propane conversion was generally lower over the 1/10 Ga₂O₃/MoO₃ catalyst. The increase in selectivity due to the increased MoO₃ content (lower Ga₂O₃ content) was to be expected and is largely due to the lower conversion.

Ga_2O_3 is the active component in the catalyst mixture and appears to be responsible for the activation of the propane molecule and subsequent total oxidation to CO_x .

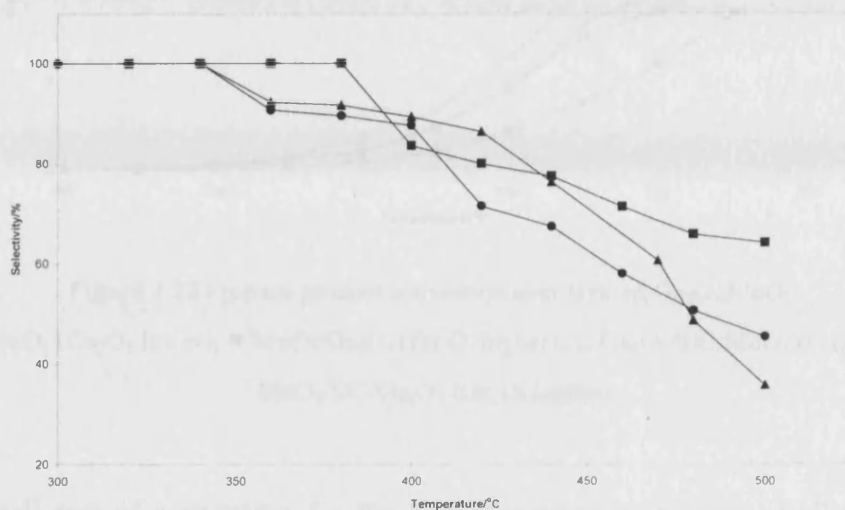


Figure 3.21 The influence of Ga_2O_3 to MoO_3 ratio for propane selectivity over dual component $\text{Ga}_2\text{O}_3/\text{MoO}_3$ catalysts: ▲ 1/1 $\text{Ga}_2\text{O}_3/\text{MoO}_3$ calcined; ● 1/3 $\text{Ga}_2\text{O}_3/\text{MoO}_3$ calcined; ■ 1/10 $\text{Ga}_2\text{O}_3/\text{MoO}_3$ calcined.

3.3.4 Propane oxidative dehydrogenation over $\text{Ga}_2\text{O}_3/\text{MoO}_3$ with varying bed arrangement

Varying the arrangement of the bed tested the effect of the individual components upon the activity of the catalyst. Figure 3.22 shows changes in propane conversion as a function of reaction temperature for the various bed compositions. The exact arrangement of the components can be found in the experimental section 2.2.3. The catalyst was arranged with either the two component oxides separated by a layer of inert silicon carbide (denoted $\text{Ga}_2\text{O}_3/\text{SiC}/\text{MoO}_3$ or $\text{MoO}_3/\text{SiC}/\text{Ga}_2\text{O}_3$) or in intimate contact (denoted $\text{Ga}_2\text{O}_3/\text{MoO}_3$ or $\text{MoO}_3/\text{Ga}_2\text{O}_3$). The Ga_2O_3 was tested in the lower or upper portion of the bed. As before, the main products were propene and CO_x .

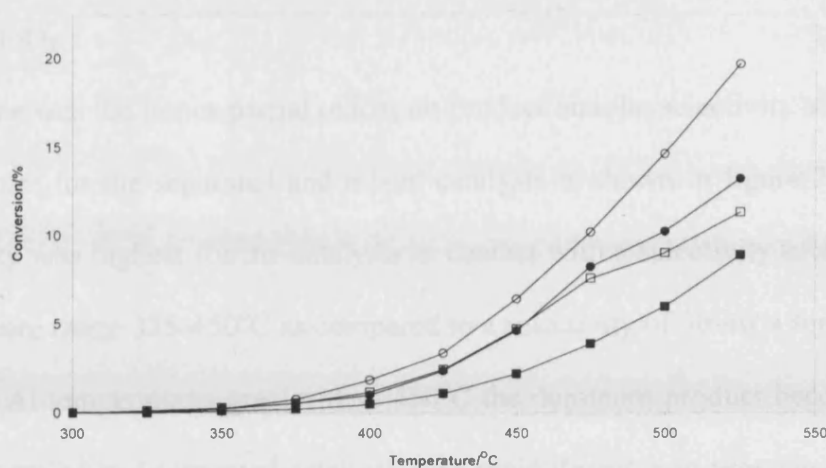


Figure 3.22 Propane product conversion over layered Ga₂O₃/MoO₃:

○ Ga₂O₃/MoO₃ (Ga₂O₃ lower); ● MoO₃/Ga₂O₃ (Ga₂O₃ higher); □ Ga₂O₃/SiC/MoO₃ (Ga₂O₃ lower); ■ MoO₃/SiC/Ga₂O₃ (Ga₂O₃ higher)

The overall rate of conversion for the beds separated by a layer of silicon carbide was lower than that of the beds in intimate contact. The Mo/Si/Ga catalyst (gallium in higher position) showed initial propane conversion at 350°C rising to 9% at 525°C. The Ga/SiC/Mo catalyst (gallium in lower position) was more active showing initial conversion at 325°C rising to a maximum of 11% at 525°C.

With the two oxides in intimate contact the overall conversion was higher. The Ga₂O₃/MoO₃ catalyst (gallium lower position) displayed initial conversion at 325°C with a maximum conversion of 20% at 525°C. Placing the gallium in the higher position resulted in a decrease in activity with initial conversion occurring at 350°C and a maximum conversion of 13% at 525°C. Both the calcined and uncalcined 1:1 Ga₂O₃/MoO₃ mechanical mixtures were more active over the entire temperature range, showing higher conversions at lower temperatures. At temperatures greater than 450°C there is a marked difference in activity between the separated and mixed catalysts: the uncalcined mixed catalyst showed a maximum conversion of 26% at 500°C. Allowing a point of contact between the two components increased the

conversion significantly with a rate of conversion similar to that of the calcined 1:1 Ga₂O₃/MoO₃.

Propene was the major partial oxidation product and the selectivity as a function of temperature for the separated and mixed catalysts is shown in figure 3.23. Propene selectivity was highest for the catalysts in contact with a selectivity of 50-70% in the temperature range 325-450°C as compared to a selectivity of 30-40% for the separated catalyst. At temperatures greater than 450°C the dominant product becomes CO_x for both the mixed and separated catalysts. The rapid decrease in propene selectivity for the catalysts in contact (ca. 40%) is due to the increased conversion as compared to the separated catalysts.

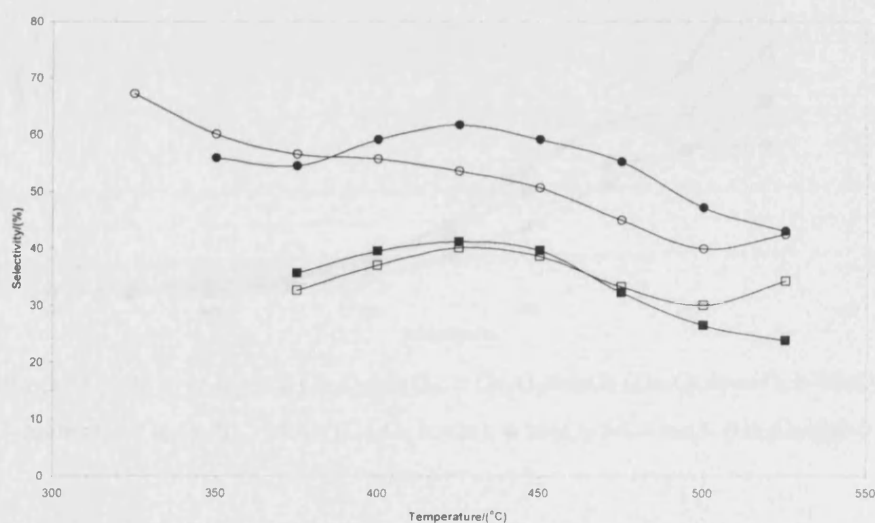


Figure 3.23 Selectivity to propene over layered Ga₂O₃/MoO₃: ○ Ga₂O₃/MoO₃ (Ga₂O₃ lower); ●

MoO₃/Ga₂O₃ (Ga₂O₃ higher); □ Ga₂O₃/SiC/MoO₃ (Ga₂O₃ lower); ■ MoO₃/SiC/Ga₂O₃ (Ga₂O₃ higher)

Propene yields are given in figure 3.24. The Ga₂O₃/MoO₃ in contact, with the gallium oxide in the lower portion of the bed, produced the highest maximum yield of propene: at 525°C the propene yield is 6.7% but due to the high temperature the dominant product is CO₂ and the selectivity to propene is just 40%. The propene yield over the separated Ga₂O₃/SiC/MoO₃ was similar to that of the catalyst in contact but decreases to 4.6% at 525°C. The lowest propene yield was over the catalysts arranged with MoO₃ in the lower portion of the bed with a maximum yield of around 3% at 525°C.

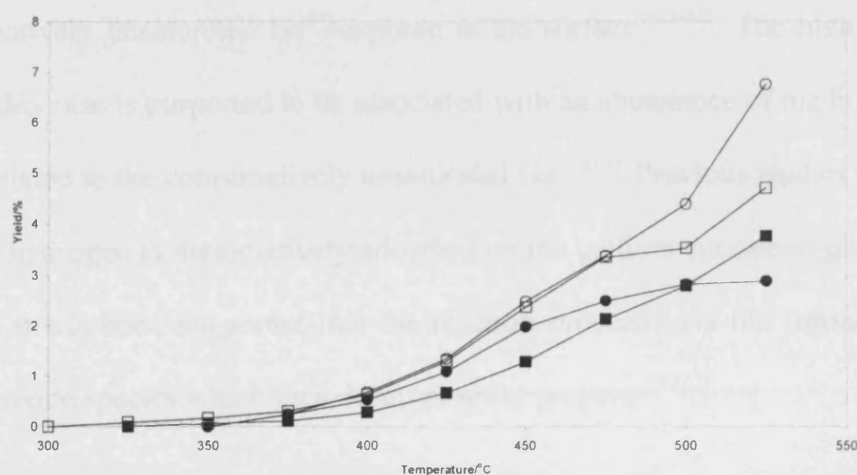
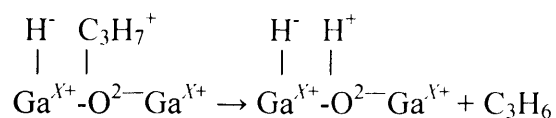
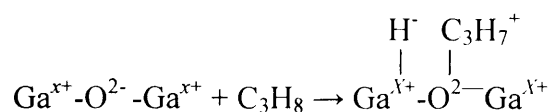


Figure 3.24 Propene yield over layered Ga₂O₃/MoO₃: ○ Ga₂O₃/MoO₃ (Ga₂O₃ lower); ● MoO₃/Ga₂O₃ (Ga₂O₃ higher); □ Ga₂O₃/SiC/MoO₃ (Ga₂O₃ lower); ■ MoO₃/SiC/Ga₂O₃ (Ga₂O₃ higher)

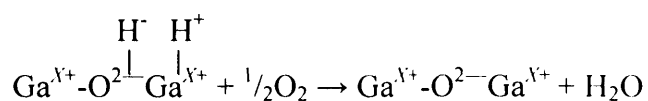
3.4 Discussion

The 1:1 Ga₂O₃/MoO₃ catalysts produced a propene yield comparable with known active propane oxidative dehydrogenation catalysts. It is therefore interesting to consider the origin of this activity. In earlier studies investigating CH₄/D₂ exchange it has been shown that the rate of reaction for Ga₂O₃ was at least two orders of magnitude greater than any other metal oxide [2-3]. The exchange reaction is used as a

probe for C-H bond activation and the data from the earlier study demonstrate that Ga₂O₃ is a very effective catalyst for alkane activation. It has also been shown that of all the gallium oxide polymorphs, β-Ga₂O₃ is the most reactive for the ODH of propane using CO₂ as an oxidant ^[9] with an intrinsic activity almost twice that of the other gallium oxide polymorphs. It is also noteworthy that Ga₂O₃ is used in combination with H-ZSM5 for the Cyclar process to convert propane to aromatics. Ga₂O₃ is implicated in alkane activation through a dehydrogenation step, although this is a non-oxidative process ^[10]. β-Ga₂O₃ is known to have a unique structure with oxide ions in distorted ccp and Ga³⁺ in distorted tetrahedral and octahedral sites with the coordinatively unsaturated Ga³⁺ exposed at the surface ^[11-12]. The high catalytic activity in this case is purported to be associated with an abundance of medium strong acid sites related to the coordinatively unsaturated Ga³⁺ ^[13]. Previous studies have also shown that hydrogen is dissociatively adsorbed on the gallium surface to give H⁺ and H⁻ ^[14], and it has been suggested that the reaction proceeds via the formation of a gallium alkoxide species which then decomposes to propene ^[9,15]:



The reduced surface may then be reoxidised by O₂ to give water:



Such a mechanism was proposed to account for the fact that gallium oxide is hardly reduced during the reaction and the temperature programmed reduction of the pure Ga₂O₃ tested in this study show that this is indeed the case (section 3.2.4). However, although both the Ga₂O₃ and MoO₃ catalysts showed no reduction below 600°C the mixed Ga₂O₃/MoO₃ showed a reduction feature at ca. 400°C indicating that reduction of the catalyst at the temperatures studied is possible. Propane conversion over Ga₂O₃/MoO₃ may follow a redox mechanism whereby propane is oxidized to propene with the simultaneous reduction of the mixed metal oxide. The reduced metal oxide is then re-oxidized by O₂.

Comparison of the propane oxidation over Ga₂O₃ and MoO₃ showed that the conversion over Ga₂O₃ was considerably higher than that for MoO₃. This is consistent with the ability of Ga₂O₃ to activate alkanes. On the contrary MoO₃ alone was very selective for propane oxidative dehydrogenation to propene. The same pattern was seen for the diluted MoO₃/SiC although this was not the case for the diluted Ga₂O₃/SiC. Addition of silicon carbide to the Ga₂O₃ catalyst led to a slight increase in conversion and selectivity indicating that dilution of the Ga₂O₃ component has a positive effect on catalyst activity. It may well be the case that dilution helps control over oxidation by allowing better heat removal from the bed. However, the mixing (and hence dilution) of Ga₂O₃ with MoO₃ results in a better catalyst than dilution with an inert indicating that MoO₃ plays an active role in the propane conversion and affords some control over the selectivity.

The data from catalysts with varying Ga/Mo emphasize the importance of the synergy between Ga₂O₃ and MoO₃. As the Ga/Mo ratio was decreased from 1/3 to

1/10 the behaviour of the dual component catalyst tended towards the behavior exhibited by MoO₃. Furthermore it was demonstrated that by separating the Ga₂O₃ and MoO₃ the overall activity and selectivity of the catalyst was decreased. The position of the Ga₂O₃ within the bed altered the activity. These data reiterate that the Ga₂O₃ component is important for increasing the rate of propane conversion, whilst the MoO₃ imparts selectivity to propene.

The combination of the two oxides demonstrated a synergistic effect to produce a marked increase in propene yield. The Ga₂O₃/MoO₃ catalyst has been used successfully for methane partial oxidation to methanol ^[11]. It is interesting that the addition of Ga₂O₃ to MoO₃ resulted in an increased methanol yield by promoting methane conversion, whilst maintaining the higher methanol selectivity of MoO₃. The same type of synergy was observed for selective propane oxidation in the present study and it is apparent that both reactions have similarities, as the alkanes must be activated before undergoing partial oxidation.

The characterisation data indicates that the Ga₂O₃/MoO₃ catalysts were comprised from a physical mixture of Ga₂O₃ and MoO₃. This being the case the synergy developed between the two oxides is associated with the boundary where the oxides are in contact with each other. This type of contact synergy is known for Ga₂O₃ in other reactions ^[13], and it appears that the effect is also important for propane partial oxidation.

The Ga₂O₃ phase present in the catalysts has a marked effect on the catalysts overall activity and explains the difference in activity between the calcined and uncalcined Ga₂O₃/MoO₃ mixture. Calcination of Ga₂O₃ at 650°C leads to the formation of the thermodynamically more stable β-Ga₂O₃ with the loss of the hydroxy gallium oxide. TGA analysis of the hydroxide by C. Otero Arean *et al* showed that it lost water over the temperature range 390-650 K (117-377°C) ^[15]. The studies indicate that the

presence of the hydroxy gallium oxide GaO(OH) results in a more active but less selective catalyst for propane oxidative dehydrogenation.

3.5 Conclusions

Catalysts based on a physical mixture of Ga₂O₃ and MoO₃ have been prepared and evaluated for propane dehydrogenation by partial oxidation. Characterisation studies indicated that the catalyst was comprised of a mixture of the component Ga₂O₃ and MoO₃ oxides with no formation of any new mixed phase. The Ga₂O₃/MoO₃ catalyst synergistically combined the alkane activation properties of Ga₂O₃ with the selective oxidation function of MoO₃. The yield of propene of the non-optimised Ga₂O₃/MoO₃ catalyst was comparable with a V₂O₅/TiO₂ catalyst, which is known to be active for propane ODH. Reducing the Ga/Mo ratio from 1/1 resulted in a slight decrease of propene yield whilst reducing the ratio to 1/10 resulted in a significantly reduced yield. Dilution of the Ga₂O₃ component with inert silicon carbide leads to an increase in activity and selectivity when compared to the undiluted Ga₂O₃. Ga₂O₃ on its own is good at activating propane but is not very selective; the converse is true for MoO₃. It may be the case that surface migration from one active site to another is an important factor with MoO₃ suppressing the total combustion of the propane molecule to CO_x and thus increasing selectivity.

3.6 References

- [1] J.S.J. Hargreaves, G.J. Hutchings, R.W. Joyner, S.H. Taylor, *Chem. Commun.*, (1996) 523
- [2] J.S.J. Hargreaves, G.J. Hutchings, R.W. Joyner, S.H. Taylor, *Appl. Catal. A. Gen.* 227 (2002) 191
- [3] S.H. Taylor, *Ph.D. Thesis. University of Liverpool*, 1994
- [4] F.C Munier, A. Yasmeeen and J.R.H Ross, *Catal. Today*, (1997) 33
- [5] V. Cortes Corberan, R.X. Valenzuela, Z.Olejniczak, B. Sulikowski, A. Perez Pujol, A. Fuerte and E. Wloch, *Catal. Today*, 78 (2003) 247-256
- [6] T.E. Davies and S.H. Taylor, *J. Mol. Catal. A. Chem.*, 220 (2004) 77-84
- [7] C. Otero Arean, A. Lopez Bellan, M. Penarroya Mentrut, M. Rodriguez and G. Turnes Palomino, *Micro. and Meso. Mat.*, 40 (2000) 35-42
- [8] B. Sulikowski, Z. Olejniczak and V. Cortes Corberan, *J. Phys. Chem.*, 100 (1996) 10323-10330
- [9] M. Saito, S. Watanabe, I. Takahara, M. Inaba, K. Murata, *Catal. Lett.*, 3-4 (2003) 213
- [10] Y. Yue, B. Zheng, W. Hua and Z. Gao, *J. Catal.*, 232 (2005) 143-151
- [11] E. Iglesia, J.E. Baumgartner, *Catal. Lett.*, 21 (1993) 55
- [12] N.N. Greenwood and A. Earnshaw, *Chemistry of the Elements*. Pergamon Press. 1994
- [13] M. Marezio, J.P. Rameika, *J. Chem. Phys.* 46 (1967) 1862
- [14] C. Otero Arean and M. Rodriguez Delgado, *Mat. Lett.*, 57 (2003) 2292-2297
- [15] P. Meriaudeau and M. Primet, *J. Mol. Catal.*, 61 (1990) 227
- [16] P. Meriaudeau, C. Naccache, *J. Mol. Catal.*, 59 (1990) L31

Chapter 4

Chapter 4

Cobalt oxide catalyst for the low temperature oxidative dehydrogenation of propane

4.1 Introduction

The production of chemicals by energy efficient and environmentally friendly routes is an important aim for the modern pharmaceutical and chemical industries. In particular, the facile utilisation of cheap and relatively abundant feedstocks such as short chain alkanes (C_1 - C_4) remains a challenging target ^[1, 2]. In the previous chapter, it was shown how a physically mixed Ga_2O_3/MoO_3 catalyst was capable of propane oxidative dehydrogenation at temperatures between 350°C-500°C. The results were comparable to other catalysts studied in the literature but were not as good as those regarded, and proven, to be the best such as vanadium containing oxides.

The overall aim of the project was to design multi component catalysts containing the redox and Brønsted acid functionalities so that iso-propanol can be synthesised from propane in a single stage process. This meant that it was necessary to find a catalyst capable of propane conversion at temperatures low enough to allow the resulting propene to be further hydrated to iso-propanol. The typical operating temperature for the hydration reaction over existing catalysts is between 100-300°C and given that the Ga_2O_3/MoO_3 catalyst was inactive below 350°C, it was found to be unsuitable for use in the hydration reaction.

The following chapter reports the results for propane oxidative dehydrogenation over Co_3O_4 . Co_3O_4 is an important and versatile ceramic oxide that is stable in the cubic spinel-type structure. It is used in magnetic ^[3], electrochemical ^[4] and catalytic applications and it is its application in catalysis that makes it most interesting.

According to Bond ^[5] catalysts used in dehydrogenation reactions are typically n-type semiconducting metal oxides. Co_3O_4 , however, is an example of a p-type semiconductor, which is more active in catalytic combustion. Co_3O_4 is known to be highly active for CO oxidation ^[6-8] as well as being an active component in materials used for the catalytic purification of exhaust gases ^[9]. It is its catalytic activity for hydrocarbon combustion that is the most interesting. Co_3O_4 has been reported to be the most active in hydrocarbon catalytic combustion among simple oxides ^[10,11] and a number of studies have focused specifically on propane and propene combustion ^[12,13].

It is against this background that Co_3O_4 was chosen and studied for the oxidative dehydrogenation of propane to propene. It was envisaged that it might be possible to control or hinder the total combustion reaction at low temperatures allowing the formation and propene.

4.2 Characterisation

4.2.1 BET surface areas

Table 4.1 BET surface areas of Co_3O_4 . Effect of preparation conditions.(Maximum error $\pm 10\%$)

Calcination Temperature ($^{\circ}\text{C}$)	Aged (h.)	BET surface area (m^2g^{-1})
250	1	78
400	1	35
550	1	10
250	3	79
400	3	35
550	3	12
Commercial (Avacado)	n/a	4



The BET surface areas for the cobalt oxide catalysts are shown in table 4.1. Varying the aging time between 1-3 h. had little effect on the surface areas. However, increasing the calcination temperature led to a pronounced decrease in surface area due to sintering of the catalyst. Calcination of the precursor at 250°C resulted in a catalyst surface area of c.a. 78m²g⁻¹. Calcination at higher temperatures of 400°C and 550°C resulted in surface areas of around 35 and 10m²g⁻¹ respectively. The cobalt oxide obtained from a commercial source had the lowest surface area of 4m²g⁻¹, far lower than those prepared by precipitation.

4.2.2 X-Ray Diffraction

The powder X-ray diffraction patterns for the precipitated Co₃O₄ catalysts are shown in figure 4.1. The figure shows the diffraction pattern for the precursor, the calcined catalyst (400°C; 2h) and the used catalyst (0-140°C. C₃H₈/O₂/He=1/20/79, 4800 h⁻¹). The precursor was obtained by precipitation of the corresponding nitrate and drying for 16 hrs at 120°C.

The precursor is highly amorphous with no definite phases present in the pattern. Calcination of the precursor at 400°C gave rise to the spinel Co₃O₄. The position of the diffraction peaks fits well to cubic spinel type structure of the Co₃O₄ as confirmed by JCPDS data and is in good agreement with the literature ^[6]. No other crystalline phases could be detected indicating that the spinel cobalt is the only crystalline phase formed, however, reflections from some of the crystal planes are missing from the pattern.

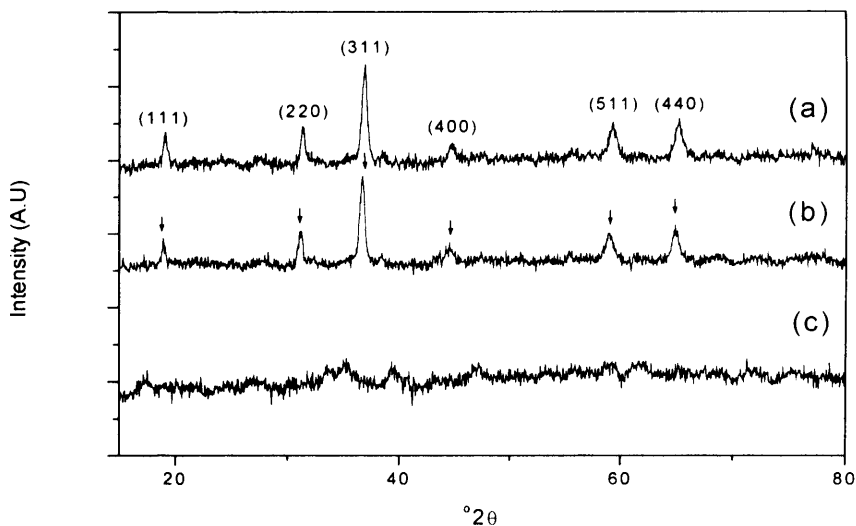


Figure 4.1 X-ray diffraction patterns of Co_3O_4 . (a) Co_3O_4 used in reaction, (b) Fresh Co_3O_4 , (c) Co_3O_4 precursor

The diffraction pattern from the used Co_3O_4 catalyst showed no major changes from the fresh. There is a minor difference in the intensity and definition of some of the diffraction peaks, which may be as a result of the further heat treatment during the reaction or surface restructuring due to reduction.

Figure 4.2 shows the x-ray diffraction pattern for the precipitated cobalt oxide compared to the commercial sample obtained from Avocado. The commercial catalyst is more crystalline than its precipitated counterpart with diffraction peaks from crystal planes attributed to Co_3O_4 that are not present in the precipitated catalyst. The prepared Co_3O_4 is more amorphous and does not show diffraction from the (422), (731) or (751) crystal planes that are present in the commercial sample.

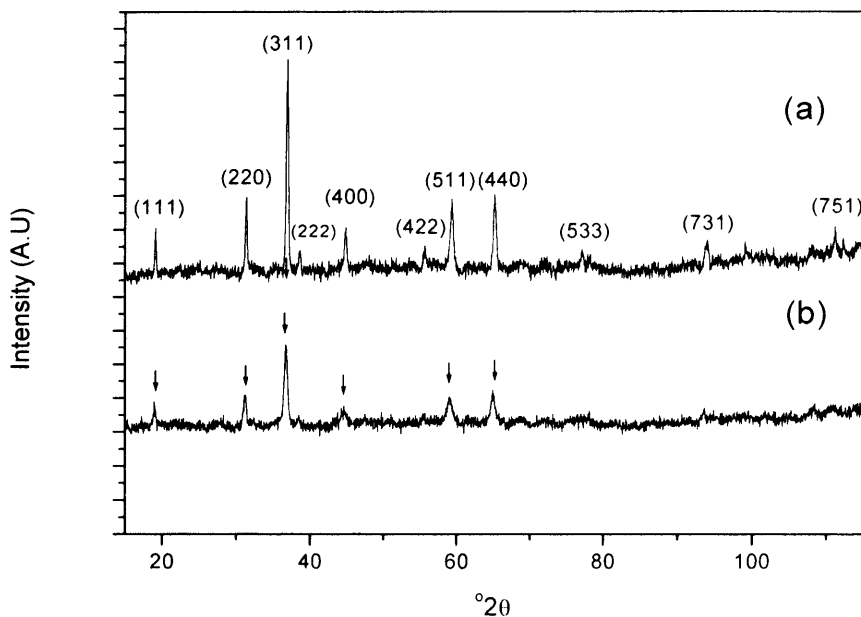


Figure 4.2 X-ray diffraction patterns of Co_3O_4 . Comparison with commercial Co_3O_4 . **(a)** Commercial Co_3O_4 (Avocado), **(b)** precipitated Co_3O_4 .

4.2.3 Temperature programmed reduction

Temperature programmed reduction and oxidation experiments were conducted as described in the experimental (section 2.3.5: catalyst = 0.05-0.1g, flow = 50 ml min⁻¹ 10% H_2 /Ar, ramp rate = 10°C min⁻¹). Figure 4.3 shows the temperature-programmed oxidation of the cobalt precursor. The major oxidation feature occurs at 290°C and corresponds to the formation of the stable Co_3O_4 .

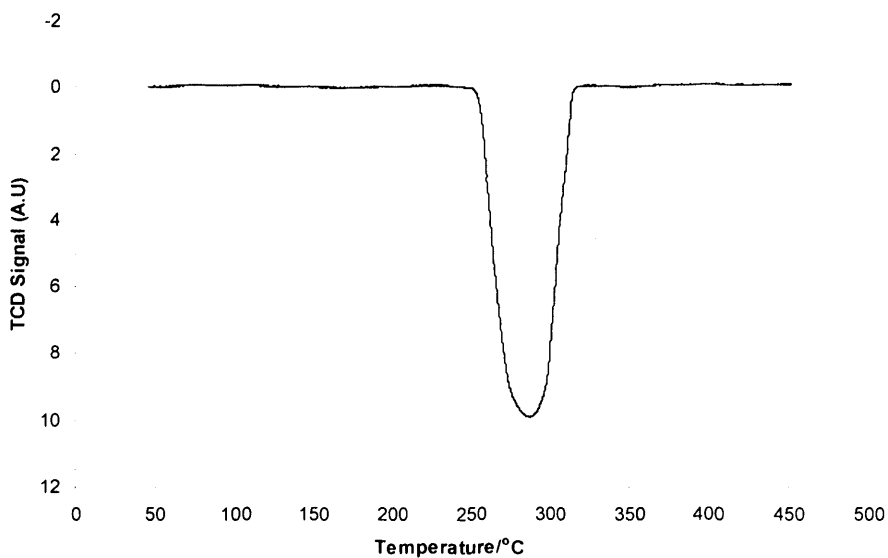


Figure 4.3 Temperature programmed oxidation of cobalt oxide precursor.

Figure 4.4 shows the TPR profiles for the freshly prepared catalyst and the activated catalyst (400°C, 2 h, 10% O₂/He). Activation of the catalyst prior to the test is necessary to remove CO₂ associated with the surface. Both catalysts show major

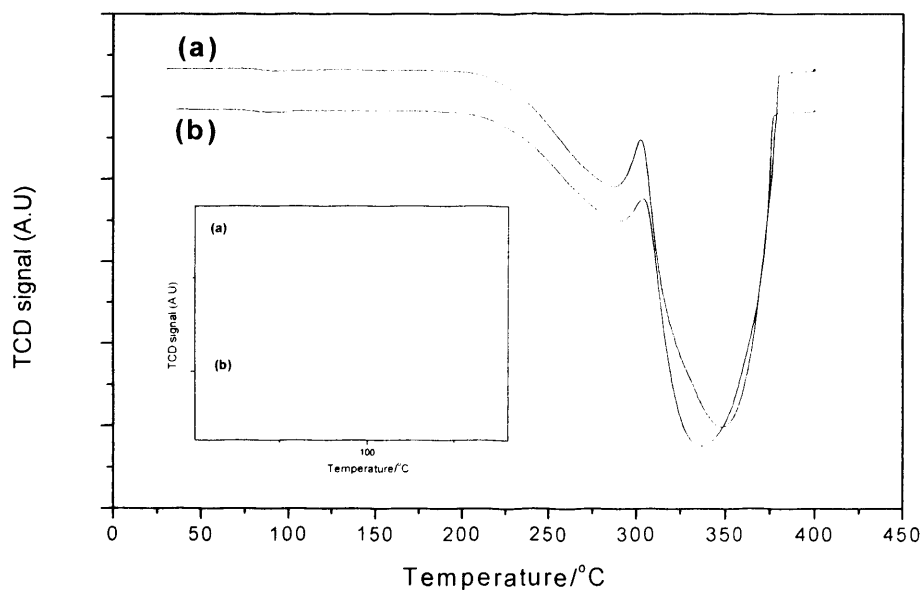


Figure 4.4 Temperature programmed reduction of: (a) fresh precipitated Co₃O₄ (b) Activated Co₃O₄.
Inset: Close up of the low temperature reduction feature

reduction peaks at c.a. 290°C and c.a. 350°C attributed to the reduction of Co_3O_4 to CoO and from CoO to Co [6]. There is little difference between the two profiles other than a slight decrease in the temperature of the major $\text{CoO} \rightarrow \text{Co}$ reduction peak, which shifts from 350°C to 330°C for the activated catalyst.

A surprising low intensity reduction feature was also observed at 90-100°C and is shown in the inset. This reduction feature was present in both the fresh and activated catalyst and remained largely unchanged after activation. This reduction feature is difficult to assign to any specific species and given its low intensity may be the result of reduction of a specific active centre or oxygen species present on the surface.

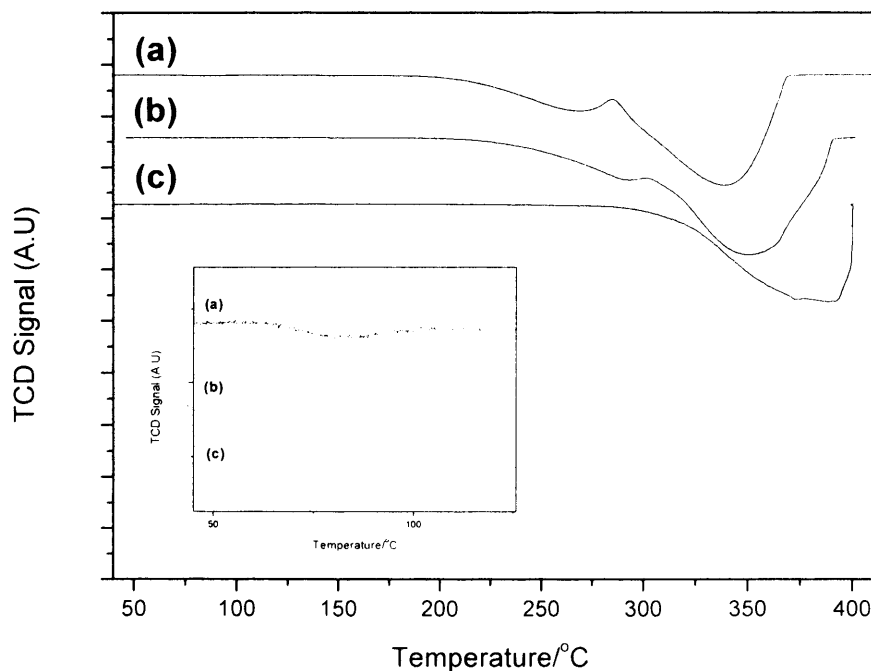


Figure 4.5 Temperature programmed reduction of: (a) fresh precipitated Co_3O_4 (b) used Co_3O_4 (c) Commercial Co_3O_4

Figure 4.5 shows the TPR profiles for the fresh, used and commercial Co_3O_4 catalysts. The catalyst was tested against a commercial sample to see if the preparation method used here produced a catalyst with differing properties. Also, in research done by others ^[15], the Co_3O_4 catalyst studied has been from a commercial source. The fresh catalyst, (a), showed the same reduction peaks mentioned previously including the low-temperature reduction feature at 80-100°C. The TPR profile of the post-reaction catalyst, (b), showed no low-temperature reduction feature indicating that *in situ* reduction of the catalyst had occurred during the reaction. The two larger reduction features are also seen to shift to higher temperatures.

The 80-100°C reduction feature was also missing from the commercial Co_3O_4 , (c). The two major peaks present in the fresh catalyst at 268°C and 338°C are not as well defined in the commercial sample, and the onset of H_2 consumption is at higher temperatures. Table 4.2 gives the precise temperatures of the reduction peaks for the Co_3O_4 catalyst tested.

Table 4.2 Temperature of reduction peaks

Catalyst	Reduction Peak (°C)
Fresh precipitated Co_3O_4	81, 268, 338
Used Co_3O_4	293, 350
Commercial Co_3O_4	373(Sm. Shoulder), 389

4.3 Results

4.3.1. Initial experiments

The Co_3O_4 catalyst was prepared as described in experimental section 2.1.3. The catalyst was tested in the 25-140°C temperature range. After the first test the catalyst was reactivated *in situ* (400°C, 3h, flow=20ml min⁻¹, O₂//He=10/90) and tested again. The exact conditions are described in the experimental section 2.2.4. The results for propane conversion can be seen in figure 4.6. Each data point is the average of 3 injections. The reaction data in the work were reproducible with a precision of ±4%

The catalyst showed initial activity at 60°C with a conversion of ca. 0.1% rising to 4% at 140°C. The only products were propene and CO₂. Such a low temperature of conversion is surprising for propane oxidative dehydrogenation, which typically operates in the 350-600°C temperature range. Reactivation of the used catalyst led to a decrease in activity. The reactivated catalyst was no longer active at 60°C and showed initial activity at 80°C with propene in trace concentrations. The conversion at 140°C was 0.6%, far lower than that of the fresh Co_3O_4 .

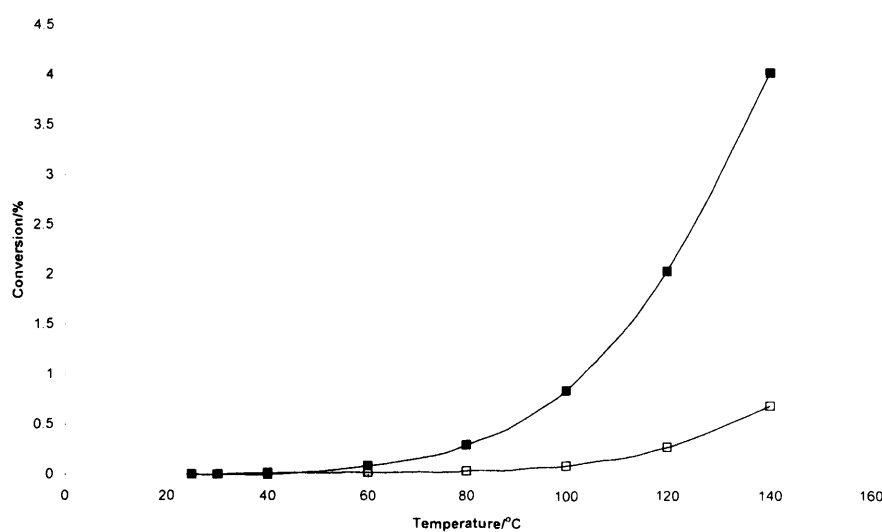


Figure 4.6 Propane conversion over fresh and reactivated Co_3O_4 : (■) fresh Co_3O_4 (□) reactivated Co_3O_4 (400°C, 3 h, flow=20ml min⁻¹, O₂/He=20/80)

The selectivity to propene over both the fresh and used Co_3O_4 is shown in figure 4.7. The fresh Co_3O_4 catalyst shows a maximum selectivity of 28% at 140°C, as CO_2 is the dominant reaction product. The selectivity to propene remains stable, with maximum propene selectivity not exceeding 28% beyond 100°C. The reactivated catalyst showed a higher selectivity to propene but only as a result of the lower conversion. As with the fresh catalyst the selectivity is seen to rise, increasing from 32% at 80°C to 39% at 140°C.

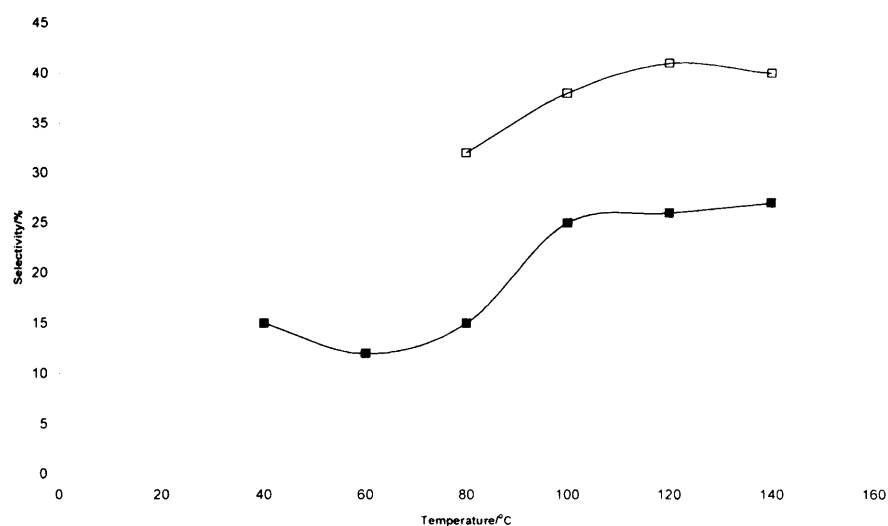


Figure 4.7 Propene selectivity over fresh and reactivated Co_3O_4 : (■) fresh Co_3O_4 (□) reactivated Co_3O_4 (400°C, 3 h, flow=20ml min⁻¹, O₂/He=20/80)

In the initial experiments on the Co_3O_4 catalyst the selectivity was found to increase when the used catalyst was treated at 400°C for 2h in 10% flowing O₂. It was envisaged that *in situ* pre-treatment of the fresh Co_3O_4 prior to testing may increase the activity and selectivity of the catalyst. It had been suggested that the CO_2 present in the original catalytic runs had not been a product of the reactants but had come from the catalyst itself, possibly associated with the surface and is driven off as the temperature of the reaction is increased. The results seen below seem to indicate that

this is indeed the case. Figure 4.8 shows the decrease in CO₂ concentration with time on line at 40°C. The catalyst was tested in a 10% O₂/He flow with no propane present. After approximately 150 minutes the CO₂ concentration was seen to decrease to 0%. If the reactor temperature is increased, more CO₂ is driven off the catalyst, the concentration of which then decreases to 0%. In subsequent experiments it was found that the optimum conditions for the total removal of CO₂ was *in situ* calcination at 400°C for 2h in a 20 ml min⁻¹ 10% O₂/He flow. Pre-treatment at temperatures greater than this resulted in a decrease in catalytic activity due to sintering of the catalyst and lower surface areas. Tests conducted on the empty reactor and an inert silicon carbide sample showed no CO₂ present in the feed (see appendix) indicating that the CO₂ was from the catalyst.

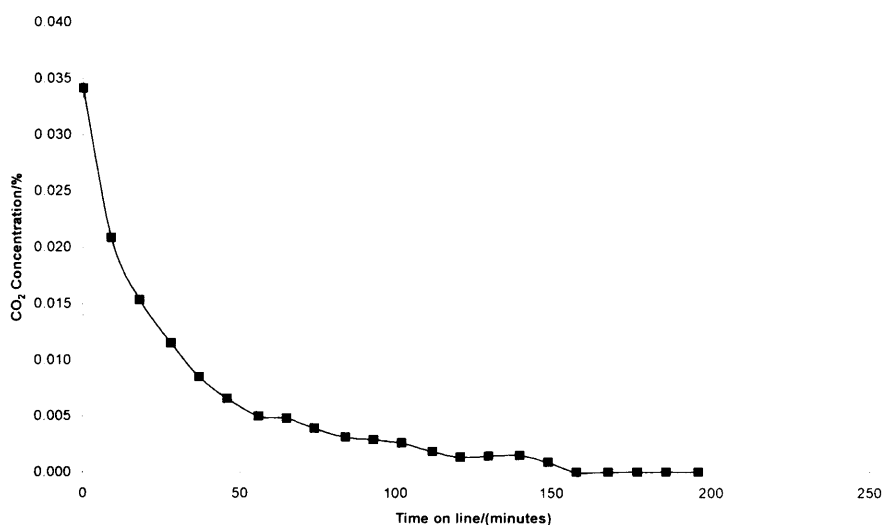


Figure 4.8 Effect of catalyst pre-treatment at elevated temperatures. 40°C; 10% O₂/He CO₂ concentration as a function of time on line

The results for propane conversion over the pre-treated Co₃O₄ can be seen in figure 4.9. The *in situ* calcination of the catalyst prior to the reaction was found to decrease the overall activity of the catalyst, however, the light off temperature of the catalyst

was decreased to ambient. Initial activity starts at 25°C, albeit with very low conversion, not achieving greater than 0.4% below 80°C. Above this temperature there is an increase in conversion achieving a maximum of 1.2% at 140°C. This is a lot lower than the untreated catalyst, which shows a maximum conversion of 4.0% at 140°C. It appears that the *in situ* pre-treatment lowers the light off temperature but also lowers the activity of the catalyst.

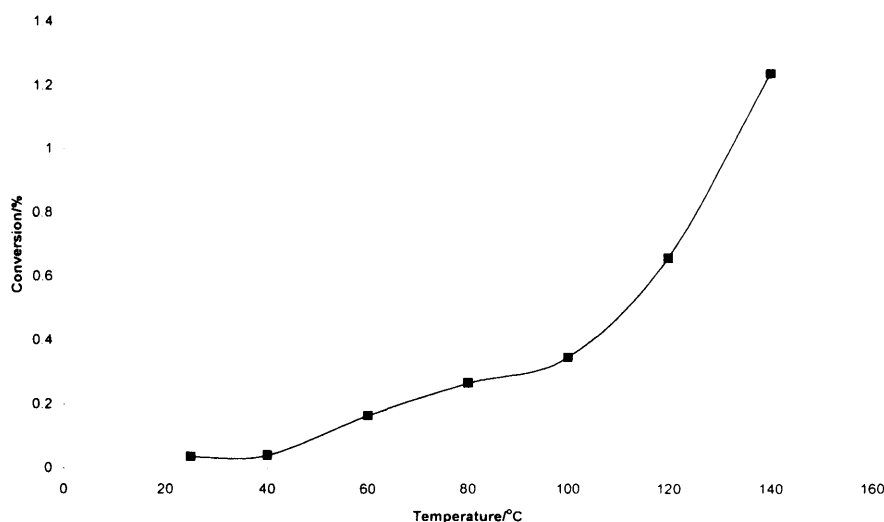


Figure 4.9 Propane conversion over pre-treated Co_3O_4 : Co_3O_4 (calcined 400°C, 3h.); *in situ* pre-treatment at 400°C, 2h, $\text{O}_2/\text{He} = 10/90\%$, 20ml min^{-1} .

Although the pre-treatment had a negative effect upon the conversion, it had a marked effect on the low-temperature selectivity of the catalyst. Figure 4.10 shows the selectivity to propene as a function of temperature for the pre-treated catalyst. The catalyst was 100% selective for propene below 80°C. Above this temperature the selectivity decreases, as the dominant reaction product becomes CO_2 . At 140°C the selectivity is 76%, as the temperature is increased the selectivity continues to decrease. It appears that the optimum selectivity and activity occurs in the temperature range 25-140°C.

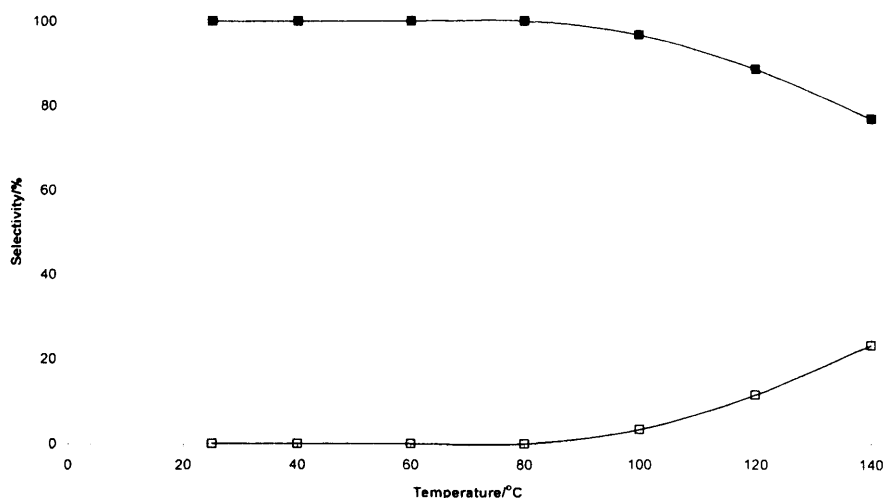


Figure 4.10 Selectivity to products over pre-treated Co_3O_4 : Co_3O_4 (calcined 400°C , 3h.); *in situ* pre-treatment at 400°C , 2h, $\text{O}_2/\text{He} = 10/90\%$, 20ml min^{-1} . (■) Propene; (□) Carbon dioxide.

As a result of the low conversion the propene yield was also very low, not achieving greater than 1%. The profile follows that of the conversion with the yield remaining at less than 0.5% up to 100°C . It is only at temperatures greater the 100°C that the propene yield increases with any significance. The maximum propene yield was just 0.95% at 140°C as can be seen in figure 4.11.

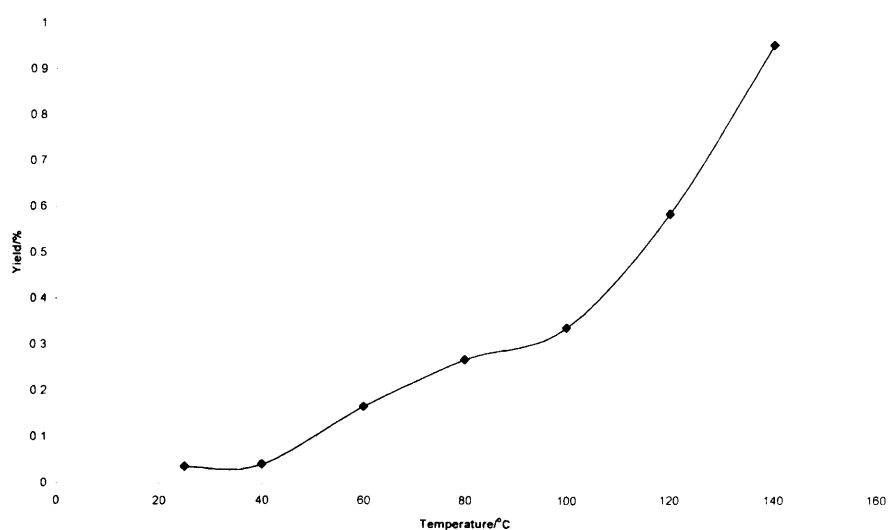


Figure 4.11. Propene yield over pre-treated Co_3O_4 : Co_3O_4 (calcined 400°C , 3h.); *in situ* pre-treatment at 400°C , 2h, $\text{O}_2/\text{He} = 10/90\%$, 20ml min^{-1} .

4.3.2 Variation in O₂ concentration

In an effort to increase the low-temperature conversion of the pre-treated Co₃O₄, the catalyst was tested in varying O₂ concentrations. The results for propane conversion are shown in figure 4.12. The catalyst was activated *in situ* prior to the run (400°C, 2h, 20 ml min⁻¹ 10% O₂/He flow).

With 0% O₂ in the feed the catalyst was still active at 25°C and showed conversions of 0.1% at 60°C. The overall conversion at temperatures below 80°C was comparable to the conversions obtained with oxygen concentrations of 10-35%. Above 80°C the conversion decreases to c.a. 0.1% and remains low with increasing temperature. Increasing the oxygen concentration to 99% resulted in a decrease in overall conversion. There was no conversion below 80°C and at 140°C the conversion achieves only 0.4% as compared to 1% in lower O₂ concentrations. However, the conversion in the 80-140°C temperature range is greater than when no gas-phase oxygen is present. Varying the O₂ concentration

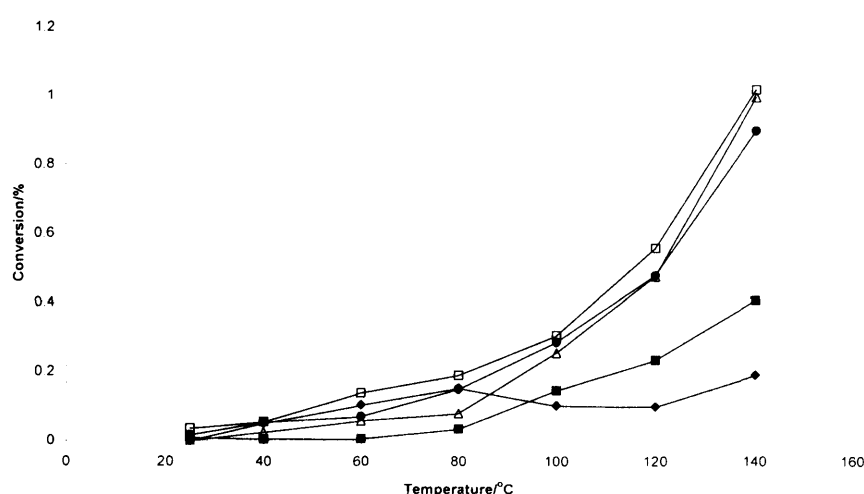


Figure 4.12 Effect of varying O₂ concentration on propane conversion.

Percentage O₂ in feed (♦) 0%, (Δ) 10%, (□) 20%, (●) 35%, (■) 99%

between 10-35% had little effect upon the activity of the catalyst. The catalyst was active at 25°C and in each case followed a similar reaction profile; at 60°C the conversion is approximately 0.1% and rises to 1% at 140°C. The optimum concentration for maximum conversion appears to 20%. Interestingly repeat runs showed that in the temperature range 25-80°C the conversions at each concentration were irreproducible and differed at each temperature between repeat reactions. However, the catalyst was active at ambient temperatures, and conversion was seen to increase gradually with increasing temperature never achieving higher than 0.2% below 80°C. Given the energy required to activate oxygen it is probably the case that molecular oxygen plays no part in the reaction at temperatures lower than 80°C. The activity and selectivity is quite possibly the result of lattice oxygen, which is consumed during the reaction rendering the catalyst inactive. The catalyst is not re-oxidising due to the low temperature.

The selectivity to propene for varying O₂ concentrations is shown in figure 4.13. Varying the concentration from 10-35% resulted in no change to the low-temperature selectivity. The catalyst was 100% selective for propene up to 80°C. At 140°C the selectivity decreased to around 80% in all cases.

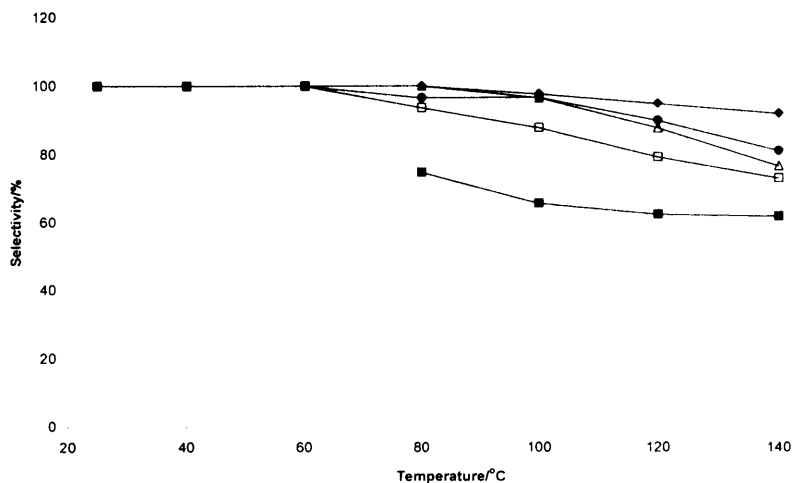


Figure 4.13 Effect of varying O₂ concentration on propene selectivity.

Percentage O₂ in feed; (◆) 0% (Δ) 10% (□) 20% (●) 35% (■) 99%

With no oxygen in the feed the selectivity decreases to only 90% at 140°C, the total combustion reaction is suppressed by the limiting oxygen concentration. Increasing the O₂ concentration to 99% resulted in over oxidation of the propene to CO₂ and consequently, a decrease in selectivity to 60% at 140°C.

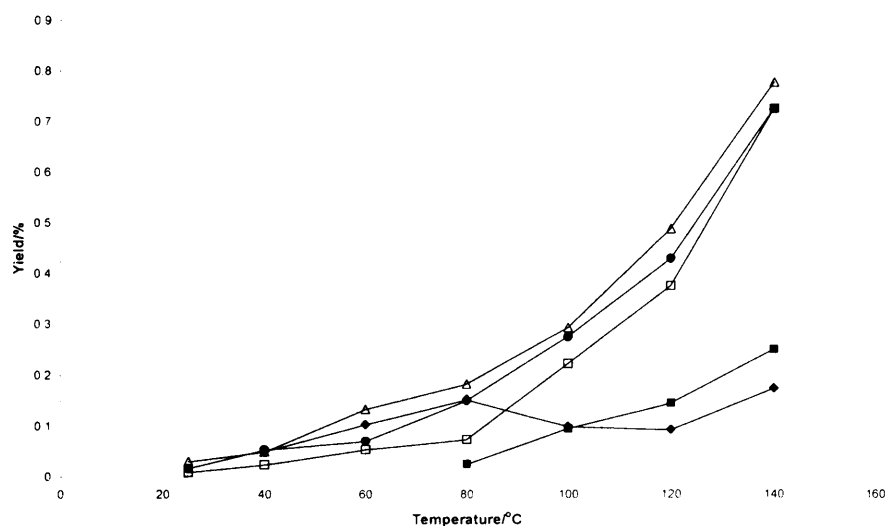


Figure 4.14 Effect of varying O₂ concentration on propene yield.

Percentage O₂ in feed; (◆) 0% (Δ) 10% (□) 20% (●) 35% (■) 99%

As a result of the low conversion the overall propene yield is low, not achieving greater than 1% (figure 4.14). With 0% O₂ in the feed the catalyst achieves a maximum yield of just 0.15%. Increasing the O₂ concentration to 10% increased the propene yield across the entire temperature range with a maximum yield of 0.8% at 140°C. Further increase in the oxygen concentration to 35% resulted in a decrease in yield. Saturating the feed with O₂ resulted in no propene production below 80°C. Above 80°C the yield is seen to increase with increasing temperature, but still remains relatively poor with a maximum conversion of just 0.2% at 140°C.

From the data it appears that varying the oxygen concentration between 10-35% has little effect on the conversion in the temperature range 25-80°C. Without gas-phase oxygen the reaction still proceeds, with conversions comparable to those when O₂ is present. In an O₂ saturated atmosphere the catalyst favours the combustion pathway and due to over dilution of the reactant propane with a competitive diluent i.e. O₂, the low temperature activity is lost and the conversion remains low.

4.3.3 Variation in calcination conditions

The effect of varying the ageing times and calcinations conditions were tested and the results for propane conversion and selectivity can be seen below in figure 4.15. The catalyst aging times were 1h and 3h. The resultant precursors were then calcined at 250°C, 400°C and 550°C. The 6 catalysts were prepared as described in the experimental section 2.1.3. Each catalyst was activated *in situ* prior to the run (400°C for 2h in a 20 ml min⁻¹, 10% O₂/He flow) and tested under typical conditions (C₃H₈/O₂/He=1/20/79, 4800 h⁻¹)

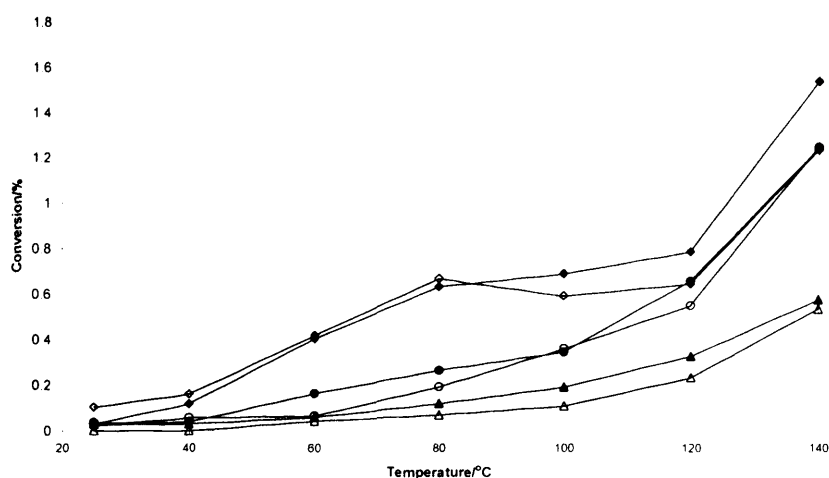


Figure 4.15 Effect of ageing time and calcination temperature on propane conversion over Co_3O_4 catalyst. (◆) Calcined 250°C/1h ageing (◇) Calcined 250°C/3h ageing (●) Calcined 400°C/1h ageing (○) Calcined 400°C/3h ageing (▲) Calcined 550°C/1h ageing (△) Calcined 550°C/3h ageing

It is worth noting that it took less time to activate the catalysts calcined at higher temperatures, there was more CO_2 associated with the catalyst calcined at 250°C than the catalyst calcined at 550°C.

Varying the ageing time between 1 and 3hrs had little effect on the catalyst activity. The reaction profiles for the different ageing times are broadly similar. Varying the calcination temperature of the Co_3O_4 had a marked effect on the activity of the catalyst. The Co_3O_4 calcined at 250°C displayed the highest rate of conversion increasing from 0.1% at 40°C to 1.5% at 140°C; this was to be expected given its higher surface area and low temperature of calcination. Calcination of the catalyst at higher temperatures resulted in a decrease in overall conversion. At 140°C the catalysts calcined at 400°C and 550°C show conversions of ca. 1.2% and 0.4% respectively.

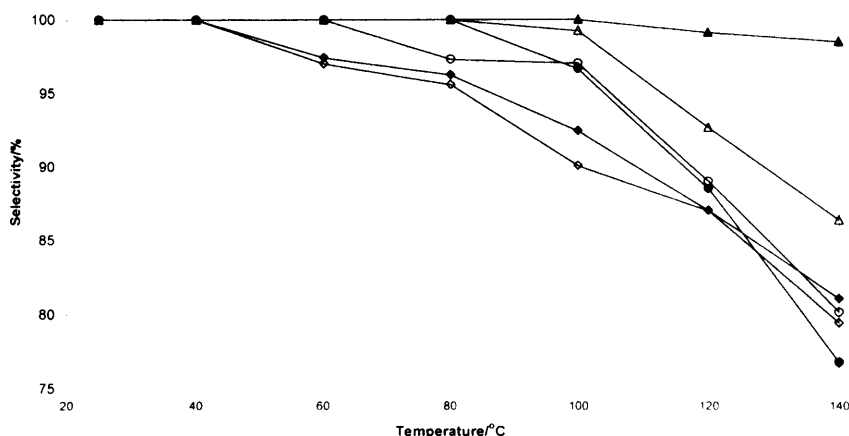


Figure 4.16 Effect of ageing time and calcination temperature on propene selectivity over Co_3O_4 catalyst. (◆) Calcined 250°C/1h ageing (◇) Calcined 250°C/3h ageing (●) Calcined 400°C/1h ageing (○) Calcined 400°C/3h ageing (▲) Calcined 550°C/1h ageing (△) Calcined 550°C/3h ageing

The selectivity to propene as a function of temperature is shown in figure 4.16. Again, varying the ageing time had little effect on the catalyst. The selectivity profiles for the 250°C and 400°C calcined Co_3O_4 are the same for both ageing times. Curiously, the 1h aged, 500°C calcined Co_3O_4 was more selective than its 3h aged counterpart with a selectivity of 97% at 140°C as compared to 85%.

The high activity of the 250°C-calcined Co_3O_4 resulted in a low selectivity. Selectivity drops from 100% at 40°C to 80% at 140°C. Calcining the precursor at higher temperatures increased the low temperature selectivity but at 80°C the selectivity decreases rapidly as the total combustion reaction becomes dominant. Calcination of the precursor at 400°C leads to a more active and selective catalyst overall. Calcination of the precursor at 550°C leads to a more selective catalyst but only due to the lower conversion.

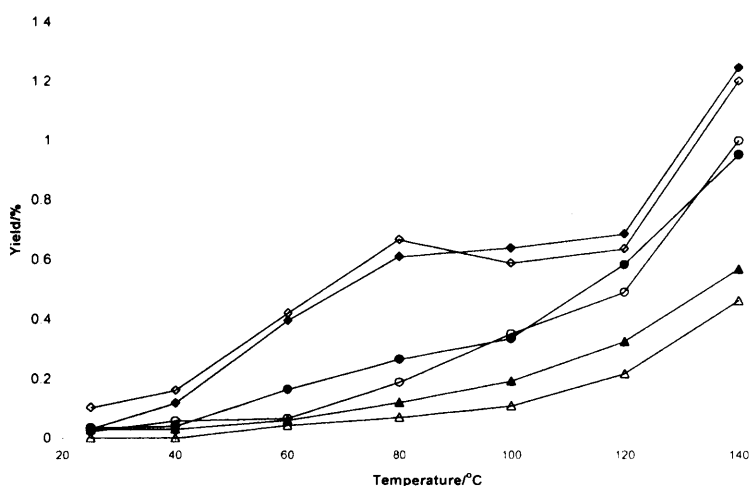


Figure 4.17 Effect of ageing time and calcination temperature on propene yield over Co_3O_4 catalyst.
 (◆) Calcined 250°C/1h ageing (◇) Calcined 250°C/3h ageing (●) Calcined 400°C/1h ageing (○)
 Calcined 400°C/3h ageing (▲) Calcined 550°C/1h ageing (△) Calcined 550°C/3h ageing

Propene yields are given in figure 4.17. Varying the ageing time between 1h and 3h had little effect on the yield. The catalyst calcined at 250°C gave the highest yield of 1.2% at 140°C, but with a propene selectivity of ca. 80%. At the lower temperature of 80°C the catalyst is far more active than the others tested with yields of 0.5% at 97% selectivity as compared to yields >0.3% for the catalysts calcined at higher temperatures. The catalyst calcined at 400°C showed a maximum yield of ca. 0.9% at 140°C. Increasing the calcination temperature to 550°C lowered the total propene yield.

4.3.4 Variation in flow rate

The effect of flow rate on the oxidative dehydrogenation of propene over Co_3O_4 was tested and the results are presented below. The catalyst tested was prepared as described in the experimental section 2.2.1. The precursor was calcined at 400°C for

2h. The reaction conditions were as previous but with varying flow rate. The concentration of the reactants remained the same in all experiments. ($C_3H_8/O_2/He=1/20/79$). Prior to testing the catalysts was activated *in situ* ($400^\circ C$ for 2h in a 20 ml min^{-1} 10% O_2/He flow).

The results for propane conversion are presented in figure 4.18. Increasing the gas hourly space velocity from 4800 h^{-1} to 19200 h^{-1} resulted in a decrease in conversion over the entire temperature range. All low temperature activity was lost with the light off temperature increasing to $60^\circ C$. The maximum conversion at $140^\circ C$ decreased to less than 0.4% for all flow rates greater than 4800 h^{-1} .

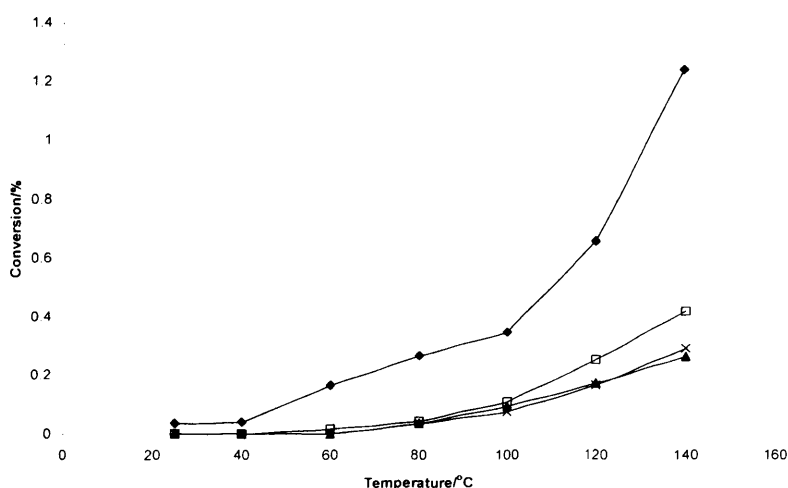


Figure 4.18 Effect of flow rate on propane conversion over Co_3O_4 catalyst: space velocities (♦) 4800 h^{-1} (x) 2400 h^{-1} (□) 14400 h^{-1} (▲) 19200 h^{-1}

The selectivity to propene as a function of temperature is shown in figure 4.19. Increasing the flow rate led to a loss of low temperature activity and hence no propene yield below $60^\circ C$. At temperatures greater than $80^\circ C$ the catalyst remained approximately 80% selective to propene. Space velocities of 4800 h^{-1} led to a more selective catalyst. The catalyst was 100% selective to propene in the temperature range $25-80^\circ C$. Above $80^\circ C$ the selectivity is seen to decrease with increasing

temperature. At 140°C the selectivity drops to below 80%. At higher temperatures it appears that increasing the space velocity does have the effect of increasing selectivity. At 140°C the selectivity for the catalyst running with higher flow rates remains greater than 80%.

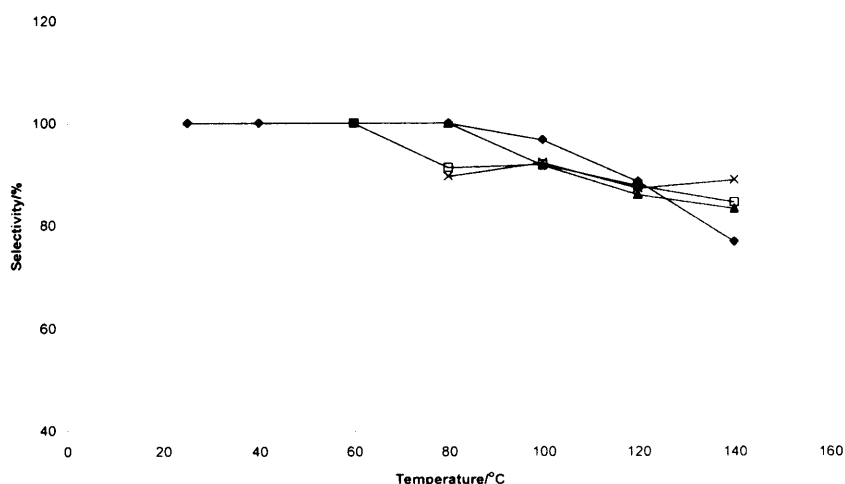


Figure 4.19 Effect of flow rate on propene selectivity over Co_3O_4 catalyst: space velocities (◆) 4800 h⁻¹ (×) 2400 h⁻¹ (□) 14400 h⁻¹ (▲) 19200 h⁻¹

It seems that at low temperatures a longer contact time is necessary for the catalyst to be active but at higher temperatures (>80°C) decreasing the contact time prevents over oxidation of the alkene to CO_2 .

4.3.5 Steady state activity

The CoOx catalyst was retested in the smaller reactor using 0.25g of sample. The reaction mixture was 20ml min⁻¹ comprising 1% propane in synthetic air mixture. ($\text{C}_3\text{H}_8/\text{O}_2/\text{He}=1/20/79$). The fresh catalyst was first tested until it showed complete deactivation before being reactivated at increasing temperatures for a period of 2h in 10% O_2 in He. After each reactivation the catalysts were retested for activity the

results for which are given in figure 4.20. The temperature of the reaction was 40°C and the selectivity to propene 100%. The freshly prepared Co_3O_4 showed rapid deactivation at 40°C with conversion decreasing from 0.05% to 0% in 80 minutes.

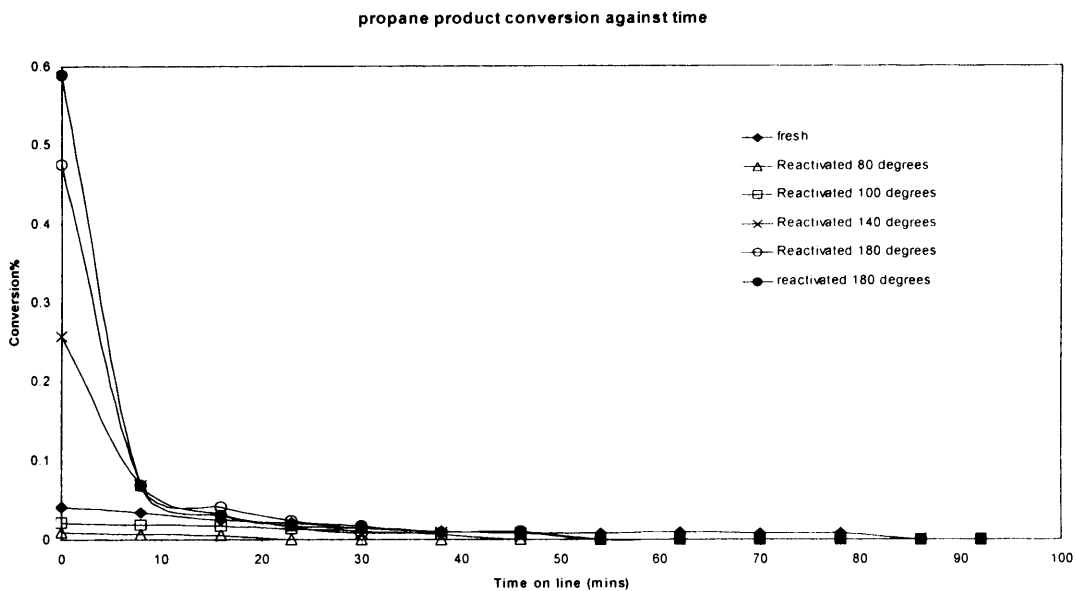


Figure 4.20 Steady state activity of Co_3O_4 at 40°C and the effect of reactivation at increasing temperature. Propane conversion as a function of time on line.

Calcination of the catalyst at 80 and 100°C gave rise to moderate activity displaying half of the original conversion of the fresh catalyst. The reactivated catalysts also deactivated more rapidly than the fresh and displayed zero conversion in less than 30 minutes. Reactivation of the catalyst at 140°C increased the initial conversion to almost 10 times that of the fresh but again deactivation was rapid with conversion dropping from 0.25% to less than 0.1% in 10 minutes, reaching zero conversion in approximately 45 minutes. Reactivation at 180°C resulted in the highest initial conversion of ca. 0.5% but again deactivation was rapid.

Although the selectivity to propene at 40°C is 100% the conversion at this temperature is very small and does not exceed 0.6 %. In order to increase the conversion and catalyst lifespan, the reaction temperature was increased, the results for which are shown in figure 4.21. In each case a fresh Co_3O_4 catalyst was used and was activated *in situ* prior to each run. The temperature of the reaction increased in 20°C increments.

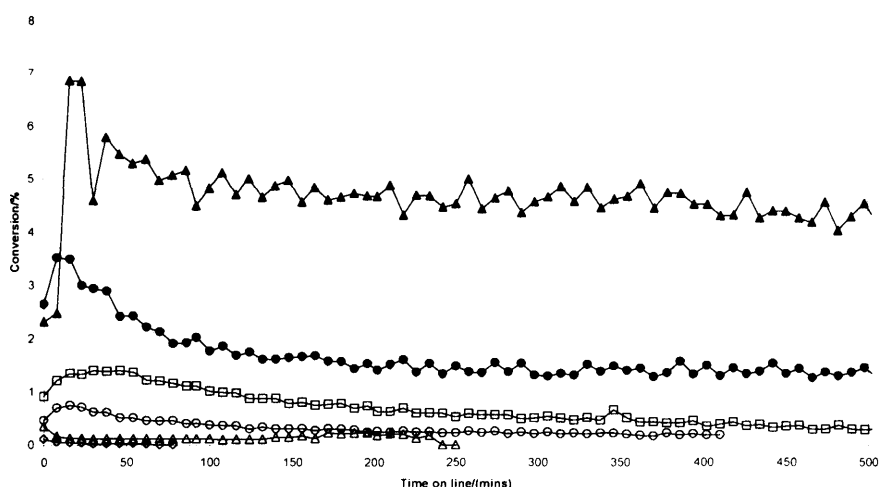


Figure 4.21 Steady state propane conversion over Co_3O_4 at different reaction temperatures as a function of time on line. (\diamond) 60°C, (Δ) 80°C, (\circ) 100°C, (\square) 120°C, (\bullet) 140°C, (\blacktriangle) 150°C

Increasing the temperature of the steady state reaction resulted in an increase in conversion and catalyst stability. At 60°C the conversion was still extremely low at 0.1% and decreased to 0% after approximately one hour. Increasing the reaction temperature to 80°C increased the initial conversion to 0.35% but the activity still decreased with time on line. At 80°C total deactivation took 250 minutes. At 100°C the conversion was still less than 1% and again the catalyst was not stable and deactivated steadily to 0% conversion after 400 minutes. At 120°C the conversion reaches 1% and the catalyst lifespan is increased to ca. 660 minutes. The catalyst still

shows steady deactivation with time on line with the conversion decreasing to less than 0.5% after 500 minutes. It is only when the reaction was run at 140°C that the conversion remained stable. The catalyst displayed a maximum conversion of 3.5% that decreased to 1.5% after 100 minutes. The catalyst showed no deactivation with time on line and maintained steady state conversion for the duration of the experiment. Increasing the temperature further to 150°C increased the maximum conversion to 5.5% that steadily decreased to 4% before becoming stable. It seems that temperatures of 140°C and greater are required for stable turnover of the catalyst.

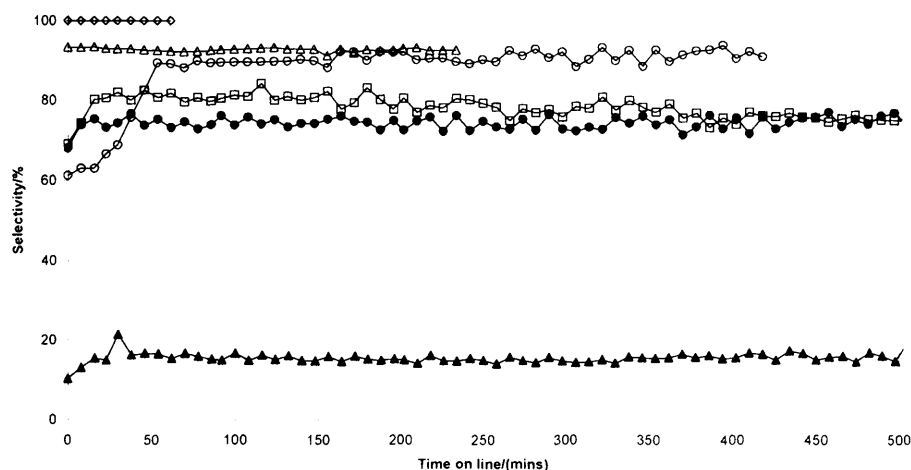


Figure 4.22 Selectivity to propene with steady state conversion over Co_3O_4 at different reaction temperatures as a function of time on line. (\diamond) 60°C, (Δ) 80°C, (\circ) 100°C, (\square) 120°C, (\bullet) 140°C, (\blacktriangle) 150°C

The selectivity to propene is shown in figure 4.22. Increasing the temperature of the reaction resulted in the expected decrease in selectivity. At 60°C the catalyst is still 100% selective to propene but the propane conversion at this temperature is near zero. Increasing the temperature by 20°C resulted in a decrease in selectivity with the selectivity at 80°C stabilising at ca. 92%. Running the catalyst at 100°C resulted in a

selectivity to propene of ca. 92%, similar to that of the catalyst run at 80°C. At 140°C, where the catalyst is stable, the selectivity is 75% and remains so for the duration of the experiment. At 150°C there is a large drop in selectivity. At this temperature the dominant reaction becomes the total combustion of propane with propene selectivity decreasing to just 15%.

The catalysts tested at 60°C and 80°C gave the lowest yields overall not achieving greater than 0.1% propene. Increasing the reaction temperature to 120°C increased the yield by a factor of five with the maximum propene yield being 0.5%. The highest yield was shown over the Co_3O_4 ran at 140°C. The catalyst gave a maximum yield of ca. 1% propene at 76% selectivity. Increasing the temperature of the reaction to 150°C resulted in a significant decrease in propene selectivity and hence a decrease in the yield to just 0.7%

4.3.6 Improved conversion with lower space velocities

In an effort to increase the low temperature conversion of the cobalt catalyst a 10g batch was prepared and tested in a large-scale reactor. The preparation of the catalyst is described in the experimental (section 2.1.3). A description of the apparatus used along with the specific reaction conditions is described in section 2.2.2. The reaction was conducted at 40°C and the selectivity to propene throughout the reaction was 100%. The propane conversion as a function of time on line is shown in figure 4.23 along with the propane conversion over the reactivated sample.

Propane conversion in the large-scale reactor turned out to be a lot lower than expected. Initial conversion at time zero was just 0.68% and decreased to less than 0.1% after 100 minutes.

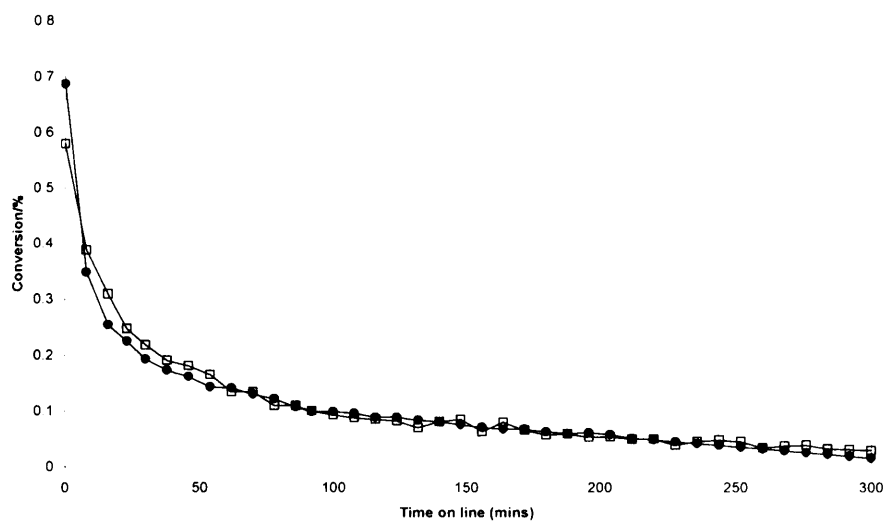


Figure 4.23 Propene conversion at 100% selectivity over 10g Co_3O_4 at 40°C . GHSV = 120 h^{-1}

It was envisaged that by using 40 times the original amount of catalyst the overall conversion would increase by the same factor. This was not the case. However, the catalyst lifetime was increased and reactivation of the catalyst (400°C , 2h. $10\%\text{O}_2$) resulted in an activity identical to that of the fresh. The total yield was extremely low rapidly decreasing to $<0.1\%$ after 100 minutes online

4.3.7 Comparison with commercial sample

The laboratory prepared Co_3O_4 was compared to a commercial Co_3O_4 . The commercial sample was used as received and was tested under identical conditions to the prepared sample. The catalyst was tested against a commercial sample to see if the preparation method used here produced a catalyst with differing properties. Also, in research done by others, the Co_3O_4 catalyst studied has been from a commercial source ^[15]. The results for propane conversion are presented in figure 4.24.

The commercial catalyst showed no activity below 140°C, light off occurred at 150°C with a conversion of 0.1%. This rose to a maximum of 0.4% at 200°C, significantly lower than the prepared catalyst which was active at room temperature and achieved a maximum conversion of 1.2% at 140°C.

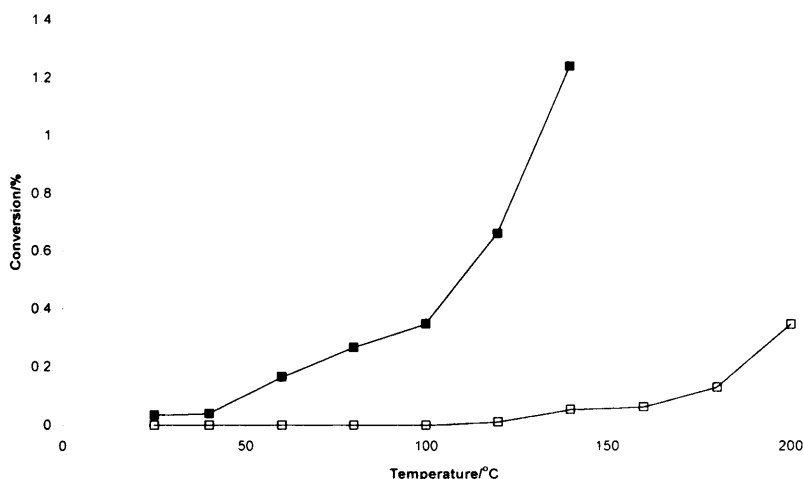


Figure 4.24 Propane conversion over commercial and prepared Co₃O₄: (■) Prepared Co₃O₄; (□) Commercial Co₃O₄

Selectivity data is presented in figure 4.25. The commercial Co₃O₄ catalyst was generally less selective than the prepared catalysts. A maximum selectivity of 75 % was achieved with the commercial catalyst at 175 °C, and propene selectivity decreased as the temperature was increased. The commercial Co₃O₄ was less active and selective than the prepared catalyst and displayed no low temperature activity.

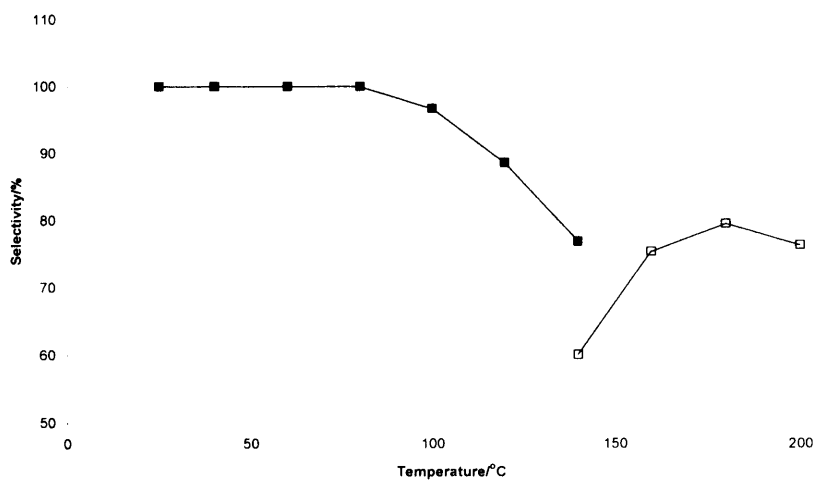


Figure 4.25 Selectivity to propene over commercial and prepared Co₃O₄; (■) Prepared Co₃O₄; (□) Commercial Co₃O₄

4.3.8 *In situ* reductions

From the results reported so far it has been found that the Co₃O₄ catalyst is active and 100% selective below 80°C. Above this temperature, however, the reaction profile is seen to change, with selectivity reducing with increasing temperature. Temperature programmed reduction of the cobalt oxide samples also showed a minor reduction feature present at approximately 80-90°C. This feature was only found in the prepared active catalyst and was not present in the used or commercial cobalt oxide. The following experiment tested the effect of the controlled removal of the reducible species by *in situ* reduction of the catalyst with H₂. The exact conditions for the reduction are given in the experimental section 2.2.7. The effect of reduction on the propane conversion is shown in figure 4.26.

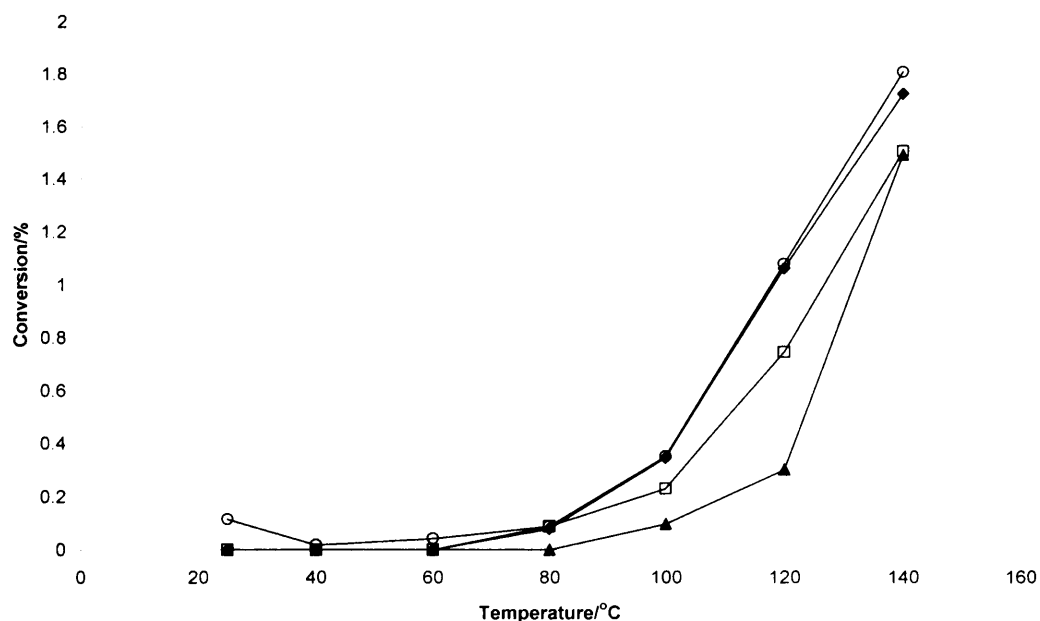


Figure 4.26 Propane conversion over Co_3O_4 reduced at increasing temperatures. (◆) Reduced 80°C
(□) Reduced 150°C (▲) Reduced 200°C (○) Unreduced Co_3O_4 comparison

Reduction of the catalyst at 80°C resulted in a total loss of activity below 80°C. The reduced catalyst showed initial activity at 80°C with conversion of 0.08%. This increased to 1.7% at 140°C. Interestingly, the reaction profile above 80°C is identical to that of the unreduced fresh catalyst indicating that the reducible species at 80-90°C seen in the TPR may well be responsible for the low temperature activity. Further reduction at 150°C resulted in an overall decrease in conversion over the entire temperature range. The catalyst was still active at 80°C but the maximum conversion at 140°C was 1.4%. Reduction at 200°C resulted in a shift in the light off temperature to 100°C and a further reduction in overall conversion.

The selectivity to propene as a function of temperature for the reduced catalyst is shown in figure 4.27. As before the unreduced catalyst was 100% selective to

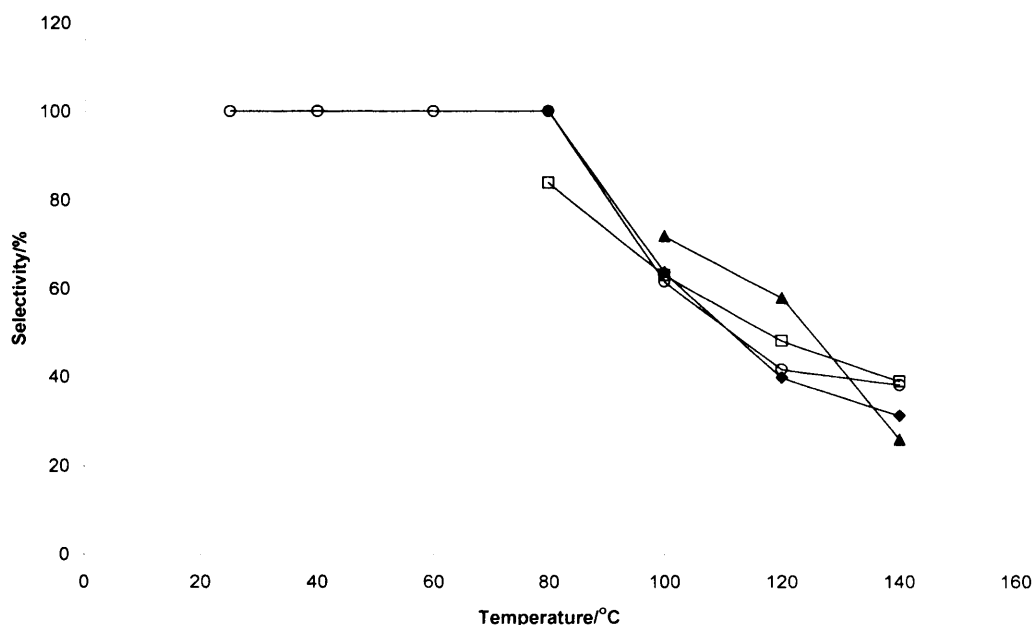


Figure 4.27 Selectivity to propene over Co_3O_4 reduced at increasing temperatures. (◆) Reduced 80°C (□) Reduced 150°C (▲) Reduced 200°C (○) Unreduced Co_3O_4 comparison

propene at temperatures lower than 80°C. The catalyst reduced at 80°C showed similar decrease in selectivity as the unreduced catalyst. It was 100% selective at 80°C decreasing to 35% at 140°C. The selectivity of the catalyst reduced at 150°C was lower than that for the unreduced catalyst. It was still active at 80°C but with a lower selectivity of 84% which decreased to 40% at 140°C. Further reduction at 200°C resulted in the light off temperature shifting to 100°C; the selectivity at this temperature was lower again at 72% reducing to 21% at 140°C.

4.4 Discussion

From the results seen above, the Co_3O_4 catalyst prepared was found to be active and selective for the oxidative dehydrogenation of propane to propene at low temperatures. It is interesting to consider the origin of the exceptional behaviour. X-ray diffraction analysis of the prepared catalyst (figure 4.1) showed that it comprised the cubic spinel type Co_3O_4 . This catalyst has proven itself to be a highly active and effective catalyst for a number of different reactions including low-temperature CO oxidation [6-8], as well as hydrocarbon combustion and oxidation [10-13,14]. In a study on the role of acidity in oxidation reactions Busca *et al* summarised previous data and described Co_3O_4 as a binary oxide with strong reducibility, strong nucleophilicity and a highly ionic metal-oxygen bond [15]. These highly ionic metal oxides with highly reducible cations are usually excellent total oxidation catalysts and some of them can have a selective behaviour in ODH reactions. Indeed the precipitated catalyst studied here was very selective for the ODH of propane to propene. The results from the catalytic reaction showed that Co_3O_4 was capable of activating propane at ambient temperatures with 100% selectivity to propene. However, the conversion was very low and the Co_3O_4 was found to deactivate very rapidly. The critical temperature range for this 100% selectivity was found to be 25-80°C. It appears that within this temperature range the catalyst is capable of activating the weakest C-H bond with reduction of the surface site possibly resulting in the formation of a surface alkoxy species. Further hydrogen abstraction would then be necessary before desorption of the propene product and consequent hydration of the surface. The formation of hydroxide species on the surface may be the reason for the rapid deactivation with the temperature being too low to facilitate desorption. It was shown that altering the O_2

concentration had little effect on the activity at temperatures lower than 80°C indicating that it plays no part in the reaction. It is unlikely that at such low temperatures activation of the gas phase O₂ is possible. And, consequently, there is no re-oxidation of the active site or indeed promotion of water formation.

It is equally likely that deactivation occurs as a result of surface bound CO₂ from over oxidation of the propane molecule. It was shown in section 4.3.1 that the fresh catalyst needed to be heated in order to drive off CO₂. It is possible that over oxidation of the propane molecule is also occurring with the CO₂ molecule being too tightly bound to desorb at such low temperatures. Jansson *et al* conducted TPO experiments on cobalt oxide involved in CO combustion. The deactivated catalyst showed presence of surface carbonates and carbon. However, the authors state that this is not the source of the deactivation. They suggest that deactivation occurs due to reconstruction of the surface hindering the redox cycle ^[6]. Interestingly another group, Cunningham *et al*, concluded the opposite, in that the carbonates are responsible for the deactivation ^[16].

The nature of the reaction changes quite clearly at 80°C. Above this temperature there is typically a drop in selectivity due to over oxidation of propane to CO₂. Interestingly no other products were observed throughout the reaction. The catalyst deactivates rapidly at temperatures lower than 130°C, and it is only at 140°C that the catalyst shows steady state activity. It may be the case that temperatures of 140°C and higher are necessary for re-oxidation of the catalyst from gas phase oxygen.

Temperature programmed reduction studies of the fresh catalyst showed a reduction feature around 80°C. The same reduction feature was not observed with a deactivated catalyst or the inactive commercial sample. It is thought that this low temperature reduction feature is associated with a surface oxygen species that effects the low temperature selective oxidation. This postulation is enforced by experiments in which

the fresh catalyst was treated with hydrogen *in situ* at 80°C for 120 minutes prior to being tested for propane oxidative dehydrogenation (section 4.3.8). The pre-treated catalyst showed no activity for propane ODH. Regeneration of the pre-treated catalyst at 180°C for 2h in a 10%O₂/He mixture resulted in the propane conversion and selectivity to propene being fully restored to that of the fresh catalyst.

The precise nature of the active site responsible for this high activity is as yet unknown but a number of authors support the theory that within spinels (Co^{tet} (II) Co₂^{oct} (III)O₄), the high catalytic activity is related to the weaker Co^{oct} (III)-O bond [17-19]. The precise nature of the active oxygen species is indeterminable from the experimental data but work done by others indicated the presence of physisorbed or chemisorbed electrophilic (O₂²⁻, O⁻ and O₂⁻) and nucleophilic (O²⁻)^[6,20]. Although there is disagreement in the role of each oxygen species. Further tests are necessary to probe the precise nature of the active species present but it is believed that increasing the concentration of the low-temperature reducible species seen in the TPR experiments may result in an increase in the activity.

4.5 Conclusions

Co_3O_4 prepared by precipitation of the corresponding nitrate was found to be active for the oxidative dehydrogenation of propane to propene at ambient temperatures. Initial tests found the catalyst to be active but highly unselective due to the presence of CO_2 . Further tests revealed that the CO_2 produced in the temperature range 25-80°C was in fact from the catalyst itself not a product of the reaction. This surface CO_2 was easily removed prior to the reaction by pre-treatment of the catalyst at temperatures of 400°C in a 10-20% oxygen atmosphere. The activated catalyst was 100% selective below 80°C. Temperature programmed reduction of the catalyst showed the presence of a reducible oxygen species at 80-90°C which was attributed to the low temperature activity. At temperatures greater than 80°C the selectivity decreases as the competing combustion reaction becomes dominant. Steady state activity is only possible at temperatures greater than 140°C but the selectivity to propene at these higher temperatures is lower.

4.6 References

- [1] J.A. Labinger, J.E. Bercaw, *Nature*, 417 (2002) 507-514
- [2] J.M. Thomas, R. Raja, G. Sankar, R.G. Bell, *Nature*, 398 (1999) 227-230
- [3] S.A. Makhlof, *J. Magn. Magn. Mater.*, 246 (2002) 184
- [4] M. Koinuma, T. Hirae, Y. Matsumoto, *J. Mater. Res.*, 13 (1998) 837
- [5] G. Fierro, M. Lo. Jacono, M. Inversi, R. Dragone, P. Porta, *Top. Catal.* 10 (2000) 39
- [6] J. Jansson, A.E.C. Palmqvist, E. Fridell, *J. Catal.*, 211 (2002) 387
- [7] J. Jansson, *J. Catal.*, 194 (2000) 55.
- [8] H.K. Lin, H.C. Chiu, H.C. Tsai, S.H. Chien and C.B. Wang, *Catal. Lett.*, 88 (2003) 169
- [9] P.-Y Lin, M. Skoglundh, J. Lowendahl, J.-E. Otterstedt, L. Dahl, K. Jansson, M. Nygren, *Appl. Catal. B. Env.*, 6 (1995) 237-254
- [10] J.E. Germain, *Catalytic Conversion of Hydrocarbons*, Academic Press, New York, 1967
- [11] G.K. Boreskov, J.R. Anderson and M. Boudart, Editors, *Catalysis Science and Technology*, Vol.3, Springer Verlag, New York, 1982, p. 39.
- [12] E. Finocchio, G. Busca, V. Lorenzelli, V. Sanchez Ecribano, *J. Chem. Soc., Faraday Trans.*, 92 (1996) 1587-1593
- [13] G. Busca, E. Finocchio, Lorenzelli, G. Ramis, M. Baldi, *Catal. Today.*, 49 (1999) 453-465
- [14] E. Finocchio, R.J. Willey, G. Busca and V. Lorenzelli, *J. Chem. Soc.*, 93 (1997) (1)175-180
- [15] G. Busca, E. Finocchio, G. Ramis and G. Ricchiardi, *Catal. Today.* 32 (1996) 133-143

- [16] D.A.H. Cunningham, T. Kobayashi, N. Kamijo and M. Haruta, *Catal. Lett.*, 25 (1994) 257
- [17] P. Jacobs, A. Maitha, J.G.H Reintjes, J. Drimal, V. Ponec, H.H. Brongersma, *J. Catal.*, 147 (1994)
- [18] M. Shelaf, M.A.Z Wheeler, H.C Yau, *Surf. Sci.*, 47 (1975) 697
- [19] C. Yau, M. Shelaf, *J. Phys. Chem.*, 78 (1974) 2460
- [20] J. Haber, W. Turek, *J. Catal.*, 190 (2000) 320

Chapter 5

Chapter 5

Nanocrystalline Cobalt Oxide: a catalyst for selective oxidation under ambient conditions

5.1. Introduction

The following chapter expands upon the research conducted previously on Co_3O_4 catalysts for the oxidative dehydrogenation of propane to propene. In the previous chapter it was shown how precipitated bulk Co_3O_4 was capable of propane conversion at temperatures as low as ambient with 100% selectivity. However, the conversion at these temperatures was very low and only reached 1% at 140°C. Steady state activity was possible at 140°C but with a reduced selectivity of ca. 75%. Temperature programmed reduction of the active catalyst showed the presence of an 80-100°C reducible species which evidence suggests was responsible for propane conversion to propene at ambient temperature with 100% selectivity. The overall aim of this study was to assess the potential of a bi-functional catalyst for the direct conversion of propane to iso-propanol. It was realised that it would require a catalyst capable of activating the alkane at temperatures low enough to allow the subsequent hydration step. In the following chapter this work is expanded upon to include other Co_3O_4 polymorphs prepared by a variety of different methods. Particular attention is paid to Co_3O_4 nanoparticles prepared by mechanochemical synthesis. Nanomaterials currently receive a high degree of interest from many fields of science, such as medicine, optics, energy and computing^[1], as well as catalysis. Nanomaterials have opened a new era for many catalytic reactions due to their particular characteristics^[2].

In fact when materials approach molecular dimensions their properties usually change when compared with a bulk material. For example nanocrystalline materials present different adsorption capacities, high surface area and increased accessibility of the active sites. Unfortunately, many of them have a limited stability and usually cannot tolerate severe reaction conditions.

The nanocrystalline Co_3O_4 catalyst was tested for propane dehydrogenation using the reaction conditions tested previously. The results indicated that the nanocrystalline Co_3O_4 was the best catalyst tested so far and hence was used in conjunction with an acid catalyst to test the possibility of direct conversion of propane to iso-propanol. The final section of the chapter investigates an approach for the direct conversion of propane to iso-propanol and details the design of multi-component catalysts containing redox and Brønsted acid functionalities to show how iso-propanol can be synthesised directly from propane in a single stage process.

5.2. Characterisation

5.2.1 BET surface areas

The BET surface areas of the Co_3O_4 samples were determined as described in experimental section (2.3.4.). The results are given below in table 5.1.

Table 5.1 BET surface areas of Co_3O_4 , (Maximum error $\pm 10\%$)

Co_3O_4 sample	BET surface area (m^2g^{-1})
Co_3O_4 precursor	64
Precipitated Co_3O_4	35
Commercial Co_3O_4	4
Co_3O_4 calcined from nitrate	14
High valence $\text{Co}_3\text{O}_4/\text{Co}_2\text{O}_3$	32
Solid state Co_3O_4 precursor. Dried 120°C	81
Solid state Co_3O_4 calcined 300°C	159
Solid state Co_3O_4 calcined 450°C	134
Solid state Co_3O_4 calcined 600°C	117

The Co_3O_4 uncalcined precursor had a surface area of $64\text{m}^2\text{g}^{-1}$, which decreased to $35\text{m}^2\text{g}^{-1}$ after calcination. The commercial catalyst had the lowest surface area of $4\text{m}^2\text{g}^{-1}$. Preparing the catalyst by the solid-state method had a marked effect on

surface area. The surface area of the solid-state precursor was $81\text{m}^2\text{g}^{-1}$, which was larger than the precipitated precursor. The surface area of the solid-state catalyst calcined at 300°C is $159\text{m}^2\text{g}^{-1}$, nearly 5 times that of the precipitated catalyst. Further calcinations at higher temperatures lead to a decrease in surface area for the 450°C and 600°C , dropping to $134\text{m}^2\text{g}^{-1}$ and $117\text{m}^2\text{g}^{-1}$ respectively. This decrease in surface area is as a result of the higher thermal treatment which causes sintering of the catalyst. Preparation of the catalyst by a mechanochemical route results in a catalyst with a much larger surface area. Such an increase would have a marked effect on the activity due to a higher proportion of active surface sites being exposed. The catalyst prepared by calcination of the nitrate at 800°C had a lower than average surface area of $14\text{m}^2\text{g}^{-1}$, such a small surface area is typical of an oxide prepared at higher temperatures. The higher valence Co_3O_4 has a surface area of $32\text{m}^2\text{g}^{-1}$, slightly lower than the precipitated catalyst and possibly due to distortion of the typical spinel structure by the Co_2O_3 phases present in the system.

5.2.2 X-ray diffraction

X-ray diffraction data was obtained using the equipment and methods described in the experimental (section 2.3.1.) All the new samples were tested and compared to the precipitated and commercial samples tested previously. The X-ray diffraction patterns can be seen below in figure 5.1. As seen previously the commercial sample is the most crystalline with diffraction peaks attributed to pure Co_3O_4 ($2\theta^\circ$ of 31.2, 36.8, 59.3 and 65.2). The same peaks are present in the sample calcined from the nitrate but are slightly weaker and display a certain amount of broadening. The high valence

cobalt oxide shows diffraction peaks from Co_2O_3 , $2\theta^\circ$ of 38.6 and 67.8. These peaks are relatively weak and broad indicating a certain amount of disorder within the system. Small peaks at $2\theta^\circ = 19.0$ and 65.2 are present and these are attributed to the (111) and (440) planes. The high

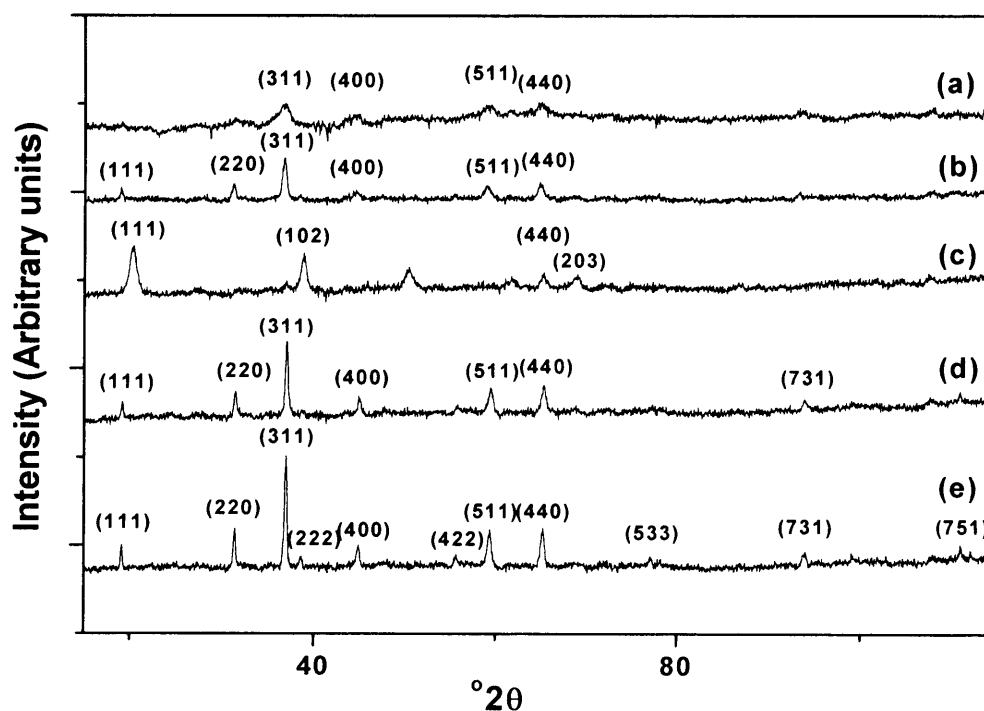


Figure 5.1 X-ray diffraction pattern of Cobalt oxide catalysts: (a) Co_3O_4 nanoparticles (b) Co_3O_4 precipitated from nitrate (c) High Valence $\text{Co}_3\text{O}_4/\text{Co}_2\text{O}_3$ (d) Co_3O_4 calcined from nitrate (e) Commercial Co_3O_4

valence sample appears to be a mixture of both Co_3O_4 and Co_2O_3 . This is consistent with the literature, which suggests that the cobalt oxide formed by this method comprises both Co_3O_4 and Co_2O_3 [3]. Interestingly the sample also shows peaks at $2\theta^\circ = 50.5$ and 61.7 . These are phases are from neither Co_3O_4 nor Co_2O_3 and cannot be attributed to any other phases in the JCPDS database. The XRD pattern for the precipitated sample indicates that it comprises pure Co_3O_4 although the broader,

weaker diffraction peaks would indicate that it is more amorphous than the other samples. The diffraction pattern of the sample prepared by solid-state reaction is indicative of a nano-crystalline sample. The broadness of the low-intensity peaks indicates that the particle size is too small to allow sufficient diffraction. The sample shows very weak and broad diffraction peaks at $2\theta = 36.8, 59.3$ and 65.2 , attributable to Co_3O_4 .

Crystallite size was determined by use of the Scherrer equation. The exact method is described in experimental section (2.3.1). Peak broadening was compared to a highly crystalline silicon sample (see appendix). The result for which are shown in table 5.2.

Table 5.2 Co_3O_4 crystallite size as determined by the Scherrer equation.

Co_3O_4 sample	Crystallite size (nm)
Precipitated Co_3O_4	34
Commercial Co_3O_4	108
Co_3O_4 calcined from nitrate	44
Solid state Co_3O_4 calcined 300°C	12
Solid state Co_3O_4 calcined 600°C	17
Used precipitated Co_3O_4	36

Determination of the average crystallite size by X-ray line broadening showed that the precipitated catalyst had a crystallite size of 34 nm, whilst the average crystallite size for the more active solid state prepared Co_3O_4 was 12 nm. Calcination of the nano-crystalline sample at higher temperatures results in agglomeration of the particles and hence larger crystals of 17nm. The nano-crystalline nature of the catalysts is consistent with their relatively high surface area. The commercial catalyst

had a measured average crystallite size of 103 nm, which is too large to be classed as nano-crystalline. The Co_3O_4 sample prepared by calcination of the nitrate had an average crystallite size of 44 nm, between that of the commercial and precipitated. The crystallite size of the used precipitated sample is 36nm, larger than the fresh sample. This may be as a result of sintering of the catalyst during the reaction.

5.2.3 Temperature programmed reduction

The temperature programmed reduction studies were conducted using the methods described in the experimental section (2.3.5). The results for the temperature programmed reduction of the nano-crystalline Co_3O_4 are shown in figure 5.2.

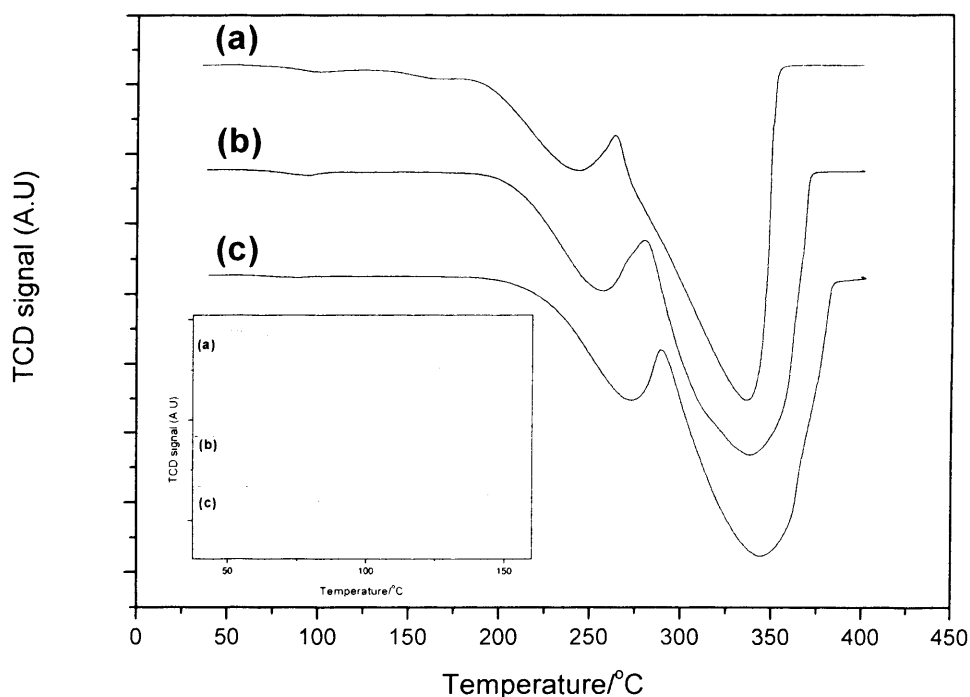


Figure 5.2 Temperature programmed reduction of Co_3O_4 nanoparticles: (a) Co_3O_4 calcined 300°C (b) Co_3O_4 calcined 450°C (c) Co_3O_4 calcined 600°C. Inset: expansion of low-temperature feature at 80-100°C

The major reduction peaks at ca. 270°C and 350°C are as a result of the reduction of $\text{Co}_3\text{O}_4 \rightarrow \text{CoO}$ (270°C) and $\text{CoO} \rightarrow \text{Co}$ (350°C)^[4]. The precise temperature of the reductions is given in table 5.3. Increasing the calcination temperature of the catalyst resulted in a shift in the reduction peaks to higher temperatures. This shift in temperatures is as a result of the increased stability of the sample due to the higher calcination times.

Table 5.3 Temperature of reduction peaks and areas of the low temperature reduction feature.

Catalyst	Reduction Peak (°C)	Area of low temperature peak (81-98°C)	Area normalized for catalyst mass
Nanocrystalline Co_3O_4 calcined 300°C	98, 243, 336	0.90	14
Nanocrystalline Co_3O_4 calcined 450°C	93, 257, 338	0.09	1.5
Nanocrystalline Co_3O_4 calcined 600°C	88, 257, 345	0.004	0.1
Precipitated Co_3O_4	81, 268, 338	0.03	0.5

Inset in figure 5.2 is an expansion of the 80-100°C temperature range. As with the precipitated catalyst the low temperature peak is still present and is seen to shift to lower temperatures with increasing calcination temperature. This pattern is surprising given that one would expect the peak to shift to higher temperatures. The values in the last column of table 5.3 denote the areas of the low temperature peak for each catalyst. With increasing calcination temperature the total concentration of the reducible species is seen to decrease. The catalyst calcined at 300°C shows the highest concentration of the reducible species with a peak area of 0.9. This value drops to just 0.004 for the 600°C calcined catalyst.

Comparison of the nanocrystalline catalyst with the precipitated and commercial sample can be seen below in figure 5.3.

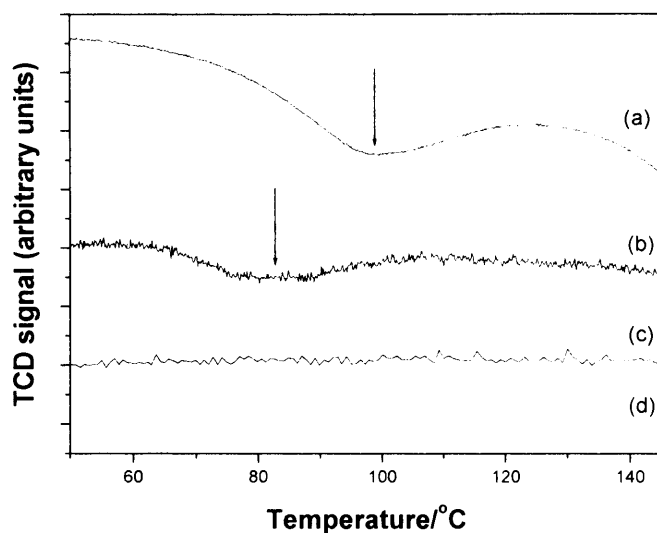


Figure 5.3 Temperature programmed reduction profiles for (a) fresh nanocrystalline Co_3O_4 calcined 300°C , (b) precipitated Co_3O_4 , (c) fresh commercial Co_3O_4 (Avocado) and (d) used at 40°C nanocrystalline Co_3O_4 .

The nanocrystalline sample has a larger concentration of reducible species in the $80\text{-}100^\circ\text{C}$ temperature range. The 80°C reduction peak is smaller for the precipitated catalyst than for the nanocrystalline sample. The commercial catalyst, which was proven inactive for propane conversion shows no reduction peak below 100°C . The TPR of the used nanocrystalline sample also showed no low-temperature reduction peak. From the previous work the low temperature activity of the Co_3O_4 catalyst was attributed to the presence of this $80\text{-}100^\circ\text{C}$ reducible species. The nanocrystalline sample appears to have this species present in larger concentrations and, as with the precipitated catalyst, the activity disappears with removal of this low temperature species. TPO experiments on the used nanoparticle catalyst are shown below in figure 5.4. It can be seen that heating in O_2 reoxidises the catalyst in the $80\text{-}100^\circ\text{C}$ region

and in higher concentrations. This higher concentration is as a result of the smaller particle sizes and hence the higher surface area.

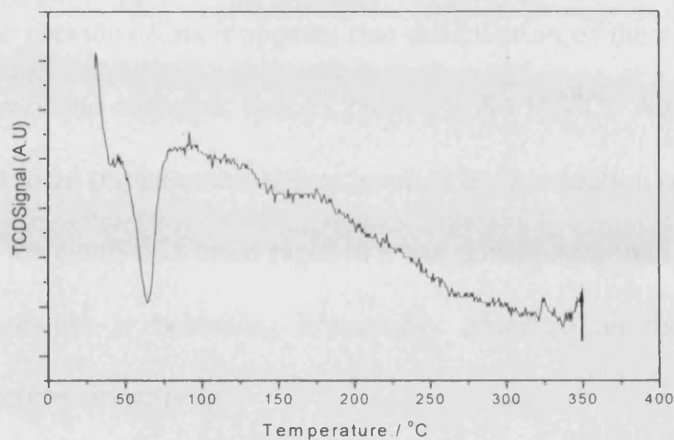


Figure 5.4 Temperature programmed oxidation of used Co_3O_4 nanoparticle catalyst

The Co_3O_4 nanoparticle catalyst was also subjected to experiments in a wet atmosphere. The temperature programmed reduction profiles for both the fresh and used catalyst are presented in figure 5.5.

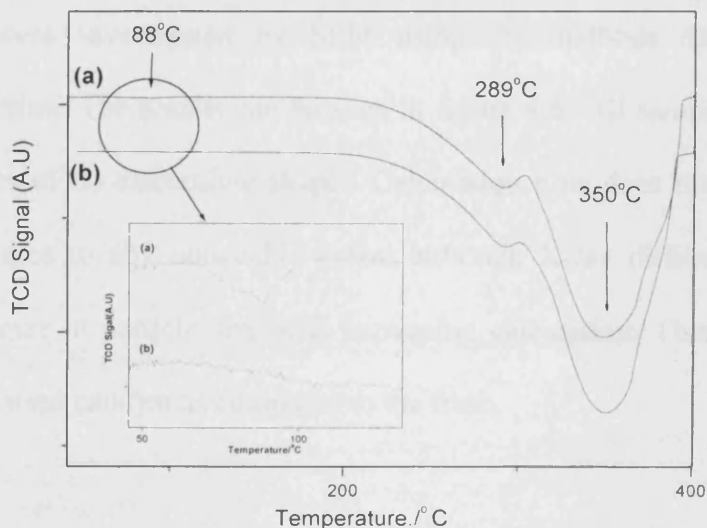


Figure 5.5 Temperature programmed reduction of Co_3O_4 nanoparticles: (a) before reaction, and (b) after reaction in wet atmosphere: Inset: expansion of low-temperature feature at 80-100°C

Treatment of the catalyst in a wet atmosphere resulted in rapid deactivation resulting in the loss of the 80-100°C reduction peak. Treatment of the catalyst at low temperatures did not affect the reducibility of the major reduction peaks at 289°C and 350°C. As in the previous tests it appears that deactivation of the catalyst occurs as a result of the loss of the reducible species present at 80-100°C. Again reactivation of the used catalyst in an oxygen atmosphere resulted in re-oxidation of the used species. Deactivation of the catalyst is more rapid in a wet atmosphere than in dry, this would indicate that moisture is becoming irreversibly adsorbed on the catalyst surface resulting in a decrease in activity.

5.2.4 Scanning Electron Spectroscopy

The catalysts were investigated by SEM using the methods described in the experimental section. The results can be seen in figure 5.6. All samples consisted of irregular particles of no discernible shape. Calcination time does not affect particle size or surface area to any noticeable extent although X-ray diffraction data does indicate an increase in particle size with increasing calcination. There is no visible difference in the used catalyst as compared to the fresh.

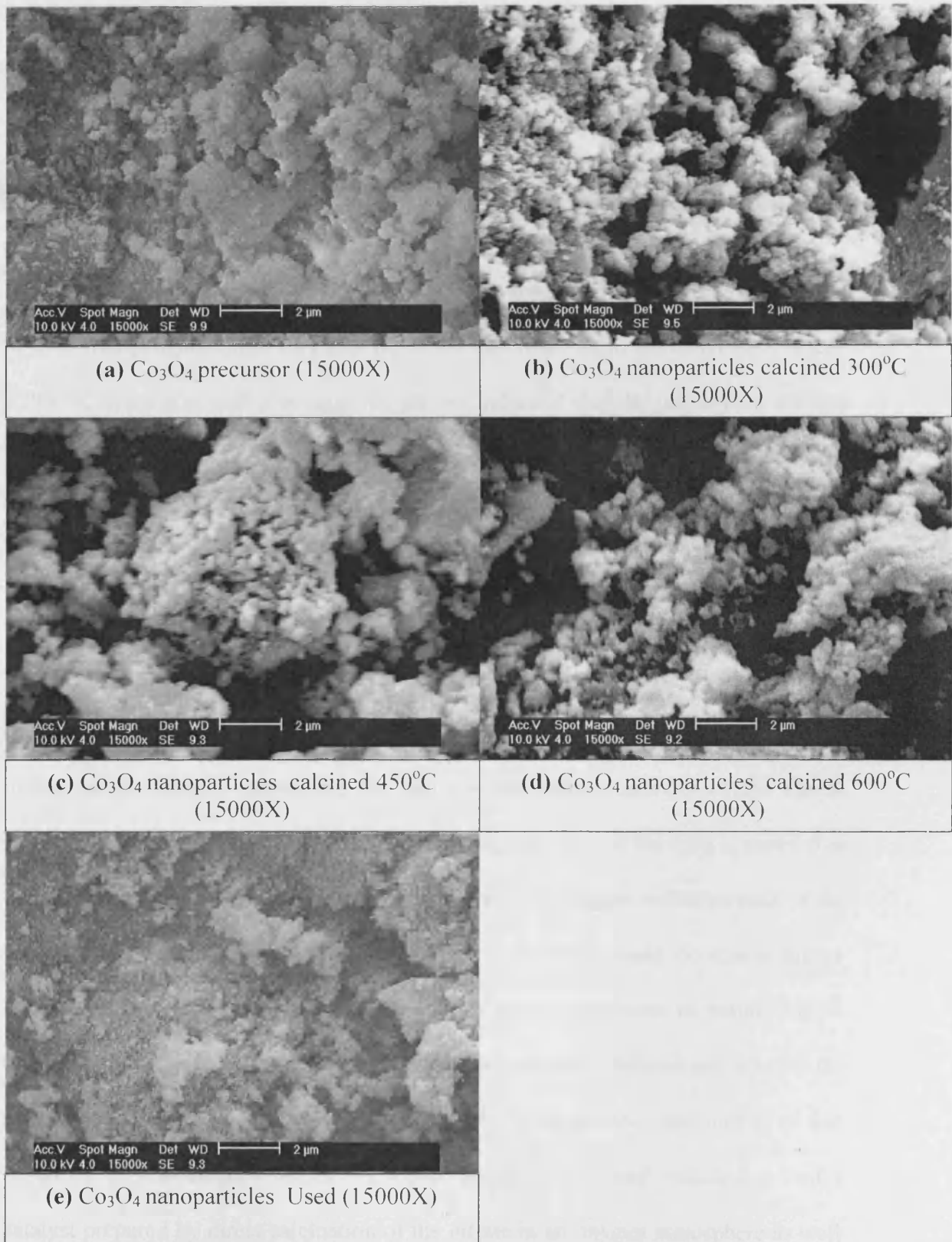


Figure 5.6 SEM of Co_3O_4 nanoparticles.

5.3 Results

5.3.1 Variation in preparation methods

So far the cobalt oxide catalyst tested was prepared by precipitation of the corresponding nitrate. This method resulted in a catalyst that was both active and selective for the direct conversion of propane to propene at low temperatures. However, although it displayed 100% selectivity to the desired product the conversion at these temperatures was very low not achieving more than 1% conversion below 120°C. Comparison with a commercial sample indicated that the preparation method played an important part in the production of an active catalyst. In an effort to increase the activity a series of cobalt oxide samples were prepared using different methods and the results compared to the original precipitation method.

A higher Co oxide system was prepared using the method described in experimental section 2.1.5. TPR experiments done previously (Section 4.2.3.) indicated the presence of a low temperature reducible species, which may well be highly active oxygen responsible for the low temperature activity of the Co₃O₄ catalyst. It has been stated previously that the high activity of the Co₃O₄ material is related to the weakness of the Co (III)-O bond i.e. to the higher oxidation state of the metal cation ^[5-7]. It was envisaged that such a material would contain a higher concentration of active oxygen species and be more amorphous in nature due to distortion of the typical Co₃O₄ spinel structure. A number of methods are reported for the preparation of a higher cobalt oxide system ^[3, 8]; the method used here is of that described by Christoskova *et al.* ^[3]. Other preparations tested included a Co₃O₄ catalyst prepared by direct calcination of the nitrate in an oxygen atmosphere as well

as cobalt oxide nanoparticles prepared by mechanochemical synthesis. The preparation of a cobalt nanostructure was of considerable interest because of the unique properties inherent in nanomaterials due to their particle size. A number of preparations have been reported ^[9-11]. The preparation method used has been described elsewhere ^[9] and the specific details are given in experimental section 2.1.4. The preparation methods used along with the experimental details are highlighted in table 5.4 below.

Table 5.4 Preparation of Co₃O₄ catalyst by different methods and their experimental details

Co ₃ O ₄ Catalyst preparation methods	Experimental details
Precipitated cobalt oxide	Precipitated from Co(NO ₃) ₂ •6H ₂ O
Mechanochemical synthesis	Prepared from Co(NO ₃) ₂ •6H ₂ O and NH ₄ HCO ₃ according to $2\text{Co}(\text{NO}_3)_2 \cdot 6\text{H}_2\text{O} + 5\text{NH}_4\text{HCO}_3 \rightarrow \text{Co}_2(\text{OH})_2\text{CO}_3 + 4\text{NH}_4\text{NO}_3 + \text{NH}_3 + 4\text{CO}_2 + 14\text{H}_2\text{O}$
Thermal treatment of nitrate	Calcined $\text{Co}(\text{NO}_3)_2 \cdot 6\text{H}_2\text{O} \xrightarrow{\Delta} \text{Co}_3\text{O}_4$
Precipitated higher cobalt oxide	$\text{Co}(\text{NO}_3)_2 \cdot 6\text{H}_2\text{O} + \text{NaOH} + \text{NaOCl} \longrightarrow \text{Co}(\text{OH})_2 \xrightarrow{\Delta} \text{CoO}_x$

Figure 5.7 shows the propane product conversion over the variously prepared Co₃O₄ catalysts. The reaction conditions were as described in the experimental section 2.2.4. Each data point at a given temperature is the average of three injections. The reaction data in the work were reproducible with a precision of ±4%

The catalyst prepared by calcinations of Co(NO₃)₂•6H₂O displayed the lowest overall conversion. Light off occurred at 60°C with 0.04% conversion and increased to only 0.8% at 140°C. It was less active than the other Co₃O₄ catalysts, which were all active at ambient temperature. The precipitated catalyst displayed the same

activity as described previously with initial activity at 25°C. Maximum conversion at 140°C was 1.2%.

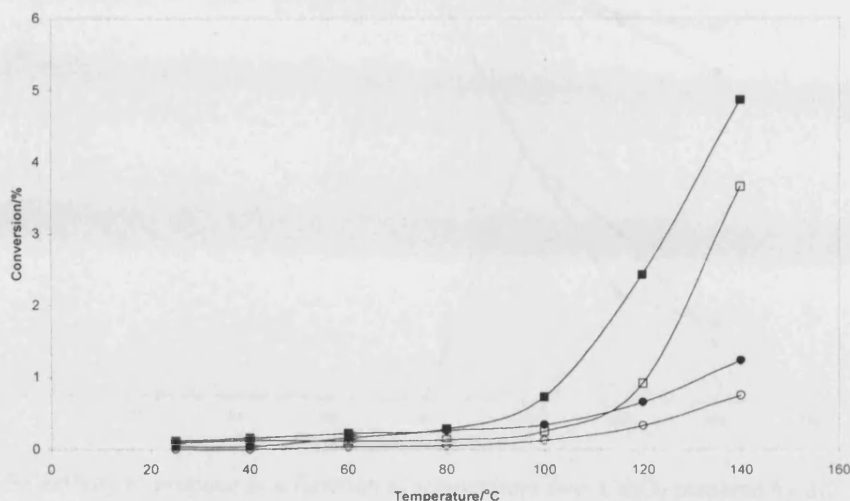


Figure 5.7 Propane conversion over Co_3O_4 prepared by different methods: (■) Co_3O_4 nanoparticles (○) Co_3O_4 calcined from nitrate (□) high valence Co_3O_4 (●) Co_3O_4 precipitated from the nitrate

The higher valence CoO_x was more active than the precipitated Co_3O_4 . At 25°C the conversion was twice that of the precipitated sample showing 0.09% conversion as compared to 0.04% for the precipitated sample. At 140°C the conversion is seen to rise to 3.7%, nearly 4 times that of the precipitated catalyst. The best results came from the cobalt oxide nano-particles prepared by the mechanochemical method. Again the catalyst was active at 25°C giving a conversion of 0.11%, the highest conversion at this temperature seen so far. The Co_3O_4 nano-particles remained the most active over the entire temperature range with maximum conversions of ca. 5% at 140°C. This is far better than the precipitated catalyst that has been studied.

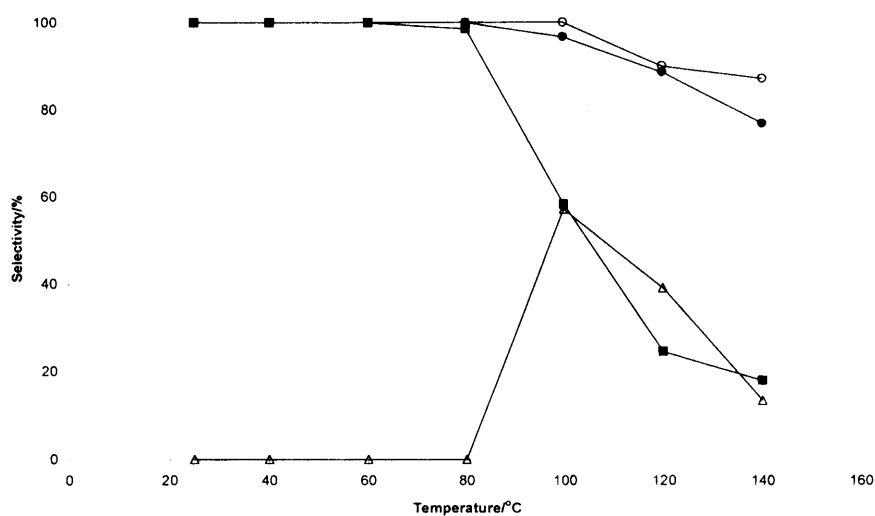


Figure 5.8 Selectivity to propene as a function of temperature over Co₃O₄ prepared by different methods; (■)Co₃O₄ nano-particles (○)Co₃O₄ calcined from nitrate (△) high valence Co₃O₄ (●) Co₃O₄ precipitated from the nitrate

The selectivity to propene as a function of temperature is given in figure 5.8. The catalyst prepared by calcination of the nitrate was the most selective being 100% selective up to 100°C. Above this temperature the selectivity decreased to 87% but was still the highest overall. However, this high selectivity was only due to the low conversion. The precipitated Co₃O₄ was 100% selective up to 100°C but again the selectivity decreased above this temperature dropping to 76% at 140°C. The higher valence Co₃O₄ was the least selective overall. Although the catalyst was active at ambient temperature the primary product was CO₂, no propene was seen at temperatures below 80°C. Propene production only became apparent at 100°C but with a maximum selectivity of 57% which rapidly decreased to 13% at 140°C. The Co₃O₄ nanoparticles were 100% selective up to 80°C but showed a large decrease in selectivity at higher temperatures falling to 58% at 100°C and decreasing further still to just 18% at 140°C. This lower selectivity is as a result of the higher activity of the

catalyst. However, it is this higher activity that makes the Co_3O_4 nanoparticle catalyst the most interesting, especially in the 25-80°C temperature range where the catalyst showed the highest conversion with 100% selectivity to propene.

The propene yields as a function of temperature are shown below in figure 5.9. The Co_3O_4 prepared by calcinations of the nitrate showed the lowest yield with no propene production below 100°C above this temperature the yield rises to 0.5% at 140°C, as did the high valence CoO_x . The highest yields were displayed by the precipitated and nanoparticle catalysts with maximum yields of around 0.9% at 140°C, none of the catalysts tested gave a yield greater than 1% over the entire temperature range. Again it is the nanoparticle catalyst that proved the most interesting with the highest yields in the 25-80°C temperature range.

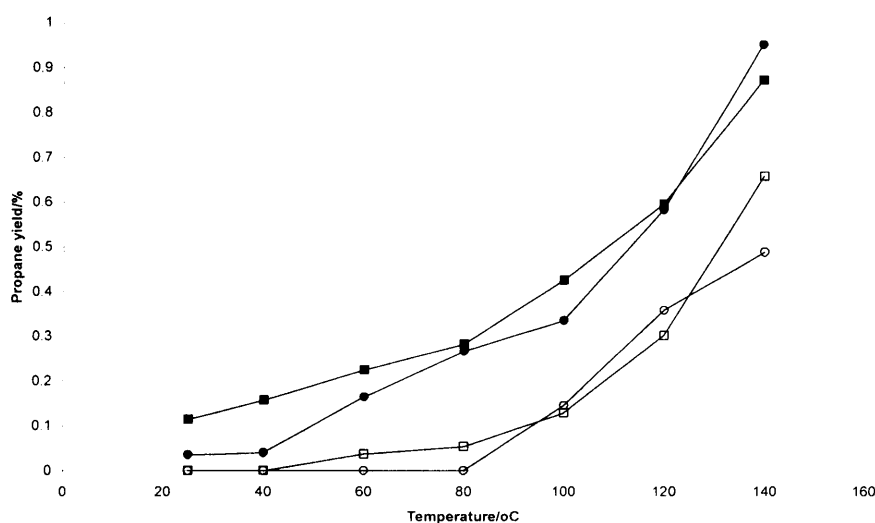


Figure 5.9 Propane yields as a function of temperature over Co_3O_4 prepared by different methods: (●) Co_3O_4 nanoparticles (○) Co_3O_4 calcined from nitrate (□) high valence Co_3O_4 (■) Co_3O_4 precipitated from the nitrate

The higher activity of the nanoparticle catalyst can be related to the increased surface area allowing more exposure of the surface active sites. The surface area of the nanoparticle catalyst is $159\text{m}^2\text{g}^{-1}$ as compared to just $35\text{m}^2\text{g}^{-1}$ for the precipitated sample.

5.3.2 Cobalt oxide nanoparticles

In an effort to increase the activity and to study the effect of preparation conditions a series of Co_3O_4 nanoparticles were synthesised using the methods described previously and calcined at increasing temperatures of 300°C , 450°C and 600°C . The reaction conditions were as before (section 2.2.4). The results for propane conversion and a comparison to the already tested precipitated Co_3O_4 are presented below in figure 5.10.

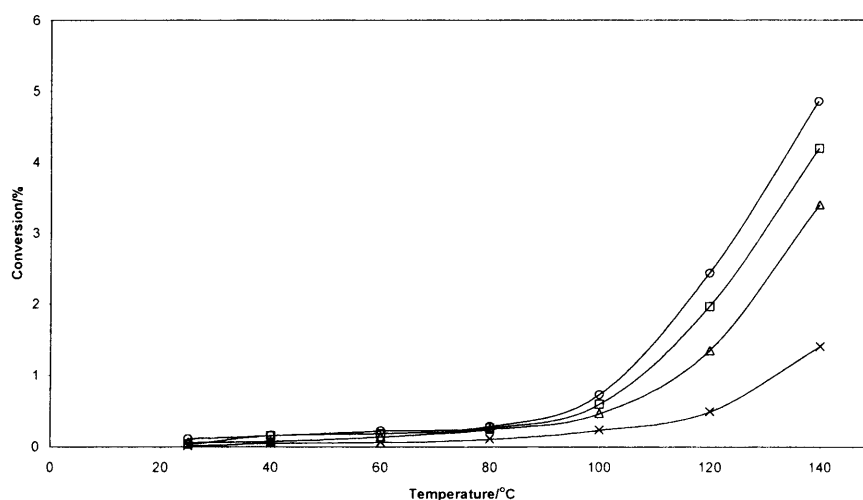


Figure 5.10 Propane product conversion as a function of temperature over mechanochemical synthesised Co_3O_4 nanoparticles. Effect of calcination temperature and comparison to original precipitated catalyst: (x) Precipitated catalyst calcined 400°C ; (Δ) Co_3O_4 nanoparticles calcined 600°C ; (\square) Co_3O_4 nanoparticles calcined 450°C ; (\circ) Co_3O_4 nanoparticles calcined 300°C .

The rate of propane conversion over the nanoparticle Co_3O_4 is appreciably greater than over the precipitated catalyst. Calcination at 300°C led to the most active catalyst with initial propane conversion of 0.1%, as compared to 0.01% for the precipitated sample. This rose to a maximum of 4.8% at 140°C : 5 times that of the precipitated

Co₃O₄. Increasing the calcination temperature resulted in a decrease in activity, with propane conversion at 140°C dropping to 4.2% for the 450°C and 3.4% for the 600°C calcined catalyst. This pattern was constant over the entire temperature range especially below 80°C where propane conversion over the catalyst calcined at 600°C decreases to near that of the precipitated. This decrease in conversion with increasing calcination temperature is consistent with previous data (section 4.3.3) and is as a result of agglomeration of the nano-scale particles. As seen in section 5.2.1, increasing the calcination time also led to a decrease in surface area.

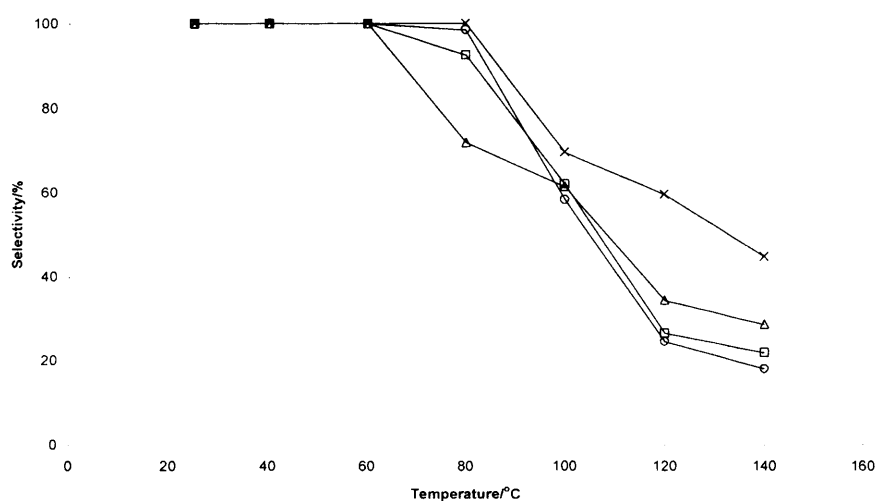


Figure 5.11 Selectivity to propene as a function of temperature over mechanochemical synthesised Co₃O₄ nanoparticles. Effect of calcination temperature and comparison to original precipitated catalyst: (x) Precipitated catalyst calcined 400°C; (Δ) Co₃O₄ nanoparticles calcined 600°C; (□) Co₃O₄ nanoparticles calcined 450°C; (○) Co₃O₄ nanoparticles calcined 300°C.

The selectivity to propane as a function of temperature can be seen above in figure 5.11. The lower selectivity for the nano-particle catalyst is consistent with the increased conversion. All of the catalysts were 100% selective to propene below 80°C. Above this temperature the selectivity over the nanocrystalline catalysts

decreases, falling to around 22% at 140°C. Curiously, at 80°C the decrease in selectivity was greater for the catalyst calcined at 600°C than for the 300°C calcined catalyst. One would expect the less active catalyst to remain more selective over the entire temperature range due to the lower conversion.

The precipitated catalyst displayed a lower selectivity to propene than that seen in previous tests but was still the most selective overall, remaining 100% selective at 80°C and decreasing steadily to 44% at 140°C.

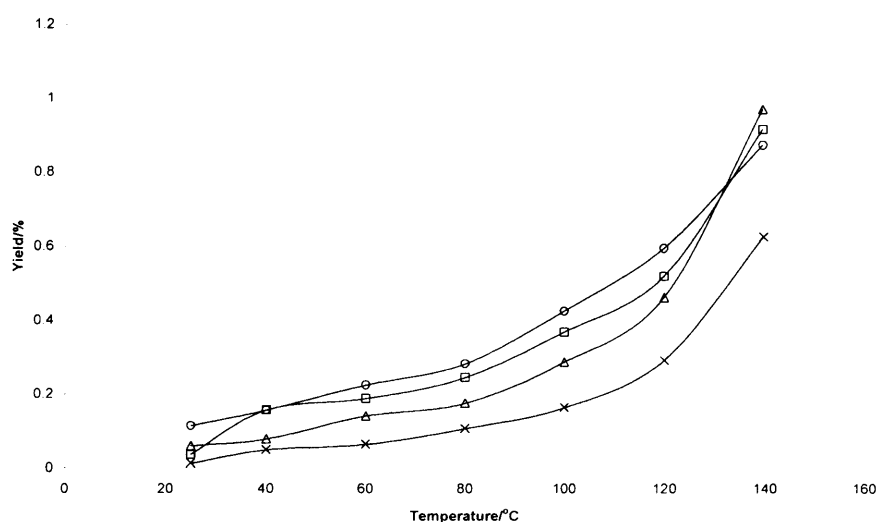


Figure 5.12 Propene yield as a function of temperature over mechanochemical synthesised Co_3O_4 nanoparticles. Effect of calcination temperature and comparison to original precipitated catalyst: (x) Precipitated catalyst calcined 400°C; (Δ) Co_3O_4 nanoparticles calcined 600°C; (\circ) Co_3O_4 nanoparticles calcined 450°C; (\square) Co_3O_4 nanoparticles calcined 300°C.

The propene yields as a function of temperature are shown in figure 5.12. The propene yield over the nanocrystalline Co_3O_4 is greater than the precipitated catalyst over the entire temperature range. Below 80°C the catalyst calcined at 450°C gives the highest yield of 0.2%, which increases to ca. 1% at 140°C. The catalyst calcined at 600°C gives the lowest yield below 120°C, but this is still greater than the precipitated

catalyst, which shows a maximum yield of 0.6% at 140°C. At 140°C the nanoparticle catalyst displays yields between 0.8 and 1%, nearly twice that of the precipitated catalyst. The higher selectivity of the 600°C calcined catalyst results in the highest yields of 1% at 140°C.

5.3.3 Steady state measurements

Previously (section 4.3.5) the steady state activity of the precipitated catalyst was tested at 40°C. It was found that the catalyst deactivated rapidly, reaching 0% conversion in approximately 1h. Reactivation of the catalyst was found to increase the initial conversion but after 6 reactivations the catalyst was inactive. The same experiment was conducted on the nanocrystalline catalyst calcined at 300°C. The 300°C calcined catalyst was chosen for the experiment due its higher activity in the 25-100°C temperature range. The catalyst remained 100% selective to propene throughout the experiment and was reactivated *in situ* at 180°C between each run. As with the precipitated catalyst reactivation at 180°C for 2h was necessary for the total removal of all traces of CO₂. The results for propane conversion as a function of time on line are displayed in figure 5.13.

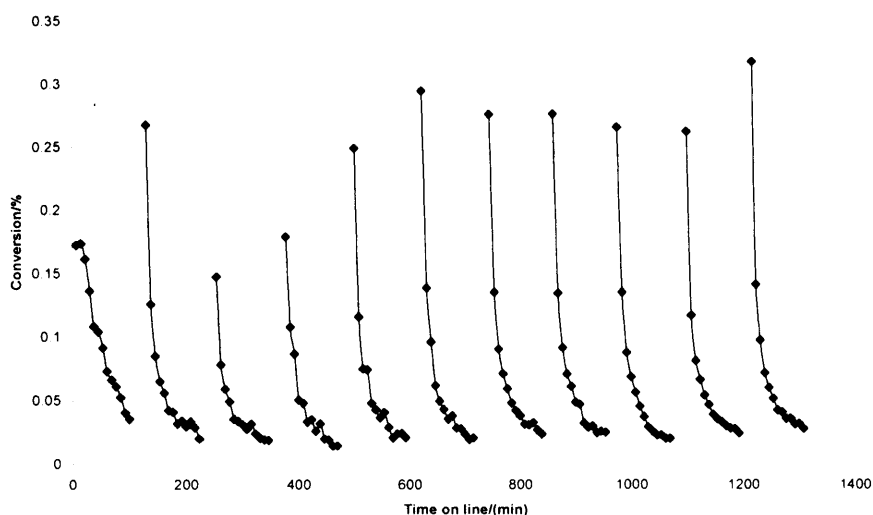


Figure 5.13 Deactivation profile at 40°C of the Co_3O_4 catalyst prepared by solid state reaction. After reactivation the catalyst was regenerated at 180°C and the cycle repeated 9 times.

Once the catalyst was deactivated it was possible to regenerate the activity for propane conversion. Heating in air restored the original catalyst activity. Regeneration at 80, 100 and 140°C for 2h restored partially the catalyst activity to that observed for the fresh catalysts. Regeneration at 180°C resulted in fully re-activated catalysts with activity identical to the fresh catalyst. After the first few reactivation and regeneration cycles the catalyst profile with time on stream was extremely reproducible. These data indicate that the catalyst was regenerated fully even after several deactivation and regeneration cycles. The ability to operate the catalyst in a reproducible cycle means that propane selective oxidation can be performed at low temperature followed by regeneration at elevated temperature. Again the conversions at these temperatures is very low decreasing from 0.5% to less than 0.05% after approximately 2h but this is still better than the precipitated catalyst which showed a maximum conversion of just 0.25% and deactivated in half the time. From these data it appears that not only is the nanoparticle Co_3O_4 more active for longer but also more stable; it was possible to reactivate the catalyst 9 times without any loss of either activity or selectivity.

5.3.4. Effect of water on Co_3O_4 nanoparticles

In this section the effect of humidity on the low temperature conversion of propane to propene is studied. It was envisaged that the highly active and selective nanocrystalline Co_3O_4 could be use in conjunction with a suitable hydration catalyst for the one-step direct conversion of propane to propene. The role of water in the reaction mechanism is important to this study, as the aim was to carry out the dehydrogenation and hydration reactions in a concerted manner. Although the oxidative dehydrogenation step for propane activation will contain a concentration of water in the feed that will aid the hydration of propene to iso-propanol it may be well be too small a concentration to have a positive effect. Current alkene hydration reactions using heterogeneous catalyst operate with a concentration of water in the feed to facilitate the re-hydration of the acid catalyst. However the presence of water can also influence the reaction by acting as an inhibitor and by quenching thermal and radical reactions.

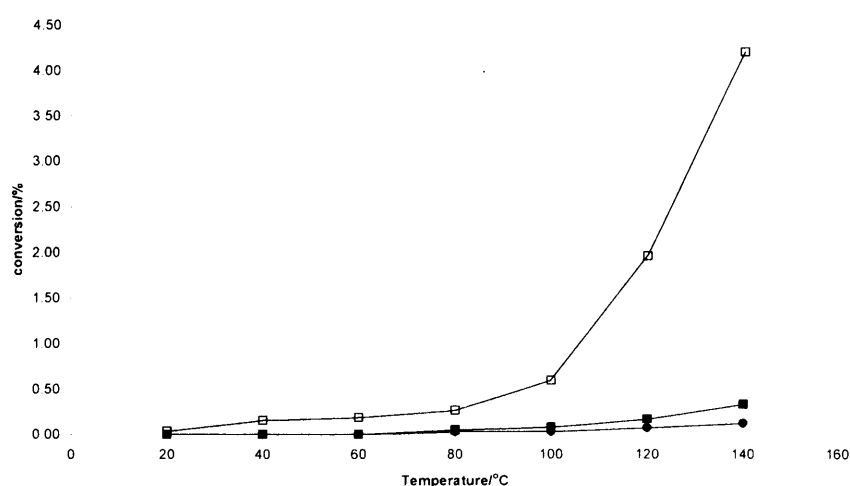


Figure 5.14 Propane product conversion as a function of temperature over Co_3O_4 nanoparticles. Effect of water on catalyst activity. (□) No water in feed (■) Water in feed (0°C) 0.611 KPa (●) Water in feed (8-10°C) 1.15 KPa. Temperature in parenthesis refers to temperature of sampler used to achieve the corresponding vapour pressure

Introduction of water to the feed resulted in a decrease in conversion across the entire temperature range (figure 5.14). With a minimal amount of water in the feed the low temperature reactivity was suppressed with light-off shifting to 60°C. At 140°C the conversion reaches a maximum of 0.3%, far lower than the maximum conversion in a dry atmosphere. With higher concentrations of water in the feed the activity is suppressed further, initial conversion is at 80°C and only increases to 0.1% at 140°C. It appears that water has a negative effect upon the activity of the catalyst. Previous work on Co_3O_4 deactivation by water has shown similar results with Yau *et al* finding that CO oxidation is inhibited by surface bound H_2O . At these low temperatures it is possible that water is becoming irreversibly adsorbed, blocking the active surface sites and inhibiting catalytic turnover ^[12]. Cunningham *et al* also stated that there is competition between CO and moisture for the active sites with similar results being found by other groups ^[13].

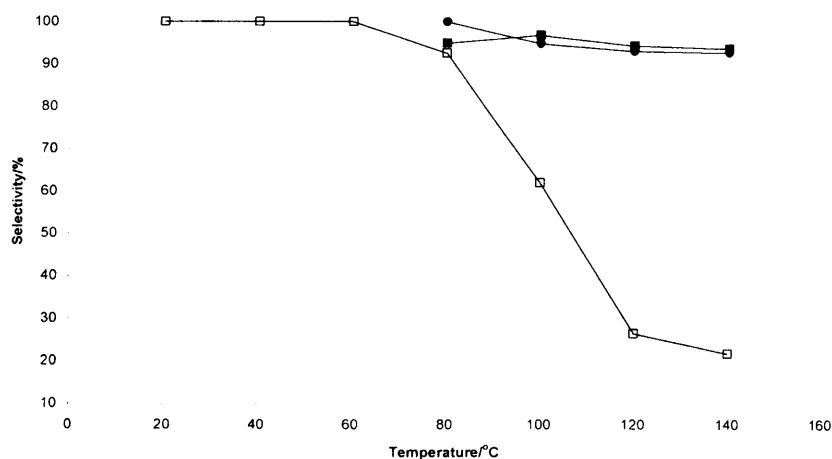


Figure 5.15 Selectivity to propene as a function of temperature over Co_3O_4 nanoparticles. Effect of water on catalyst activity. (□) No water in feed (■) Water in feed (0°C) 0.611 kPa (●) Water in feed (8-10°C) 1.15 kPa. Temperature in parenthesis refers to temperature of sampler used to achieve the corresponding vapour pressure

As a result of the lowered conversion the selectivity for the catalyst in a wet atmosphere is high, remaining above 90% throughout the experiment (figure 5.15). It appears that the presence of water suppresses both the dehydrogenation and total combustion reactions. In a dry atmosphere the selectivity is as previously with a rapid decrease above 100°C as CO₂ becomes the dominant reaction product. The high conversions seen over the nanocrystalline Co₃O₄ are only as a result of the extremely low conversion.

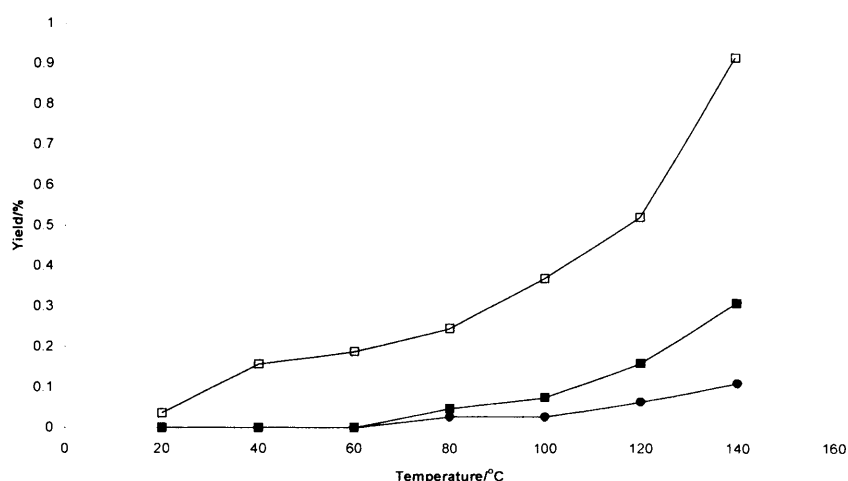


Figure 5.16 propene yield as a function of temperature over Co₃O₄ nanoparticles. Effect of water on catalyst activity. (□) No water in feed (■) Water in feed (0°C) 0.611kPa (●) Water in feed (8-10°C) 1.15 kPa. Temperature in parenthesis refers to temperature of sampler used to achieve the corresponding vapour pressure

The results for propene yield as function of reaction temperature are given in figure 5.16. The results for propene yield in a wet atmosphere are quite poor with yields being half that of the catalyst in a dry atmosphere. No propene is produced below 80°C and the maximum yield at 140°C is just 0.3%. Increasing the water pressure resulted in a further decrease in yield not achieving greater 0.1% at 140°C.

5.3.5 Conversion of propene to iso-propanol over acid catalysts

Initial experiments into iso-propanol production focused on the secondary propene hydration step. A series of acid catalysts with known hydration capabilities were selected and prepared for propane hydration to isopropanol. These included a 70 wt% $\text{H}_3\text{PO}_4/\text{SiO}_2$ catalyst prepared as described in experimental section 2.1.6 and a number of heteropolyacids used as received. 0.4g of catalyst was used in each case with the catalyst bed being saturated with water prior to the reaction. Propene was introduced to the feed after a 1h stabilisation period. The exact details of the experimental conditions are described in the experimental section 2.4.1.

Initial experiments studied the effect of temperature on the reaction with the water partial pressure kept constant. Subsequent experiments looked at the effect of water partial pressure on the reaction.

The results for propene conversion to iso-propanol as a function of temperature are given in figure 5.17. At low temperatures only isopropanol was detected. For all catalysts, the activity increased in parallel with the increase in temperature and passed through a maximum at 100°C. Further increase in temperature led to a decrease in the rate of iso-propanol formation due to thermodynamic limitation. At the highest reaction temperatures there is an increase in the formation of the oligomerisation-cracking and etherification products.

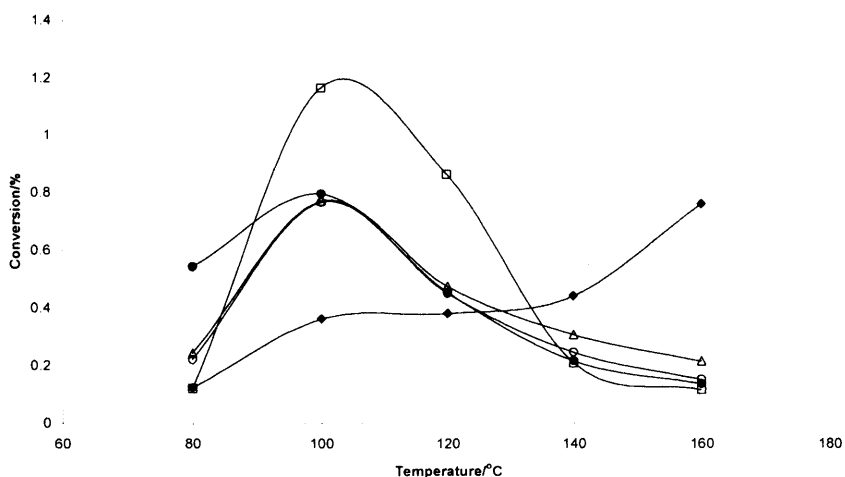


Figure 5.17 Propene conversion to iso-propanol as a function of temperature. Water partial pressure: 4.2 kPa (temperature: 30°C). (●) 70 wt%H₃PO₄/SiO₂ (○) Tungstosililic acid (□) Phosphomolybdic acid (◆) ZSM-5 zeolite (Δ) Bulk HPW

Propene conversion remained very low over the entire temperature range for all of the catalysts. The catalysts displayed similar reaction profiles with the highest conversions occurring at 100°C. The bulk HPW and tungstosililic catalyst showed near identical reaction profiles with initial conversion of 0.2% at 80°C, this rose to a maximum of 0.7% at 100°C before diminishing to 0.2% at 150°C. The 70wt%H₃PO₄/SiO₂ catalyst showed a similar trend, with a maximum conversion of 0.7% at 100°C, the rate of propanol formation then decreases with increasing temperature to just 0.2% at 150°C. Propane conversion is the highest over the phosphomolybdic catalyst with a maximum conversion of ca. 1.2% at 100°C. As with the other catalyst this decreases with increasing temperatures falling to 0.1% at 150°C. The rate of propene conversion over the ZSM-5 zeolite was different to the other catalysts showing an increase in conversion with increasing conversion. At 80°C the conversion is 0.1% and rises to 0.8% at 150°C.

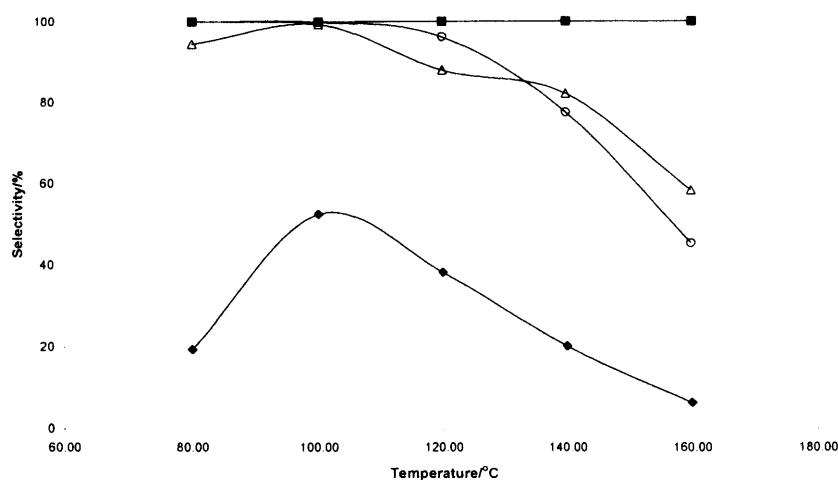


Figure 5.18 Selectivity to iso-propanol as a function of temperature. Water partial pressure: 4.2kPa (temperature: 30°C): (●) 70wt% H_3PO_4/SiO_2 (○) Tungstomolybdic acid (□) Phosphomolybdic acid (◆) ZSM-5 zeolite (Δ) Bulk HPW

The selectivity to iso-propanol as a function of temperature is given in figure 5.18. The phosphomolybdic and the 70wt% H_3PO_4/SiO_2 remained the most selective over the entire temperature range being 100% selective to iso-propanol up to 150°C. The tungstosilicic and bulk HPW displayed 100% selectivity at 100°C before decreasing to approximately 60% at 150°C. At these temperatures there is an increase in the formation of the oligomerisation-cracking and etherification products. The ZSM-5 zeolite was the least selective overall with a maximum iso-propanol selectivity of 52% at 100°C, this rapidly decreased to just 6% at 150°C. The optimum temperature for the reaction under these conditions appears to be 100°C. The most active and selective catalyst was the phosphomolybdic, giving a maximum 1.2% conversion with 100% selectivity. The 70wt% H_3PO_4/SiO_2 was also 100% selective but with a lower conversion.

The iso-propanol yields as a function of temperature are given in figure 5.19.

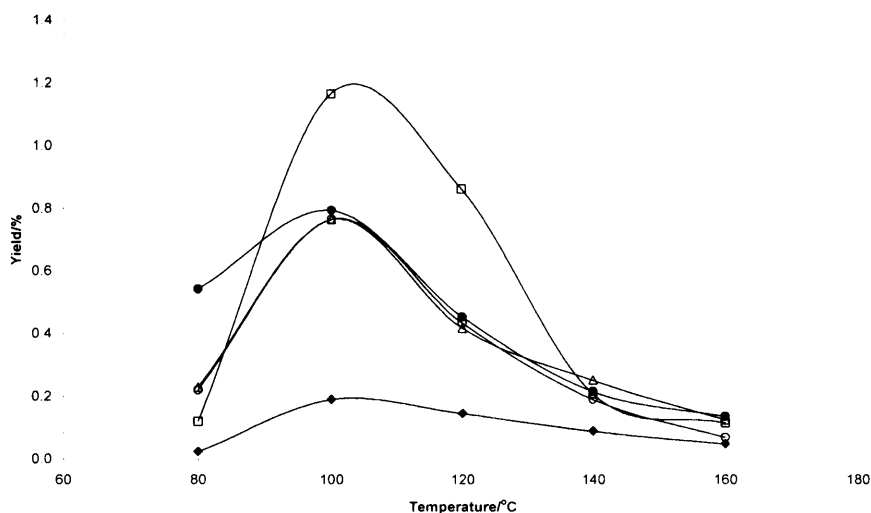


Figure 5.19 Iso-propanol yield as a function of temperature. Water partial pressure: 4.2kPa (temperature: 30°C): (●) 70wt% H_3PO_4/SiO_2 (○) Tungstosililic acid (□) Phosphomolybdic acid (◆) ZSM-5 zeolite (Δ) Bulk HPW

The most active and selective catalysts gave the highest yields. The phosphomolybdic acid catalyst gave a maximum yield of 1.2% iso-propanol at 100°C, this was with 100% selectivity. The ZSM-5 catalyst gave the lowest yield, not achieving greater than 0.2% across the entire temperature range this was as a result of the low activity and selectivity. The 70wt% H_3PO_4/SiO_2 , tungstosililic acid and bulk HPW gave similar yields across the temperature range studied with a maximum of 0.7% at 100°C.

The results from the catalytic experiments showed clearly that the most active and selective catalyst was the phosphomolybdic acid catalyst giving the highest conversion and yields with 100% selectivity. Interestingly all of the catalysts, with the exception of ZSM-5 zeolite showed a maximum conversion at 100°C. These data are in keeping with those reported in the literature which also saw a temperature of maximum conversion^[14].

5.3.6 Direct conversion of propane to iso-propanol over bi-functional catalyst

Following on from the previous work, experiments were conducted using the Co_3O_4 nanoparticles in combination with the best hydrating catalyst from the previous experiment. The direct catalytic partial oxidation of propane to iso-propanol would require a dual functioning catalyst that is able to activate propane and introduce oxygen via hydration at the lowest possible temperature in order to avoid gas phase and unselective reactions. It was envisaged that by combination of the low temperature and highly active Co_3O_4 nanoparticles with a suitable hydrating catalyst the direct conversion of propane to iso-propanol could be achieved. The catalyst studied in the following section was made by direct combination of the Co_3O_4 nanoparticles with the phosphomolybdic acid catalyst. The arrangement within the bed and the precise reaction conditions are given in experimental section 2.4.1. The catalyst was heated up to 70°C in a He/O_2 mix. Once the temperature had been allowed to stabilise propane and H_2O were introduced to the system. The sample cylinder was heated in 10°C steps and allowed to stabilise at each temperature for approx. 15-20 minutes before sample injection. Three injections were done at each temperature and the average taken. Carbon dioxide, propene and iso-propanol were the only products present. There was no evidence of any other hydration products in the reaction effluent. The results for propane conversion as a function of water concentration are given in figure 5.20.

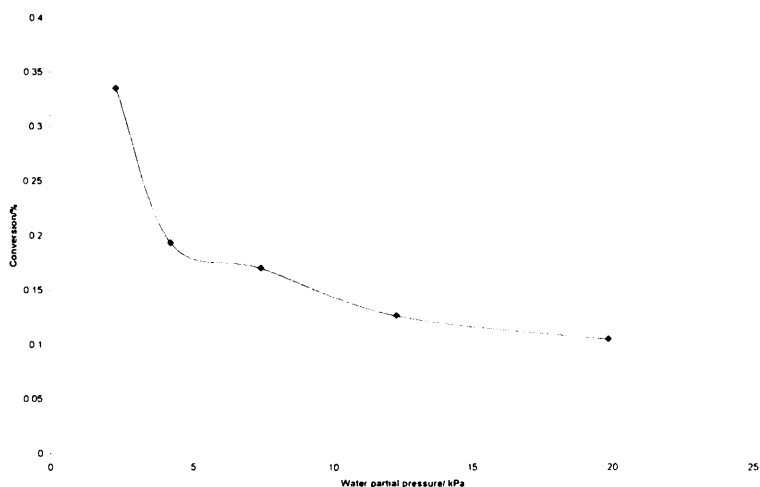


Figure 5.20 Propane conversion to iso-propanol over Co_3O_4 /Phosphomolybdic acid mixture. Conversion as a function of water partial pressure. Reaction at 100°C .

With water in the feed propane conversion over the mixed catalyst was very low with a maximum of 0.36% conversion to products. The conversion is seen to decrease with increasing water pressure. Generally the iso-propanol is present in trace amounts with carbon dioxide being the primary product. The exact conversion values are given in table 5.5.

Table 5.5 Propane conversion to iso-propanol as a function of water vapour pressure

Water temperature/ $^\circ\text{C}$	Vapour pressure/KPa	Conversion/%
20	1.2	0.33
30	2.3	0.19
40	4.2	0.17
50	7.4	0.13
60	12.3	0.10

The bifunctional catalyst is relatively inactive with propane conversion being suppressed by both water in the feed and by dilution of the active redox catalyst with the relatively inactive phosphomolybdic acid. Increasing the water concentration has a negative effect on the Co_3O_4 catalyst limiting propene production and hence limiting the total iso-propanol yield.

The selectivities as a function of water temperature are given in figure 5.21.

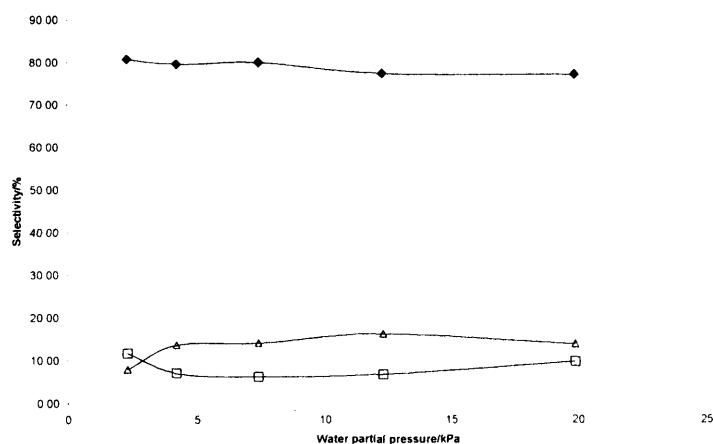
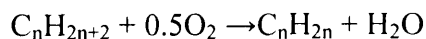


Figure 5.21 Selectivity to iso-propanol as a function of water partial pressure over

Co₃O₄/phosphomolybdic acid catalyst: (◆)CO₂ (□) C₃H₆(Δ)C₃H₅OH

The typical propane conversion over the nanocrystalline Co₃O₄ at 100°C is approximately 1% with a 97% selectivity to propene. This was not the case with the cobalt oxide used in this experiment. Tests done with no water in feed showed results of less than 0.5% conversion with only a 10-20% selectivity to propene. The primary product under these conditions was carbon dioxide with the catalyst remaining 80% selective to CO₂ throughout the whole reaction. Whether this is due to the presence of the acid catalyst or due to the cobalt oxide will have to be established. Varying the concentration of water in the system had little effect on product selectivity. The catalyst showed a maximum 14% selectivity to iso-propanol and varied little with water concentration. The same was true for the propene selectivity which was no greater than 10% throughout the reaction. Interestingly it is worth noting that even with no water in the feed, trace amounts of iso-propanol are still present. Removal of propane from the feed results in the disappearance of this peak. This could indicate

that there is sufficient water from the initial reaction to hydrate the silica catalyst according to:



Alternatively it may just be the case that the acid catalyst is itself sufficiently hydrated from the outset. Given that there is very little variation in activity with increasing water concentration this may well be the case

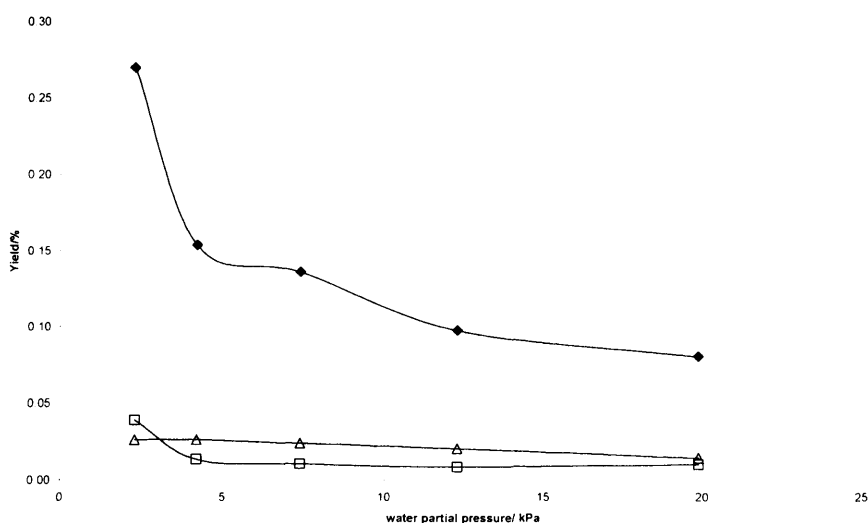


Figure 5.22 product yields as function of water partial pressure over Co_3O_4 /Phosphomolybdic acid catalyst

The product yields as function of water temperature are given in figure 5.22. Due to the poor conversions and selectivities the iso-propanol yields are very poor. There are trace amounts of propene and iso-propanol in the feed but nothing significant. All yields are below 0.5% with iso-propanol yields not exceeding 0.03%. Such low traces

of product are disappointing but not unexpected given the low temperatures employed, coupled with the limited activity of the catalysts used.

Given that the propane conversion over Co_3O_4 is suppressed by the presence of water it not surprising that the conversion is so low. The maximum yield of propene obtainable over the Co_3O_4 in a wet atmosphere at 100°C is just 0.5%. This means that there is only a trace amount of propene within the feed that can go on to react with the acid catalyst to produce isopropanol. The total iso-propanol production is limited by the activity of the redox catalyst in the system. Nevertheless, iso-propanol is still present as a product in the reaction mixture and although the conversions and selectivities are extremely low there is definite proof that the concept works. By combination of a dehydrogenation and acid catalyst the direct conversion of propane to iso-propanol was possible at 100°C .

5.4 Discussion

5.4.1 Propane oxidative dehydrogenation over bulk Co_3O_4 catalyst

In an effort to increase the low temperature activity of the Co_3O_4 catalyst a series of samples were prepared using different methods. The most active of the cobalt oxides was found to be nanoparticle Co_3O_4 prepared by mechanochemical synthesis. The cobalt oxide was synthesized by solid state reaction and the surface area of the sample was $159\text{m}^2\text{g}^{-1}$. The nano-crystalline nature of the catalyst is consistent with their relatively high surface area. Powder XRD of this material only shows the presence of Co_3O_4 with very broad diffraction peaks. The average particle size, calculated by X-ray line broadening through the Scherrer equation, was 12 nm. TPR of this sample shows two main reduction bands at c.a. 240 and 340°C , that can be attributed to the

reduction of Co_3O_4 to CoO and from CoO to Co .^[4] The low intensity reduction feature at 80-100°C, seen previously in the precipitated Co_3O_4 was present in the nanocrystalline sample and in higher concentrations. Calculation of the peak areas indicated that the concentration of reducible species was three times that of the precipitated catalyst. The most remarkable characteristic of this material is that at ambient temperature and pressure it activates propane yielding propene with 100% selectivity. Furthermore the activity of the catalyst was greater than that for the precipitated sample. Unfortunately, deactivation of the catalyst takes place and after a period, depending on the contact time employed, no further propane activity was observed.

One of the most positive aspects of this catalyst is that it can be reactivated relatively easily by heating in air at a temperature as low as 180°C (below this temperature the catalytic activity is only partially restored). Investigation of the catalyst deactivation and regeneration cycle was presented in figure 5.13. After the first few deactivation and regeneration cycles the catalyst profile with time on stream was extremely reproducible. These data indicate that the catalyst was regenerated fully even after several deactivation and regeneration cycles. The ability to operate the catalyst in a reproducible cycle means that propane selective oxidation can be performed at low temperature followed by regeneration at elevated temperature.

It is important to indicate that although propane conversion decreases with time on line for reaction temperatures below 120°C, above this temperature the propane conversion remained constant with prolonged time on line. However, the selectivity to propene was lower than 100%.

Using the nanocrystalline cobalt oxide similar experiments to those made with propane were carried out using other alkanes as substrates. In the case of ethane, activation at low temperatures and deactivation was observed as in propane. However,

important differences were apparent. To achieve the same conversion to that observed for propane *ca.* 40-50°C higher temperature was required. In addition, the selectivity to ethylene did not exceed 70%. In the case of methane no activity was demonstrated even at a reaction temperature of 100°C.

At this stage the origin of this catalytic behaviour is uncertain. However, it is probable that it is related to the presence of a very active species that reduces in the TPR experiments at 90°C (section 5.2.3). As synthesised nanocrystalline cobalt oxide exhibits this feature but the deactivated catalyst after reaction at 25 or 40°C does not. If the deactivated catalyst was calcined in air at 180°C, which are the conditions used to regenerate catalyst activity, the reduction feature reappears. Therefore, the low temperature catalytic behaviour is assigned to the presence of this very active species, which could be cobalt in a high oxidation state or a very reactive oxygen species. Thus, the deactivation of the catalyst would be due to the exhaustion of this very active species that cannot be fully reoxidised at lower temperatures. Therefore, it appears that this low temperature reduction feature is associated with a surface oxygen species that affects the low temperature selective oxidation. This postulation is enforced by experiments in which the precipitated catalyst was treated with hydrogen in situ at 80°C prior to being tested for propane oxidation (Section 4.3.8.) The pre- treated catalyst showed no activity for propane oxidation, selective or non-selective. Regeneration of the hydrogen pretreated catalyst at 180°C in air resulted in the propane conversion and selectivity to propene being fully restored to that of the fresh catalyst. In addition, the commercial Co_3O_4 catalyst did not present this reduction at *ca.* 90°C and propane oxidation results confirmed that the catalyst was inactive at low temperature. Identification of this low temperature selective oxidation site will aid in the scientific design of more effective catalysts for alkane oxidation as

catalysts that are capable of activating alkanes at low temperatures are of fundamental importance.

At this moment most of the catalysts reported in the literature for oxidative dehydrogenation of short chain alkanes (ethane, propane, n-butane) operate at temperatures over 400°C and are based on vanadium and molybdenum oxides^[15-17]. In the case of catalytic dehydrogenation in the absence of molecular oxygen the temperatures employed are even higher (>550°C) since this reaction is thermodynamically limited^[18, 19]. In contrast, for the present work very low reaction temperatures have been employed. It is true that the conversions obtained are low but if the nature of the extremely reactive species could be identified and materials could be synthesised with higher concentration of this species, very interesting catalytic results should be obtained at ambient temperature. Another problem that arises is the deactivation of the catalyst. It has been reported that the main problem of redox catalytic reactions at low temperature is the reoxidation step of the reduced catalyst^[20]. It appears that a similar effect may be operating with the nanocrystalline Co_3O_4 , strategies such as using a different oxidant or increasing reaction pressure may help to overcome this limitation. Nevertheless, the ability to operate the catalyst with high selectivity and then fully regenerate the original activity is important. This mode of operation has already been successfully commercialised by DuPont using the Riser reactor for the selective oxidation of butane to maleic anhydride at elevated temperature^[21].

The production of chemicals by energy efficient and environmentally friendly routes is an important aim for the modern pharmaceutical and chemical industries. In particular, the facile utilisation of cheap and relatively abundant feedstocks such as short chain alkanes (C1-C4) remains a challenging target.^[22,23] Presently, the activation of these hydrocarbons under benign conditions, has not yet been reported.

The efficient utilisation of short chain alkane feedstocks is highly desirable as their production volumes are set to increase significantly, due to large scale international investment in new gas to liquids technology. Experimental evidence has been found for the selective oxidation of methane to methanol at room temperature on Fe-ZSM-5 catalysts.^[24] However, the methanol product is bound strongly to the catalyst surface and upon heating it is not released into the gas phase, but decomposes to evolve carbon monoxide. A number of studies have confirmed Co_3O_4 to be the most active catalyst for alkane oxidation. Simonet *et al* reported the lowest light-off temperature of 277°C ^[25], Finocchio and co-workers obtained similar results with propane activation occurring at approximately 300°C ^[26]. There is no evidence in the literature of a cobalt oxide capable of propane conversion to propene at room temperature. However work by Finocchio *et al* attempted to determine the reaction mechanism by FTIR for propane activation. It was found that Co_3O_4 was more active than the other oxides, giving rise to substantial conversion of propane at ca. 250°C ^[27]. Its activity in the total oxidation of propene was similar to that of propane. The commercial catalyst tested by us was more active with light off occurring at ca. 120°C and a maximum selectivity to propene of approximately 80% at 150°C . The differences in activity can be attributed to the use of different commercial catalysts (In our case Avacado $4\text{m}^2\text{g}^{-1}$) and reaction conditions.

The FTIR studies by this group go some way to suggesting a simple mechanism. It states: “On Co_3O_4 we found that propene is oxidised at the allylic position giving rise to acrylate species already at room temperature”. Also: “Propane is also activated at very low temperatures, at C(1) and at C(2). Activation at C(2) gives rise to acetates.” ^[27] Although they present these results no mention is made of low temperature reaction studies on Co_3O_4 that give rise to propene, they merely state the presence of such species on the surface.

In the present work we demonstrate a catalyst that achieves selectivity to propylene of 100% at low reaction temperatures. The per pass yields to the olefin obtained are relatively low, but the results are highly significant as no other catalyst has shown any activity for this reaction under the same conditions. Presently the low yield means that considerable improvement is required before the catalyst could be considered for industrial use. However, these are still very significant fundamental results for alkane activation, since we show for the first time a catalyst capable of selectively activating propane using ideal reaction conditions: atmospheric pressure, ambient temperature and using air as an oxidant.

5.4.2 Direct oxidation of propane to iso-propanol

The direct functionalisation of propane (instead of propylene) to oxygen containing compounds presents a significant research challenge. One of the aims of this study was to find new approaches for the development of more effective catalytic routes. Processes reported so far include liquid phase heterogeneous catalytic reactions using metalloporphyrin^[28] and phthalocyanine complexes^[29] that mimic enzymes. Other routes include indirect methods whereby the propene is oxydehydrogenated at high temperatures and the unseparated effluent mixture is passed on to a second propane oxidation step^[30]. Generally, in processes such as these, a relatively high temperature is required for activation of the alkane, but unselective gas phase homogeneous reactions can then predominate and the partial oxidation product can be destroyed. Therefore, to minimise the influence of gas phase reactions, a low temperature

method has been tested using the highly selective Co_3O_4 nanoparticle catalyst in combination with a suitable hydration catalyst.

The results for iso-propanol production over a dual functioning redox/acid catalyst were quite poor. Direct impregnation of the Co_3O_4 nanoparticle catalyst with an acidic precursor containing tungstosilicic acid, phosphomolybdate acid, HPW or H_3PO_4 resulted in total loss of activity below 150°C . At these higher temperatures the sole product was CO_2 with no iso-propanol. Supporting the Co_3O_4 on an acidic support gave similar results, with the dispersion of the Co_3O_4 resulting in the dilution of the active sites and hence a no activity below 200°C . Above this temperature there is total oxidation of the alkane. The best results were achieved by the direct mechanical mixing of Co_3O_4 with the phosphomolybdic catalyst. Under these conditions iso-propanol production was possible but with very low conversion and iso-propanol selectivity.

Due to the already low product yields over both the Co_3O_4 catalyst and the hydration catalyst, the total iso-propanol yield was in trace proportions. The total iso-propanol production is limited by the activity of the redox catalyst in the system. Nevertheless, iso-propanol is still present as a product in the reaction mixture and although the conversion and iso-propenol selectivity are extremely low there is definite proof that the concept works. By combination of a dehydrogenation and acid catalyst the direct conversion of propane to iso-propanol was possible at 100°C .

5.5 Conclusions

Following on from previous work on precipitated Co_3O_4 a series of Co_3O_4 catalysts were prepared by different means and tested for propane ODH. The best results were obtained over the nano-crystalline Co_3O_4 prepared by solid-state reaction. The catalyst was active at temperature as low as ambient and displayed a conversion nearly five times that of the precipitated Co_3O_4 with 100% selectivity to propene. However above 80°C the selectivity was found to decrease rapidly to $<20\%$. The catalyst deactivated with time on stream, but activity was restored to the initial value after regeneration in air at 180°C . Consequently, the catalyst can be operated in a cyclic manner to achieve selective alkane dehydrogenation. The activation and selective oxidation of short chain alkanes at low temperatures is a major aim. Against this background, this work presents a significant breakthrough. At this stage no attempt has been made to optimise these catalysts and it is clear that they are now worthy of further study so that their potential for energy efficient and by-product minimisation can be fully appreciated for the utilisation of cheap and abundant chemical feedstocks.

The nano-crystalline catalyst was also tested in combination with a hydration catalyst for the direct conversion of propane to iso-propanol. Due to the low propene yield and wet atmosphere the propane conversion was very low but iso-propanol was detectable in the reaction effluent.

5.5 References

- [1] C.N.R. Rao and A.K. Cheetham, *J. Mater. Chem.*, 11 (2001) 2887
- [2] A.T. Bell, *Science*, 299 (2003) 1688
- [3] St.G. Christoskova, M. Styanova, M. Georgieva, D. Mehandjiev, *Mat. Chem. and Phys.*, 60 (1999) 39-43
- [4] G. Fierro, M. Lo Jacono, M. Inversi, R. Dragone, P. Porta, *Top. Catal.*, 10 (2000) 39.
- [5] J. Jacobs, A. Maltha, J.G.H. Reintjes, J. Drimal, V. Ponc and H.H. Brongersma, *J. Catalysis*, 147 (1994) 294-300
- [6] M. Shelaf, M.A.Z Wheeler, H.C Yau, *Surf. Sci.*, 47 (1975) 697
- [7] C. Yau, M. Shelaf, *J. Phys. Chem.*, 78 (1974) 2460
- [8] C. Wang, H. Lin and C. Tang, *Cat. Letters*, Vol. 94 (2004) Nos. 1-2
- [9] H. Yang, Y. Hu, X. Zang, G. Qiu, *Mat. Lett.*, 58 (2004) 387-389
- [10] J. Gau, Y. Zhao, W. Yang, J. Tian, F. Guan and Y.Ma. *J. Uni. Sci. Tech. Beijing.*, Vol. 10 No. 1 (2003) P. 54
- [11] Y. Ni, X. Ge, Z. Zhang, H. Liu, Z. Zhu, Q. Ye, *Mat. Res. Bull.*, 36 (2001) 2383-2387
- [12] Y. Yau, *J. Catal.*, 33 (1974) 108
- [13] D.A.H. Cunningham, T. Kobayashi, Kamijon, M. Haruta, *Catal. Lett.*, 25 257 (1994)
- [14] N. Essayem, Y. B. Taârit, E. Zausa and A.V. Ivonov, *Appl. Catal. A. Gen.*, 256 (2003) 225-242
- [15] R. Grabowski, *Catal. Rev. Sci. Eng.*, 48 (2006) 199
- [16] E.A. Mamedov, V.C. Corberan, *Appl. Catal. A. Gen.*, 127 (1995) 1
- [17] T. Blasco and J.M. López Nieto, *Appl. Catal. A. Gen.*, 157 (1997) 117

- [18] F. Buonomo, D. Sanfilippo and F. Trifiró, *Handbook of Heterogeneous Catalysis*, Vol. 5 Chapter 4.3.1 “*Dehydrogenation of Alkanes*” 5 (1997) 2140
- [19] P.R. Cottrell, S.T. Bakas, M.F. Bentham, J.H. Gregor, C.R. Hamlin and L.F. Smith, *Oleflex Process- The Proven Route to Light Olefins*, UOP, Des Plaines, III, (1992)
- [20] J.R. Monnier and G.W. Keulks, *J. Catal.*, 68 (1981) 51
- [21] J. Haggin, *Chem. Eng. News*, 74 (1996) 26
- [22] J.A. Labinger and J.E. Bercaw, *Nature*, 417 (2002) 507
- [23] J.M. Thomas, R. Raja, G. Sankar and R.G. Bell, *Nature*, 398 (1999) 227
- [24] V.I. Sobolev, K.A. Dubkov, O.V. Panna and G.I. Panov, *Catal. Today*, 24 (1995) 251
- [25] L. Simonet, F. Garin, G. Maire, *Appl. Catal. B. Env.*, 11 (1997) 167
- [26] E. Finocchio, G. Busca, V. Lorenzelli and V. S. Escribano, *J. Chem. Soc. Faraday Trans.*, 92(9) (1996) 1587-1593
- [27] E. Finocchio, R.J Willey, G. Busca and V. Lorenzelli, *J. Chem. Soc.*, 93 (1) (1997) 175-180
- [28] US Patent, 5 198580
- [29] R. Raja, C. R. Jacob, P. Ratnasamy, *Catal. Today*, 49 (1999) 171-175
- [30] European Patent Appl., 0117145, 9/84

Chapter 6

Chapter 6

Conclusions and future work

6.1 Ga₂O₃/MoO₃ catalysts.

A Ga₂O₃/MoO₃ catalyst, prepared by physically mixing Ga₂O₃ and MoO₃, was tested for the oxidative dehydrogenation of propane to propene. The catalyst was active and selective for the reaction with initial propane conversion occurring at 325°C for the calcined Ga₂O₃/MoO₃ mixture. A propane conversion of 5% with a selectivity to propene of ca. 76% was achieved at temperatures as low as 440°C. Calcination of the catalyst at 650°C was found to be beneficial due the formation of the more active β - Ga₂O₃ within the system. This was confirmed by tests done on the calcined Ga₂O₃ catalyst, which showed increased activity and selectivity to propene as compared to the uncalcined sample. Dilution of the Ga₂O₃ component with inert silicon carbide was found to increase the activity and selectivity of the catalyst but not to the same extent as dilution with MoO₃. This would indicate that MoO₃ plays an active part in the reaction; it may be the case that surface migration from one active site to another is an important factor with MoO₃ suppressing the total combustion of the propane molecule to CO_x and thus increasing selectivity. One of the most important factors was that the rate of propane conversion over the mixed catalysts was greater than over the individual component oxides and the best results were obtained by having the oxides in intimate contact.

The Ga₂O₃ and MoO₃ catalysts tested in this study were used as received from a commercial source with the only modification being calcination at 650°C. XRD analysis indicated the presence of α -Ga₂O₃ and γ -Ga₂O₃ as well as β -Ga₂O₃. In

previous studies the Ga_2O_3 catalyst used has been prepared by precipitation of the nitrate and subsequent calcination of the gallium hydroxide precursor to form the pure $\beta\text{-Ga}_2\text{O}_3$ ^[1]. In both this study and those conducted elsewhere the most active polymorph is found to be $\beta\text{-Ga}_2\text{O}_3$ ^[2]. In future studies it may be beneficial to investigate the effect of preparation methods on the activity of $\text{Ga}_2\text{O}_3/\text{MoO}_3$ with a pure $\beta\text{-Ga}_2\text{O}_3$ being used as opposed to a mixture of various polymorphs. A number of methods have been reported for the production of pure $\beta\text{-Ga}_2\text{O}_3$ ^[3,4].

The most active catalyst tested was found to be the calcined $\text{Ga}_2\text{O}_3/\text{MoO}_3$ catalyst with the increased activity being linked to the formation of the more active $\beta\text{-Ga}_2\text{O}_3$ upon calcination. However, calcination of the individual MoO_3 component was found to be detrimental to the activity and selectivity of the catalyst. Therefore, it can be proposed that a more active and selective catalyst may be formed by a combination of the calcined Ga_2O_3 with the uncalcined MoO_3 . Also, calcination of MoO_3 resulted in crystal growth along a specific plane. Identification of the exact phases present and their effect on catalyst activity may prove useful for the improvement of activity and selectivity.

6.2 Co_3O_4 catalysts

Following on from previous studies on alkane combustion over Co_3O_4 spinels a series of Co_3O_4 catalysts were prepared by precipitation from the nitrate and tested for the oxidative dehydrogenation of propane to propene. Initial experiments showed how fresh Co_3O_4 was capable of propane conversion at temperatures as low as ambient but with a low selectivity to propene. Subsequent experiments found that the fresh Co_3O_4

sample contained a high concentration of surface bound CO_2 . Pre-treatment of the catalyst (400°C 2h $\text{O}_2/\text{He} = 10/90$) was necessary for the complete removal of CO_2 from the surface. After activation the catalyst was capable of propane conversion at temperatures as low as ambient with a selectivity to propene of 100%. However the conversion was less than 0.5% and the catalyst deactivated rapidly at temperatures lower than 140°C . Steady state activity was possible at temperatures greater than 140°C but with a reduced propene selectivity of ca.70%.

Temperature programmed reduction of the bulk Co_3O_4 indicated the presence of reducible species at $80\text{-}90^\circ\text{C}$ that was attributed to the low temperature activity of the catalyst. Varying the O_2 concentrations had no effect on the activity or selectivity of the catalyst below 80°C indicating that it plays little part in the reaction at these temperatures. Activation of the O_2 molecule is not possible at such low temperatures and it is only at 140°C that there is any appreciable catalytic turnover. The precise reason for catalyst deactivation is unknown but there are a number of possibilities including the build up of site blocking carbonates or water on the surface over time. Another possibility is that the low temperature reducible species present is being rapidly reduced with reactivation of the surface sites not being possible. Long residence times and low alkane concentrations are beneficial to the reaction.

In an effort to improve activity and selectivity a number of Co_3O_4 catalysts were prepared by different methods and tested for the ODH of propane. Preparation of Co_3O_4 by calcination of the nitrate resulted in a poor catalyst that was inactive at temperature lower than 80°C and unselective for propene. A high-valence Co_3O_4 catalyst prepared by a precipitation-oxidation process displayed a higher rate of propane oxidation above 100°C but with a reduced selectivity as compared to the precipitated catalyst. Interesting results were found with the nano-crystalline catalyst

prepared by solid-state reaction. The rate of propane conversion at ambient temperature was greater than the precipitated catalyst and the selectivity to propene was still 100%. The higher activity is attributable to the higher surface area, $159\text{m}^2\text{g}^{-1}$ as compared to $34\text{m}^2\text{g}^{-1}$, and hence the increased concentration of active sites over the surface. Temperature programmed reduction studies indicated a higher concentration of low temperature reducible species at 80-90°C.

Unlike the precipitated catalyst the nano-crystalline Co_3O_4 could be reactivated after deactivation. The ability to operate the catalyst in a reproducible cycle means that propane selective oxidation can be performed at low temperature followed by regeneration at elevated temperature.

Further work is necessary to determine the precise nature of the active site:

- *In situ* Raman and FTIR studies using propane as adsorbent could give information on the nature of the metal oxygen bond in Co_3O_4 as well as the activated complex present on the surface.
- To determine the product and regioselectivity of the catalyst and the role of oxygen in the oxidation of propane, and to improve understanding of the selective surface chemistry
- To probe the reaction mechanism using temporal analysis of products under typical operating conditions to provide new information on the active catalyst phases and to use this information to synthesise improved catalysts

One of the main objectives of future work would be to improve the low temperature conversion and yield of the catalyst. The addition of certain promoters may be beneficial but may also lead to over oxidation and a reduction in overall selectivity.

Another possibility is to improve the selectivity of the catalyst in the 80-140°C temperature range by hindering the total oxidation reaction at the higher temperatures.

One of the major problems with the dual functioning catalyst for the conversion of propane to iso-propanol was the unfavourable reaction conditions and the low conversions and yields over both of the component catalyst. Water was found to suppress propene production over the Co_3O_4 and limit activity. Operating the system under pressure may lead to an improvement in iso-propanol production but the effect on the alkane activation step may be detrimental.

6.3 References

- [1] C. R. Hammond, *PhD Thesis, University of Wales Cardiff.* (2004)
- [2] Y. Yue, B. Zheng, W. Hua and Z. Gao, *J. Catal.*, 232 (2005) 143-151
- [3] A.W. Laubengayer and H.R. Engle, *J. Amer. Chem. Soc.* 61 (1939) 1210
- [4] I.A. Sheka., *Chemistry of Gallium.*, Elsevier Amsterdam(1966)

Chapter 7

Chapter 7
Appendix

7.1 Mass Flow Controller calibration.

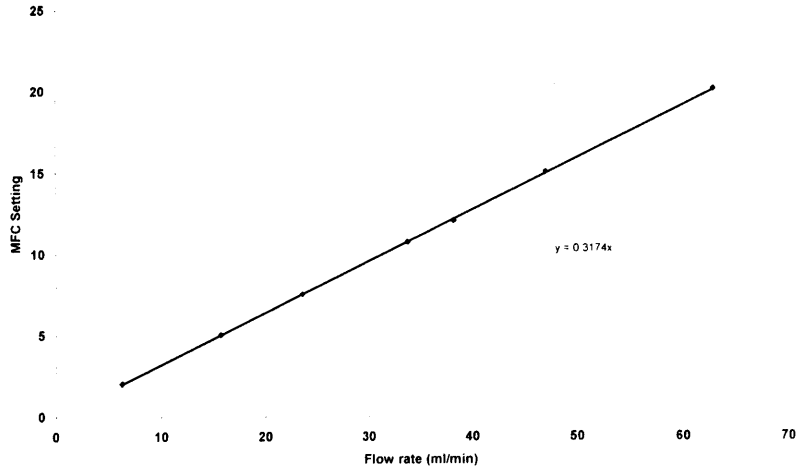


Figure 7.1.1. Helium MFC calibration

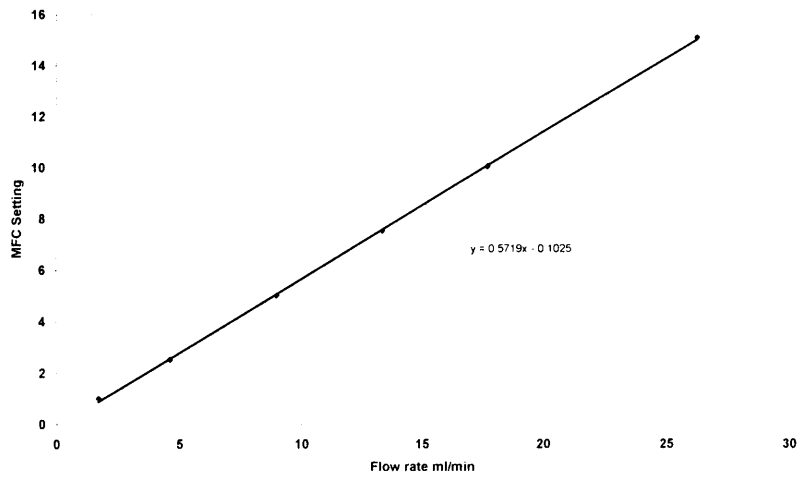


Figure 7.1.2 Oxygen MFC Calibration

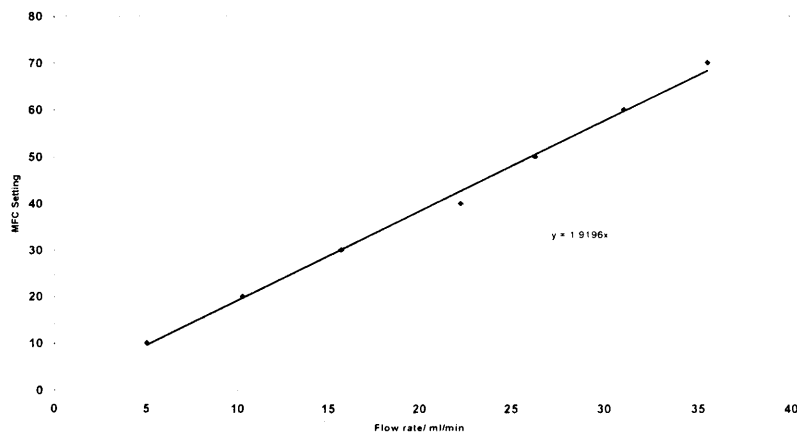


Figure 7.1.3. Propane MFC calibration

Appendix

7.2 Detector Calibration

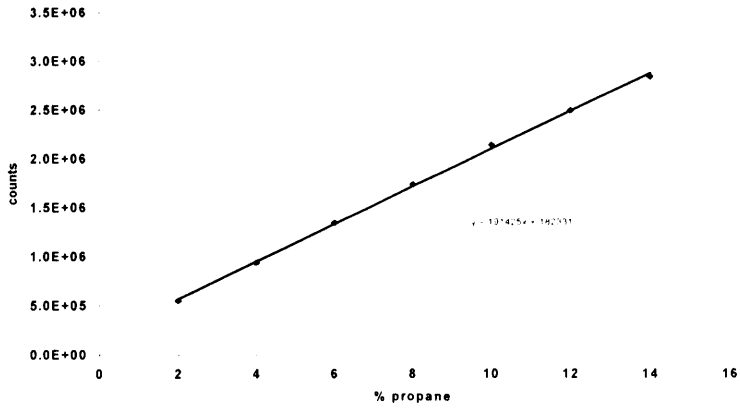


Figure 7.2.1. Calibration of FID for propane.

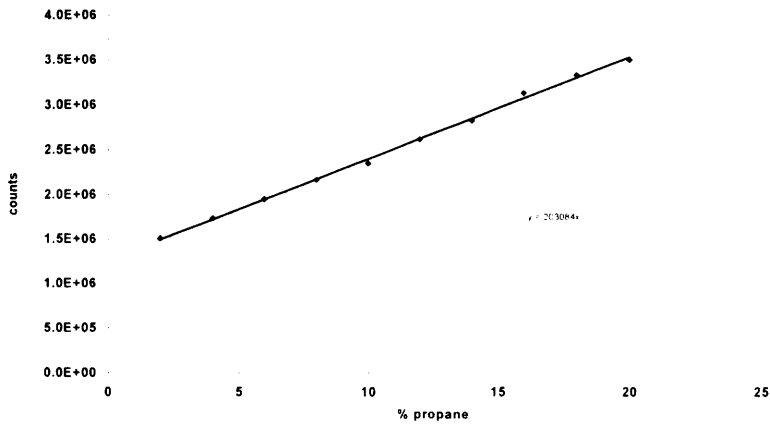


Figure 7.2.2. Calibration of TCD for propane

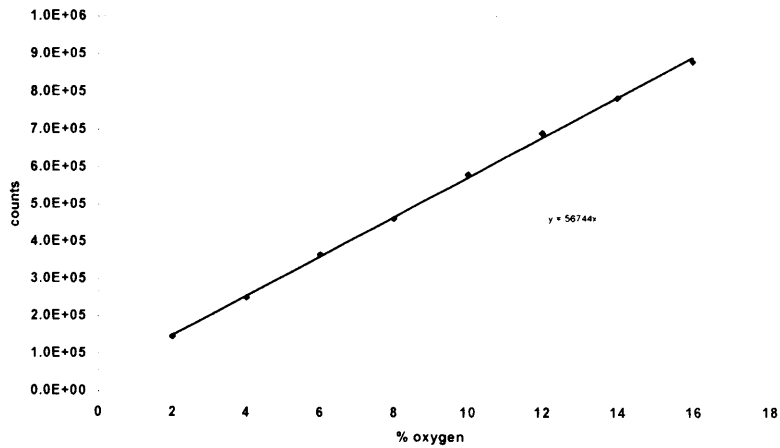


Figure 7.2.3 Calibration of TCD for oxygen

Appendix

7.3 Blank Reactor Test.

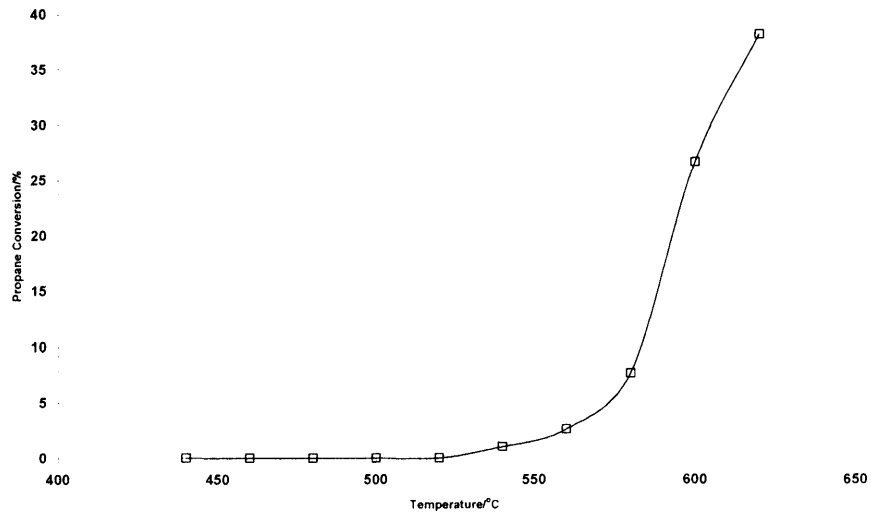


Figure 7.3.1. Propane conversion over inert silicon carbide

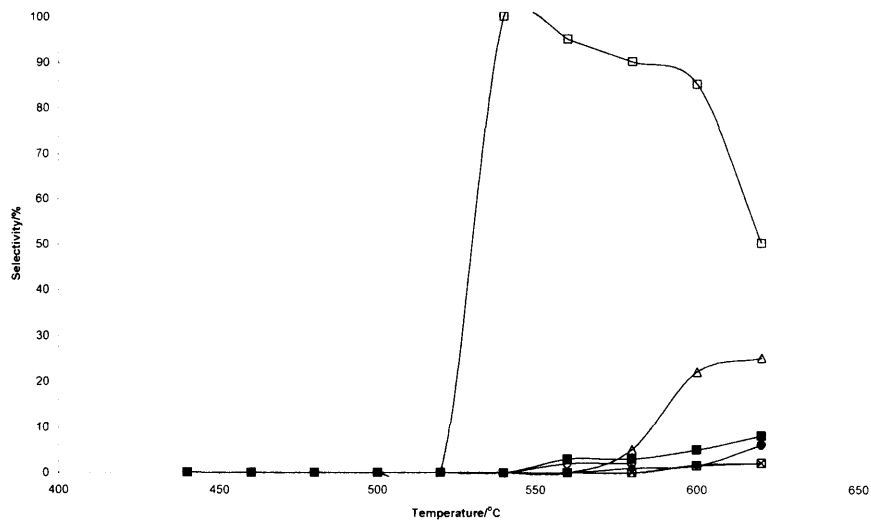


Figure 7.3.2 . Selectivity to products over inert siliconcarbide. (□) C₃H₆ (■) CH₄ (Δ) CO (●) Acrolein (X) Acetone (○) Ethane/ethane (▲)CO₂

Gemini 2360 V5.01
 Instrument ID: 236/20851/00
 Setup Group: 9 - None

Sample ID: Carbon Black Ref Date: 30/06/05 Time: 14/17/07
 Sample Weight: 0.5184 g Saturation Pressure: 780.50 mmHg
 Measured Free Space: -1.015 cc STP Evacuation Time: 1.0 min
 Analysis Mode: Equilibration Equilibration Time: 10 sec

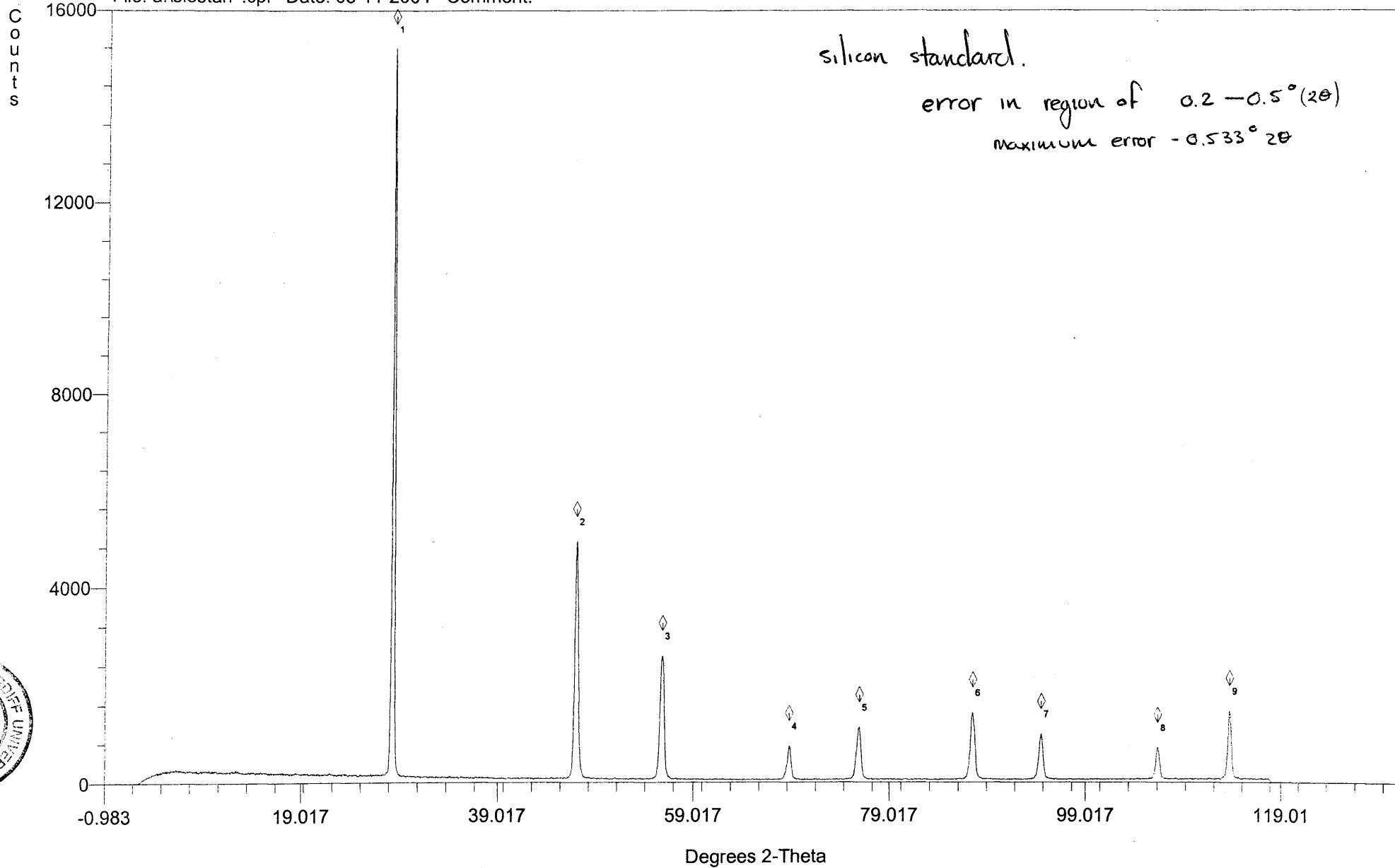
BET Multipoint Surface Area Report

Surface Area: 24.0437 sq. m/g
 Slope: 0.179763
 Y-Intercept: 0.001290
 C: 140.336349
 Vm: 5.523232
 Correlation Coefficient: 9.9998e-001

Analysis Log

Relative Pressure	Pressure (mmHg)	Vol. Adsorbed (cc/g STP)	Surface Area Point
0.0501	39.08	5.204	*
0.0751	58.58	5.490	*
0.1001	78.11	5.746	*
0.1251	97.67	5.988	*
0.1502	117.21	6.227	*
0.1752	136.72	6.470	*
0.2002	156.27	6.717	*
0.2253	175.82	6.969	*
0.2504	195.41	7.229	*
0.2754	214.96	7.489	*
0.3004	234.46	7.758	*

Carbon black standard
Expected value 24 m²g⁻¹



Silicon Standard